QCLNG-EARLY WORKS DREDGE PLUME MODELLING

Final– 7/01/2010

Prepared for:

British Gas

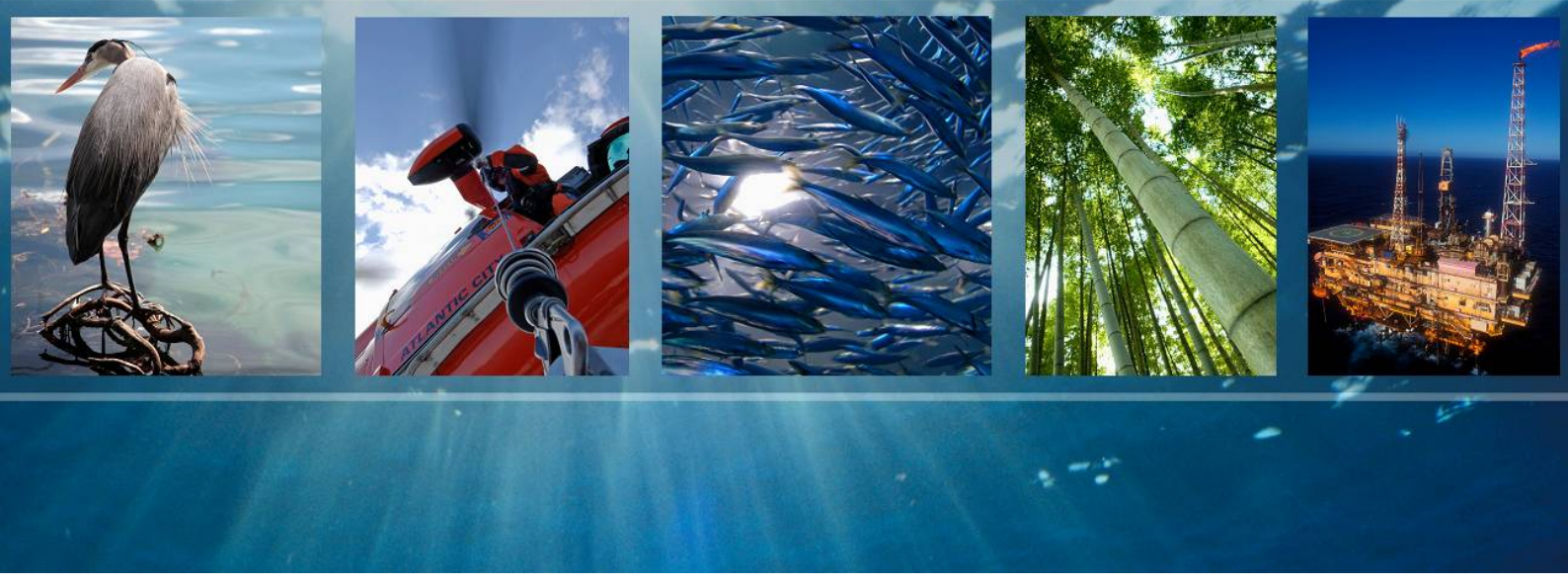

Document control form

Document draft	*Originated by*	*Edit & review*	*Authorized for release by*	*Date*
Draft 1 - Issued for internal review	Dr Sasha Zigic Dr Ryan Dunn	*Nathan Benfer*		*8th December 2009*
Draft 2 - Issued for client review			Dr Sasha Zigic	*9th December 2009*
Draft 3 after edits		*Scott Langtry*		*16th December 2009*
Final report issued to client			Dr Sasha Zigic	*7th January 2010*

Document name: QCLNG_EarlyWorks_DredgePlumeModelling_Final.doc

APASA Project Number: S125

APASA Project Manager: Dr Sasha Zigic

DISCLAIMER:

Contents

Figures

Tables

EXECUTIVE SUMMARY

British Gas (BG) commissioned Asia-Pacific ASA (APASA) to model the suspended sediment plumes and sediment deposition patterns that would result from proposed "early works" dredging within Port Curtis, adjacent to the QCLNG site. The early works program is to involve the removal of 2.14 Mm^3 of sediment, to allow for a material offloading facility (MOF) and Pioneer construction dock (construction dock), which is to be carried out as a phased approach:

Phase 1 – Dredging of MOF Stage 1 to -2.5 m below LAT (Lowest Astronomical Tide) and construction dock to -5.0 m below LAT, early July 2010; and

Phase 2 - Dredging of MOF Stage 2 to -7.8 below LAT, early September 2011.

As it is unknown whether the Fisherman's Landing reclamation site will be available by July 2010, BG had identified two alternative dredge and disposal options (or Scenarios) for MOF stage 1 and construction dock,

- Scenario 1 – removal of sediment using a cutter suction dredge (CSD) with a similar production rate to the 'Wombat', being 500 m^3/hr, and spoil pumped to the reclamation site via a floating or submerged hydraulic pipeline. Excess water (tail-water) will be returned to the marine environment, from the north-west corner of the Western Basin reclamation site via a series of outflow pipes (see Figure 1); or
- Scenario 2 - one Backhoe Dredge (BHD) will be used to remove material within the MOF and a second BHD within the construction dock. Each BHD will deposit the sediment directly into 3 supporting (six in total) Split Hull Barges (SHB), which will place the material into the existing Gladstone Port Corporation (GPC) spoil ground.

Only one dredge and disposal option is proposed for MOF stage 2:

- Scenario 3 – removal of sediment using a large CSD (~ 1,500 m^3/hr), with spoil pumped to the reclamation site via a floating or submerged pipeline. The tail-water will be returned into the marine environment through a series of overflow pipes.

An advanced sediment fate model (DREDGEMAP) was applied to simulate the transport, sinking, settlement and resuspension of the dredged material by various operations. DREDGEMAP inputs included site-specific sediment composition, production rate of the equipment, mass flux, initial vertical-distribution of sediments in the water column and details of the dredging locations for each operation (nine in total). This approach provided a realistic

estimate of the time spent and the volume of material suspended into the water column during dredging.

The model predictions for the dredging operations indicate localised plumes of TSS (total suspended sediment) would be concentrated (~ 100 mg/L above ambient) around the MOF and construction dock, with concentrations decreasing exponentially as a function of distance and current strength. During the out-going tide, sediment plumes will be advected south-east from the dredge operation toward Tide Island, which is approximately 5.5 km south-east from the MOF dredge footprint. At the turn of the tide, the plume will be pushed back up the main channel towards the mouth of Graham Creek and the Narrows (5 km north north-west from the MOF dredge foot print) at lower concentrations (~ 5 mg/L above ambient). There were episodes in the simulations where isolated patches of plumes reached visible concentrations (assumed to be > 5 mg/l), which resulted as sediment collided with land masses (i.e. South Passage Island) and formed break-away plumes, and/or sediment was resuspended from the bed. Resuspension of the fine (< 130 µm) dredged sediment was predicted as a common occurrence, due to the strong currents (up to 2 m/s) scouring the seabed within the vicinity of the operational site.

Disposal of dredged sediment from SHBs were predicted to set up very high local TSS concentrations within the sinking plume, with the entrainment of coarser sediment expected to limit the suspension time for finer sediments. Given the strong currents that run east-west, simulations indicated that the major depositional axis would be along the east-west axis. The predicted maximum area of exposure was 41 km^2 above 0.001 m (or 1 mm), with 79% of the area (or 32.2 km^2) having a thickness of less than 0.01 m. Therefore, 8.9 km^2 would be covered by a mound higher than 0.01 m.

For Scenario 1, the depth averaged median values (or typical TSS concentrations) showed an increase of 5 mg/L (above ambient) for waters directly adjacent to the MOF and construction dock. Whereas, an increase of 25 to 50 mg/L were predicted immediately adjacent to the tail-water discharge site. The 95^{th} percentile outcomes, which are indicative of worst case combinations of tidal and wave conditions, revealed 5 mg/L increases along the western shoreline of Curtis Island, including Graham Creek, the Narrows, North and South Passage Islands, in addition to waters adjacent to the tail-water discharge site. Occurrences of 10 mg/L (above background) were predicted next to the MOF and Friend Point. While 25 mg/L concentrations were found within 300 m from the tail-water outfall, along the shorelines of the construction dock, North passage and Tide Island.

The median TSS results for Scenario 2 revealed a 5 mg/L increase (above background) adjacent to the construction dock and Tide Island. Based on 95^{th} percentile statistics, 5 mg/L

concentrations were stretched over 16 km from waters south of Turtle Island to the north channel of Graham Creek. Concentration increases of 10 mg/L were predicted to occur 3.5 km north of Fisherman's Landing. While regular peaks of 25 mg/L were found within waters surrounding the MOF and construction dock dredge areas.

The median analysis of Scenario 3 dredge simulations suggested that concentrations of 5 mg/L will commonly occur in waters adjacent to North Passage Island, Tide Island and the north-east point of the reclamation site. Concentrations of 25 to 50 mg/L were estimated for waters immediately adjacent to the tail-water discharge location. The 95th percentile assessment indicated that increased concentrations of 5 mg/L extended ~ 16.5 km from Graham Creek in the north to waters surrounding Picnic Island under more extreme conditions. Concentrations up to 10 mg/L were predicted for waters surrounding both North and South Passage Islands, Tide Island, and also nearby the tail-water discharge site. Elevated concentrations of 50 mg/L are predicted for waters in the south-west corner of Tide Island, North Passage Island and in the immediate vicinity of the tail-water discharge site. A maximum concentration of 100 mg/L was predicted to occur at the tail-water discharge site.

A major component of the study involved relating the predicted TSS concentrations to light for the assessment of potential impact on seagrass productivity. This involved generating median and 95th percentile maps for the amount (%) of light reaching the seabed under ambient conditions (i.e. pre-dredging) and overlapping them with the model predictions for TSS to evaluate the expected difference in the available light reaching the seabed. Each map is defined by six contours delineating reductions of 5, 10, 15, 30, 40 and 50% of available light at the seabed.

For Scenario 1, the 50th percentile estimates (median concentrations) indicate a difference of 1% in available light at the fringe of the seagrass meadow north of the proposed Fisherman's Landing reclamation site. Up to 25% difference in the available light was indicated at the proposed tail-water outfall. The percentage difference is then predicted to decrease to a 2% reduction within 300 m of the outfall.

The 95th percentile estimates indicate a 2% reduction in light for seagrass meadows south of Fisherman's Landing. There is the potential for a 15% reduction in available light for seagrass meadows at both North and South Passage Islands. The seagrasses adjacent to Laird Point would likely experience 10% less light. Seagrass meadows north of the Fisherman's Landing reclamation site would experience a change of 5 to 25% change in light, depending on proximity to the tail-water outfall.

The median estimates for Scenario 2 indicate that a 2 to 5% difference in available light would commonly occur over seagrass meadows north and south of Fisherman's Landing. Up

to 10% reduction in available light is indicated at the tip of North Passage Island and 5% less light is indicated for meadows adjacent to Laird Point and South Passage Island.

The 95th percentile estimates indicate 10% less available light west of Compigne Island and 5% less light near Garden Island under unusual conditions. The seagrass meadows along the coastline south of Fisherman's Landing are predicted to potentially experience a 5 to 10% reduction of available light. For seagrasses adjacent to Laird Point, and North and South Passage Island's, up to a 15% reduction in the available light was indicated. Finally, a 15% change in available light was predicted for the seagrass located along the coast, north of Fisherman's Landing, under unusual conditions.

For Scenario 3, the median estimates reveal a 5% reduction in available light for seagrasses at South Passage Island and 10% at North Passage Island. For meadows adjacent to the proposed construction dock a 2% reduction was indicated as a likely occurrence. . The deeper fringes of the seagrass meadows north of the proposed reclamation site were also predicted to routinely experience a 2% reduction in available light. This reduction was around 25% at the south-western corner, adjacent to the proposed tail-water outfall.

Finally, the 95th percentile estimates indicate a 15% change in available light for meadows adjacent to Hamilton Point and along the western coastline of Curtis Island, under more unusual conditions. Seagrasses located at North and South Passage Islands could receive 10% less light. There was a potential difference of available light of 1 to 2% for meadows south of Fisherman's Landing and 2 to 25% change for seagrasses north of Fisherman's Landing.

1 INTRODUCTION

British Gas (BG) is seeking approval to embark on the "early works" dredging within Port Curtis to permit access to the QCLNG terminal on Curtis Island (refer to Figure 1). The operation is to consist of a material offloading facility (MOF) and Pioneer construction dock (construction dock), with an estimated volume of 2.14 Mm^3 to be removed in two key phases:

Phase 1 – Dredging of MOF Stage 1 to -2.5 m below LAT (Lowest Astronomical Tide) and construction dock to -5.0 m below LAT, early July 2010; and

Phase 2 - Dredging of MOF Stage 2 to -7.8 below LAT, early September 2011.

The associated dredge depths and volumes are presented in Table 1.

Asia-Pacific ASA (APASA) was commissioned to model the suspended sediment plumes and sediment deposition patterns that could be generated by the various dredging operations.

This report documents the model set-up, methodologies and data input for the dredge plume modelling tasks, and the scenario specific model results in terms of total suspended sediment (TSS) concentrations, cumulative sedimentation rates on the seabed and light attenuation.

Table 1: Dredge depth and volume removed for each location

Location	***Dredge volume (m^3)***	***Dredge depth (m LAT)***
MOF Stage 1	340,000	-2.5
Construction Dock	300,000	-5.0
MOF stage 2	1,500,000	-7.8
TOTAL	**2,140,000**	

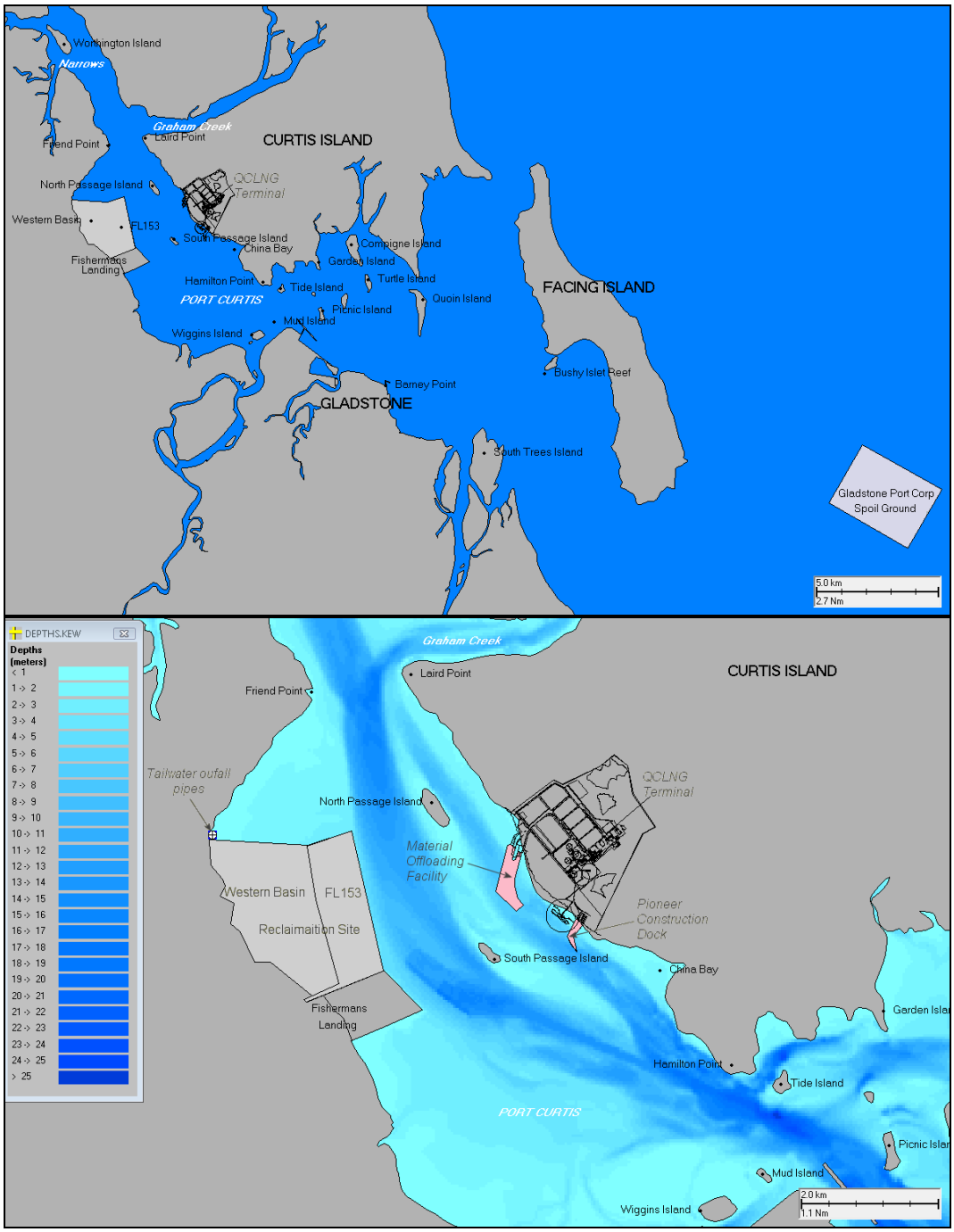

Figure 1: Top image shows the location of the QCLNG, within Port Curtis and the Gladstone Port Corporation spoil ground. Bottom image shows the dredge footprint of the material offloading facility, construction dock and the FL153 and Western Basin reclamation, relative to the existing river geometry.

2 SCOPE OF WORK

The scope of work included:

1. Integrate third party hydrodynamic and wave field data for the study area into the purpose designed, three-dimensional sediment model (DREDGEMAP);
2. Assess the cores within the MOF and construction dock to ascertain the sediment grain size classes and distribution;
3. Define the initial discharge of sediments, differential sinking and settlement of released sediments (by particle size and rates of cohesion), production rates and mass flux for each dredge operation (nine in total);
4. Simulate each dredge operation and amalgamate overlapping sources to present the cumulative effect;
5. Produce estimates for the total suspended solid (TSS) concentrations and cumulative sedimentation rates due to all overlapping operations, summarised as maps and time-series graphs at selected sensitive receptor sites; and
6. Relate predicted TSS concentrations to light attenuation, with the aim of assessing the potential change in light availability within the water-column, throughout the dredging operation.

3 STUDY DATUMS

Water depths and levels presented in this report are with respect to Lowest Astronomical Tide (LAT) unless otherwise stated and are presented in the units of meters (m).

Positions are satellite derived from the Global Positioning System using WGS 84 datum (World Geodetic System dating from 1984) and latitudes and longitudes are reported in decimal degrees.

All units are typically reported using the International System of Units (SI units).

4 CURRENT AND WAVE DATA

DREDGEMAP uses current and wave data, which varies spatially and temporally, to calculate the transport, sinking and turbulence-induced rise of the dredged material. For this project a three-month long (February to April 2009) prediction for the current field was provided at hourly time-steps by BMT-WBM from their 2-dimensional hydrodynamic model (TUFLOW), of

the existing bathymetric conditions for Port Curtis. Wave conditions were also provided by BMT-WBM from their application of a wave model (SWAN) over the area for the same period. The project team selected February to April 2009 as the period to be modelled as it captured the largest tidal ranges for the year. Figure 2 shows a snapshot of the flood and ebb tide currents within Port Curtis. For more detail regarding the current and wave modelling refer to BMT-WBM (2009).

To account for the influence of turbulence below the resolution of the current and wave data, the horizontal and vertical mixing coefficients were set to 0.5 m^2/s and 0.001 m^2/s, respectively.

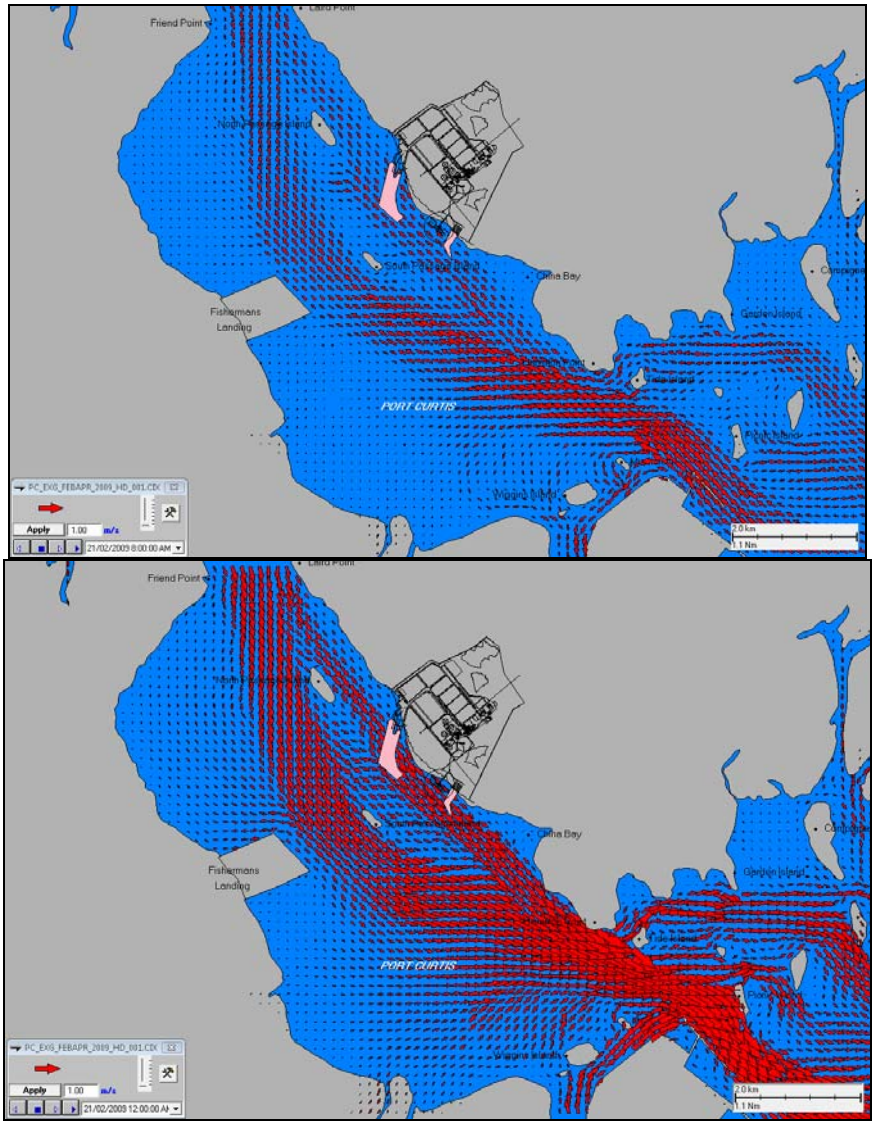

Figure 2: Snapshot of the predicted flood (top) and ebb (bottom) tide currents within Port Curtis.

5 PARTICLE SIZE DISTRIBUTION

BG had made available geotechnical analyses reports by the GeoCoastal group to identify the grain size distributions for sediment located within the MOF and adjacent to the construction dock dredge footprints. Figure 3 shows the locations of the sediment cores analysed for the dredge modelling.

The geotechnical surveys showed that the contribution of individual sediment grain size classes within the dredge areas were varied. Within the MOF, particles less than 35 μm (clay and fine silt) represented the bulk of the material, with a mean of 67 ± 18%, compared to only 23 ± 7% for sediments adjacent to the construction dock. The standard deviations for particle size classes within the MOF and construction dock ranged between 25 to 77% and 0 to 94%, respectively.

Table 2 shows the mean grain size of each sediment class representative of the MOF and construction dock.

The geotechnical survey also provided information regarding sediment density. Densities within and adjacent to the dredge areas varied across horizontal and vertical profiles ranging from 860 to 2380 kg/m^3 (dry density). Cores representative of the dredge locations and depth were characterised by a mean value of 1668 ± 204 kg/m^3. A dry bulk density of 1700 kg/m^3 was used as the model input value.

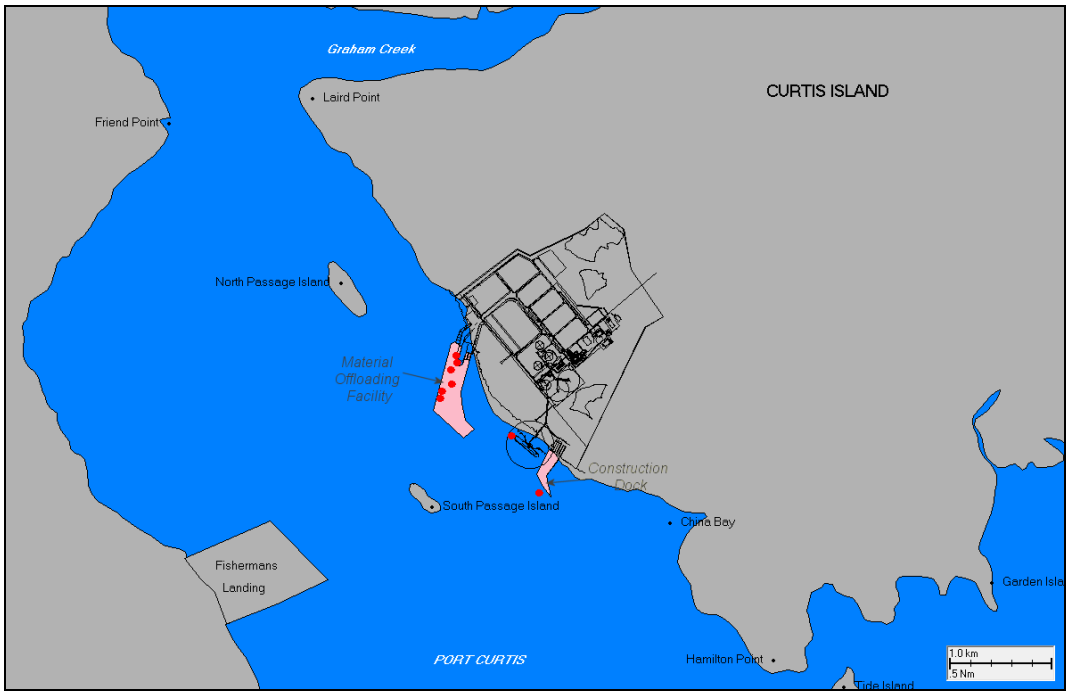

Figure 3: Location of the sediment cores analysed for the dredge modelling.

Table 2: Mean grain-size distribution representative of the material offloading facility (MOF) and construction dock.

Size range (μm)	***Mean grain size distribution for the MOF (%)***	***Mean grain size distribution for the construction dock (%)***
0-7	49	17
8-35	18	6
36-74	7	5
75-130	3	3
> 130	23	70

6 DREDGE MODEL DESCRIPTION

The fate of sediments suspended by dredging operations was simulated using a purpose-designed, three-dimensional, sedimentation process modelling system, DREDGEMAP. The model was developed by Applied Science Associates (ASA) in collaboration with the U.S. Army Corps of Engineers (USACE). This modelling system is a GIS-based application of the

model originally developed by USACE, which was developed and refined based on their experience with management of a large number of dredging and disposal operations.

DREDGEMAP computes total suspended sediment (TSS) distributions and sedimentation patterns resulting from dredging operations. The model predicts the transport, dispersion and settling of suspended sediment released to the water column using a random-walk procedure. The focus of the model is on the far-field (i.e. immediately beyond the initial release jet) processes affecting the fate of suspended sediment. The model uses specifications for the suspended sediment source strengths (i.e. mass flux), vertical distributions of sediments and sediment grain-size distributions to represent the effect of different types of mechanical or hydraulic dredges, sediment dumping practices or other sediment disturbing activities such as jetting or ploughing for trunkline burial. Multiple sediment types or fractions can be simulated simultaneously; as can discharges from moving sources.

Settling of mixtures of particles is a complex process due to interaction of the different size classes, some of which tend to be cohesive and thus clump together to form larger particles that have different fall rates than would be expected from their individual sizes. Enhanced settlement rates due to flocculation and scavenging are particularly important for clay and fine-silt sized particles (Teeter 1998, Swanson *et al*., 2004) and these processes have been implemented in DREDGEMAP. The model employs five material classes based on sediment grain sizes. The classes are biased towards the finer materials, as these are typically the most dispersive and are responsible for the greatest turbidity increases in the water column. Table 3 gives a summary of the size ranges and minimum sinking rates for each of the particle classes employed in DREDGEMAP.

The model represents the total mass of sediments suspended over time by a defined sub-sample of Lagrangian particles, allocating an equal proportion of the mass to each particle (e.g. 1/1000th of the total release if 1000 particles are used). The initial size distribution of the sediments is used to apportion the sample of Lagrangian particles to size classes.

Horizontal transport, sinking and turbulence-induced rise of each particle is modelled independently at each time step. Minimum sinking rates are calculated using Stokes equations, based on the size and density of the particle. However, sinking rates of finer classes (representing clay and silt-sized particles) are increased based on the local concentration of the same and larger particles, to account for clumping and entrainment. Deposition (i.e. the process whereby particles move from being in suspension to being settled on the bed) is calculated as a probability function of the prevailing bottom stress, local sediment concentration and size class. This formulation accounts for inhibition of deposition

where shear stress at the bed is excessive. Matter that is deposited may be subsequently resuspended into the lower water column if critical levels of bottom stress are subsequently exceeded. Mixing of resuspended sediment into higher levels of the water column will be a dynamic balance between estimates of the sinking rate and vertical mixing induced by turbulence (as specified by vertical mixing coefficients).

The model employs two different resuspension algorithms. The first applies to material deposited in the last tidal cycle (Lin *et al*., 2003). This accounts for the fact that newly deposited material will not have had time to consolidate and will be resuspended with less effort (lower shear force) than consolidated bottom material. The second algorithm is the established Van Rijn method (Van Rijn, 1989) and applies to all other material that has been deposited prior to the start of the last tidal cycle. This method calculates a constantly varying critical threshold for resuspension, based on the median (d_{50}) local particle-size distribution for settled material. In this way, the model accounts for interactions between different particle sizes. For example, finer sediments will tend to be armoured from resuspension in the presence of coarser material." Swanson *et al*. (2007) has previously summarised the justification and use for this approach. Particles initially released by operations are continuously tracked for the length of the simulation, whether suspended or deposited.

To avoid edge effects, transport is estimated in a grid-less space with the vertical and horizontal position in space recorded for each particle at the end of each time step. At the conclusion of the transport and settlement simulation phase, suspended solid concentrations (as mass per volume) and sedimentation values (as mass per area of seabed and thickness) are calculated for each time-step based on the local density of particles. Because each of the Lagrangian particles represents a larger mass of material, with each particle representing the central loci of a concentration of sediment, a Gaussian distribution is applied to the particle densities to represent the distribution of sediment mass around each of the particles for each sediment class.

To maximize resolution of the plume, contours are calculated for a uniform, user-defined, grid resolution that is independent of the resolution of the current and wave data used to calculate transport, thus supporting finer spatial differentiation of plume concentrations and avoiding underestimation of concentrations caused by spatial averaging over larger volumes/areas. Model outputs consist of water-column concentrations in both horizontal and vertical planes, time-series plots of suspended sediment concentrations, and thickness contours of sediment deposited on the sea floor.

Table 3: Grain-size classes and minimum sinking rates applied by DREDGEMAP.*

Sediment grain size class	Size range (μm)	Minimum sinking rate (m/s)
1	0-7	0.0008
2	8-35	0.0023
3	36-74	0.0038
4	75-130	0.0106
5	> 130	0.10

*Note * sinking rates are varied from these minima, based on local concentrations of sediment particles*

7 DREDGE MODELLING SCENARIOS

Two alternative dredge and disposal options (or Scenarios) are being considered for the dredging of the MOF stage 1 and construction dock, as it is unknown whether the Fisherman's Landing reclamation site will be available:

- Scenario 1 – Removal of material using a cutter suction dredge (CSD) dredge with a similar production to the 'Wombat', being 500 m^3/hr, with spoil pumped to the reclamation site via a floating or submerged hydraulic pipeline. Excess water (tail-water) will be returned to the marine environment from the north-west corner of the Western Basin reclamation site, via a series of outflow pipes (see Figure 1); or
- Scenario 2 - One Backhoe Dredge (BHD) will be used to remove material within the MOF and a second BHD within the construction dock. Each BHD will deposit the sediment directly into 3 supporting (six in total) Split Hull Barges (SHB), which will relocate it to the existing Gladstone Port Corporation (GPC) spoil ground.

For the MOF stage 2 operation only one dredge and disposal option is proposed:

- Scenario 3 - A large CSD (~ 1,500 m^3/hr) to remove the sediment and pump the spoil to the reclamation site via a floating or submerged pipeline. The tail-water will be returned into the marine environment through a series of overflow pipes.

It is likely the CSD and BHD would operate 24 hours a day, 7 days per week, with the exception of scheduled maintenances and unexpected breakdowns. To account for the downtime, an efficiency of 65% for the CSD and 53% for the BHD was factored into the

production rates to calculate the overall dredge duration for each scenario and location (see Table 4).

Table 4: Summary of dredge operations and durations for each scenario.

Scenario	Location	Dredge operation	Duration (days)
1	MOF Stage 1 and Construction Dock	CSD and land reclamation	MOF: 28.3 Construction dock: 25.0
2	MOF Stage 1 and Construction Dock	BHD and SHB	MOF: 91 Construction dock: 83.3
3	MOF stage 2	CSD and land reclamation	MOF: 64

8 SPECIFICATIONS AND ASSUMPTIONS FOR SEDIMENT MODELLING

To accurately represent the dredging operations in DREDGEMAP, the preliminary task involved an assessment of the likely sources of sediment for each scenario.

For Scenarios 1 and 3 there were two sources of suspended sediment identified:

1. Direct suspension of material by the cutter head rotation during dredging; and
2. Material suspended in the tail-water flowing out of the settling pond.

For Scenario 2 there were three sources of suspended sediment plumes identified:

1. Loss of sediment from the BHD bucket from grabbing and lifting sediment through the water column,
2. Suspension of seabed material due to the SHB propellers over shallow waters, and
3. Disposal of relocated sediment from Port Curtis into the existing GPC spoil ground.

Dewatering of the SHB was not modelled, as the BHDs typically produce high solids content and little release of sediment-laden water (QGC EIS Volume 6 Chapter 1).

The mass flux, size composition and initial vertical-distribution of sediments in the water column can be expected to vary considerably with each sediment source. The following section outlines how they were each defined in the model and the assumptions made to supplement the information provided by the proponent.

8.1 Cutter Suction Dredging

The cutter-head produces mixed size-fractions ranging from particles < 75 μm to small rock fragments. While the coarse material will settle rapidly, the finer material is suspended by the rebounded energy of the jet striking the seabed. The assumed size composition of material suspended as overflow during the operation is presented in Table 5. Within the MOF, sediment particles < 35 μm dominate the distribution (~ 67%). In contrast, only 23% contributes to the finer sediment within the construction dock and a high proportion (70%) is coarse material (> 130 μm).

Table 5: Grain size distribution (by percentage) of sediments suspended by the cutter suction dredge head.

Sediment grain size class	***Size Range (μm)***	***Grain size distribution (by %) within the MOF***	***Grain size distribution (by %) within the construction dock***
1	0-7	49	17
2	8-35	18	6
3	36-74	7	5
4	75-130	3	3
5	> 130	23	70

Vertical distributions of material from the CSD operations have been estimated from observations using an Acoustic Doppler Current Profiler (ADCP) for an operation in similar water depths by Swanson et al, (2004). Material was observed to concentrate in the lower water column, with only small concentrations reaching the surface (Figure 4).

BMT-WBM undertook a monitoring program of sediment plumes produced by the Wombat while operating near Fisherman's Landing on the 29th and 30th June 2009. During the monitoring an ADCP was mounted onto the vessel to measure current velocities and backscatter due to suspended sediments. Water samples were also collected at specific locations within the beam to calibrate the TSS/backscatter correlations. This analysis yielded estimates of the distribution of suspended sediments, by depth and distance from the centre of the plume.

The Wombat plume measurements re-affirmed the above assumption, that the sediment plumes generated are concentrated in the lower water column, as clearly seen in Figure 5 showing a cross-section of the measured TSS at one period during the 30th June 2009.

Based on these two independent observations, the vertical distribution described in Table 6 was applied to the CSD simulations in Scenarios 1 and 3.

The measured median sediment flux generated by the Wombat over 2 days was approximately 2.2 kg/s. This equated to approximately 1% of the production, which is in line with previously reported values for this type of equipment (US Army Corps of Engineers, 2008). On this basis, a 1% loss rate was applied within the model to define the sediment flux from CSD operations.

Dredging locations and the local volume to be dredged were based on maps of the areas to be dredged, as supplied by BG (see Figure 1). For Scenario 1, the area was split into 60 m sections, approximating the expected arc width of the proposed CSD. For Scenario 3, the area was split into 180 m sections, as a CSD with a much wider arc is proposed here. For each of these sections, the average depth was determined as the difference between the existing depth and the design depth. The volume to be dredged from each section was yielded by the product of the area and depth of the section. The production rate was calculated from the volume and estimated duration for each section. This approach accounts for greater discharges (for longer durations) in areas that require greater volumes to be dredged.

The path and volume information for each dredge section were combined into a time-series of changing input for the model. Dredging has been modelled as a continuous operation, without breaks for downtime, as it is not possible to predict the timing of downtimes, however, an allowance for downtime was accounted for in the production rate (refer to Section 7).

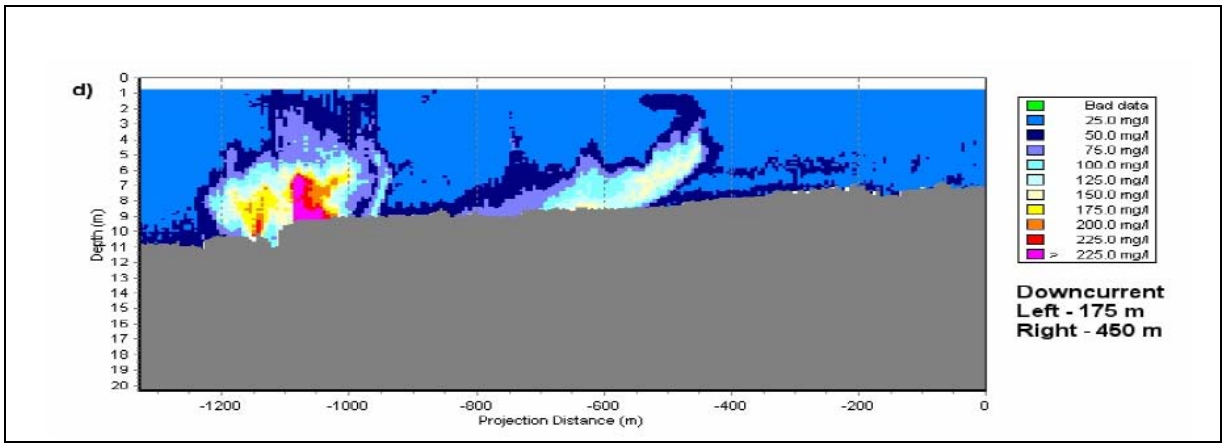

Figure 4: Example cross-section showing sediment concentrations measured by Acoustic Doppler Profiler of plumes generated by discharge of a cutter suction dredge through a hydraulic trunkline (reprinted from Swanson et al., 2004).

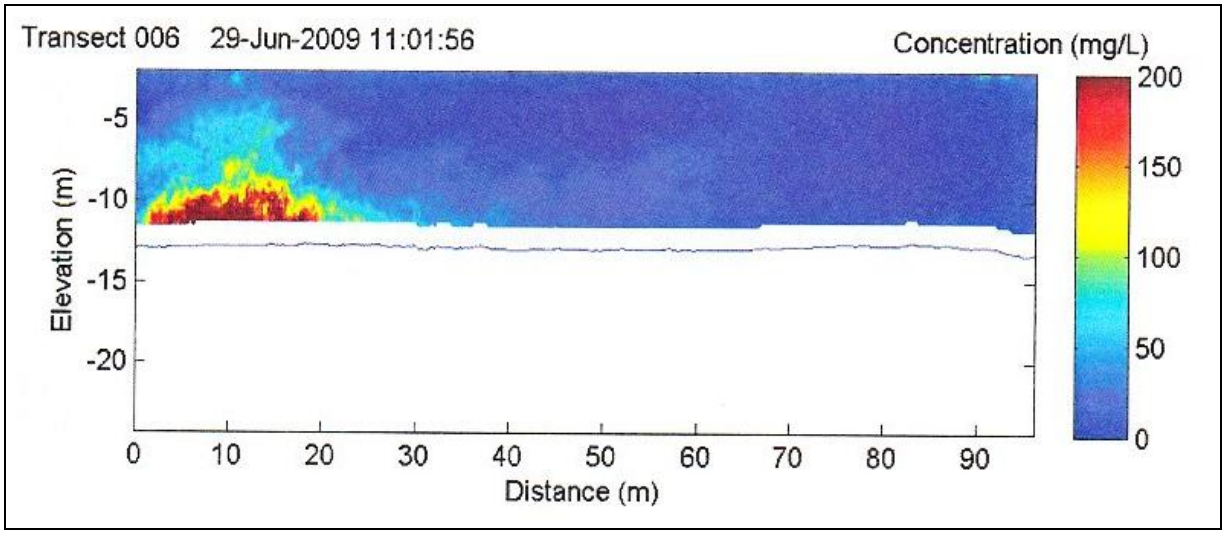

Figure 5: Cross-section of the sediment plume concentrations generated by the Wombat CSD when dredging adjacent to Fisherman's Landing on 30th June 2009 (reprinted from BMT-WBM 2009).

Table 6: Initial vertical distribution of sediments in the water column set up by loss from the cutter head.

Elevation above seabed (m)	***% of sediments***
2	5
1.6	10
1.2	15
0.8	30
0.4	40

8.2 Settling Pond Tail-Water

As described in Section 7, the spoil dredged by the CSD's will be pumped to the reclamation site via a floating or submerged hydraulic pipeline. The dredged material pumped to the settling pond, will consist of mixed size-fractions ranging from clays to rock fragments. Generally, coarse material will settle rapidly, while the fine material will remain in suspension within the tail-water and return to the marine environment, via a series of outflow pipes. As such, in Scenarios 1 and 3, the size composition of the suspended material was assumed to be characterised by 50% of sediment particles < 8 μm and 50% sediment particles between 8-35 μm.

Based on the expected output from the CSDs, BG dredging specialists estimated a flow rate at the outfall of 6,000 m^3/hr. As a conservative measure, the concentration of sediments in the tail water was set based on a maximum allowable turbidity value of 40 NTU, as specified under the Development Approvals for previous operations in the area, including the RG Tanna Coal Terminal Berth 4 and Fisherman's Landing Berth 1 dredging projects (GHD, 2009). As DREDGMAP computes suspended solids, the turbidity value of 40 NTU was converted to TSS (112 mg/L), using a relationship developed from field measurements by BMT-WBM. .

The tail-water sediment discharge was assumed to be flowing continuously out of the settling ponds for the duration of the dredge operations.

Table 7: Summary of the tail-water discharge characteristics.

Parameter	***Value***
Discharge rate (m^3/hr)	6,000 (continuous)
Sediment size (μm) distribution (%)	0-7 (50) and 8-35 (50)
Turbidity (NTU)	40
TSS equivalent (mg/L)	112

8.3 Backhoe Dredging

The BHD will use a large excavator arm fitted with an open bucket and will be mounted upon a barge. The excavator will lift material in the bucket and deliver it to a waiting hopper barge for transport to the disposal site. Past observations have shown that material is suspended

from the seabed due to the initial grab. Further suspension is generated as sediment overflows from the bucket as the bucket is lifted throughout the water column. Overflow also occurs as the bucket breaks free of the water surface and drains freely. Only sediment < 130 µm are considered "lost" (i.e. suspended into the water column), because the coarser material removed from the bucket while being lifted to the surface would fall immediately to the bottom where it would be re-dredged during subsequent grabs. As such, the distribution of material suspended by the overflow was assumed to be evenly spread between the smaller grain sizes (Table 8).

Table 9 shows the assumed vertical distribution of the material during the BHD operations. The distributions are higher at the seabed and water surface, to represent the larger loss rate of material during the initial grab and as the bucket breaks free of the water column.

Loss rates from similar operations are known to vary based on such factors as the size and type of bucket (i.e. open or closed), nature of the bed material, presence of debris, current speed and depth of water, as well as the care of the operator (Hays & Wu 2001, Anchor Environmental 2003). Reported rates compared by Anchor Environmental (2003) varied between 0.1% to 10%, with a mean of 2.1%. In the absence of measurements for the specific situation and equipment, this mean (2.1% of production rate) was assumed for all BHD operations.

Table 8: Assumed grain size distributions (by percentage) for material lost during the BHD operations.

Sediment grain size class	***Size Range (μm)***	***Grain size distribution (by %) within the MOF and***	***Grain size distribution (by %) within the construction dock***
1	0-7	25	25
2	8-35	25	25
3	36-74	25	25
4	75-130	25	25
5	> 130	0	0

Table 9: Assumptions for the initial vertical distribution of sediments in the water column set up by loss from the backhoe dredge.

Elevation above seabed (m)	***% of sediments***
2	23
1.6	16
1.2	14
0.8	19
0.4	28

8.4 Hydraulic Suspension Due to Propeller Wash

SHB are expected to transport material dredged by the BHD to the GPC spoil ground. Due to the transit time to and from the spoil ground, 3 SHB have been assumed to support each BHD. This will allow for one SHB to be either present at the dredge site, in transit, or at the spoil ground.

The SHB vessels will be propeller-driven, and because they will be operating in shallow waters, their propeller thrust would be expected to dislodge material from the seabed into the water column. The rate of the suspension would be dependant on a number of factors including engine size the number and dimensions of the propellers (hence thrust generated) the under keel clearance above the bed and the sediment type (Blaauw and van de Kaa, 1978).

The velocities produced by the wake of a propellers used during the dredge operations were computed using a methodology developed by Blaauw and van de Kaa (1978). The assumed characteristics for a SHB with an estimated capacity of 1,000 m^3 were:

- Propeller power = 800 kW
- Propeller Diameter = 1 m
- Vessel Draught = 5.0 m
- Vessel Speed = 6 knots

A calculated velocity contour for the flow velocities behind the propeller wash is plotted in Figure 6. Note that velocity fields > 2 m/s would intersect the bed at an under keel clearance of 3 m or less, in this example, and that the velocity at the bed would increase with decreasing under keel clearance. These velocity estimates were used to calculate varying shear at the bed based on the assumed vessel draft (5 m) and the local bathymetry (represented by bathymetric contours along the expected path of the SHB). Shear estimates, in turn were used to estimate erosion rates for the surface sediments, hence the flux and resulting suspended sediment concentrations varied from location to location. The initial vertical distribution of the sediments was also guided by the velocity field, with particles assumed to be mixed to approximately 2 m, with a weighting towards the upper height ( ). The particle size distribution of the bed (as determined by core samples) was assumed to represent the initial PSD of the sediment suspended by the propellers.

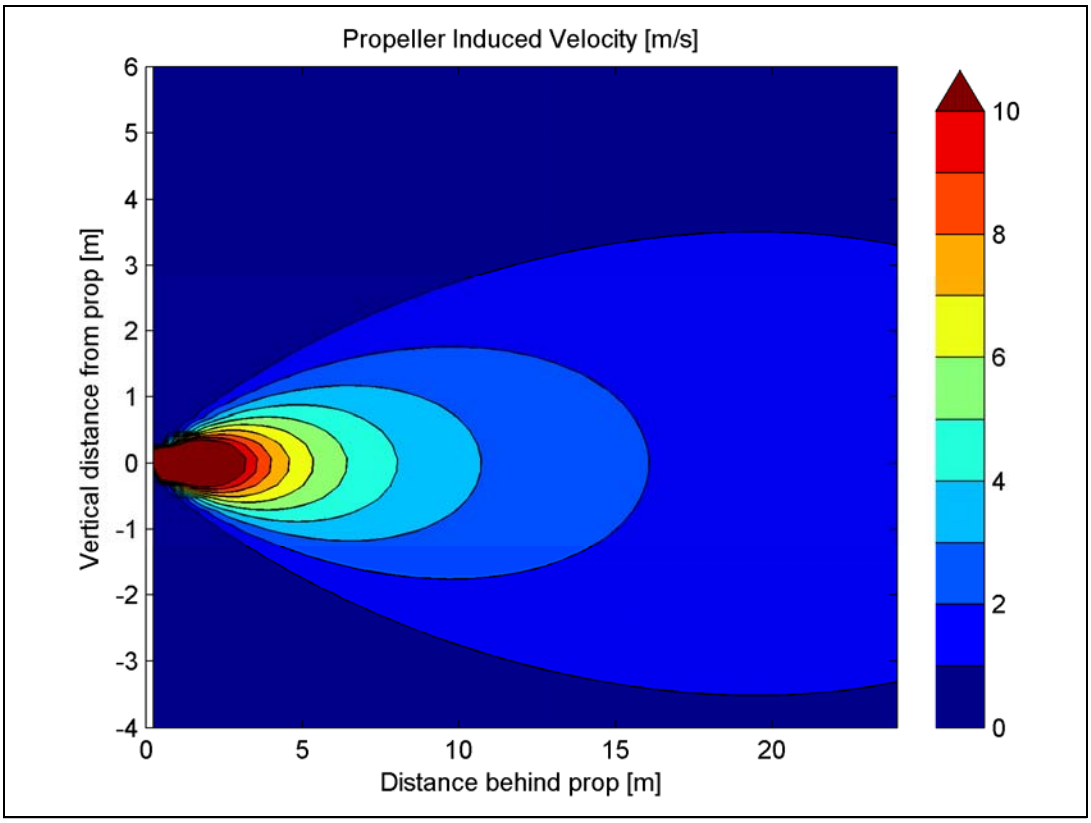

Figure 6: Computed velocity contour plot for flow behind a propeller jet. Velocity units are m/s.

Table 10: Assumed grain size distribution (by percentage) of sediments suspended by propeller wash.

Sediment grain size class	***Size Range (μm)***	***Grain size distribution (by %)***
1	0-7	20.8
2	8-35	5
3	36-74	4
4	75-130	6.9
5	> 130	63.3

Table 11: Assumptions for the initial vertical distribution of sediments in the water column set up by propeller wash.

Dumping	
Depth Above Seabed (m)	**% of Sediments**
1.97	5
1.96	20
1.94	50
1.27	20
0.015	5

8.5 Relocation of Sediment into the Existing GPC Spoil Ground

Once the supporting SHB is full it will steam to the GPC spoil ground to dispose of the sediment filled by the BHD. Once over the spoil ground the hopper will open to release the sediments from the bottom of the hull, at a depth of approximately 5 m below sea level. Previous observations of sediment dumping from hopper vessels (e.g. Swanson *et al.,* 2004) have shown that there is an initial rapid descent of solids, with the heavy particles tending to entrain lighter particles, followed by a billowing of lighter components back into the water column after contact with the seabed (Figure 7). A proportion of the lighter components will also remain suspended and may be trapped by density layers, if present.

Because simulations in this study focussed on the far-field fate of sediment particles due to transport and sinking after the initial dump phase, simulations were run with the initial vertical distribution specified to represent the post-collision phase for a case where a high proportion of the sediments are resuspended after collision with the seabed. This is summarised in Table 12.

The disposal of the spoil was assumed to take place over a 10-minute period, along 100m transects within the centre of the spoil ground.

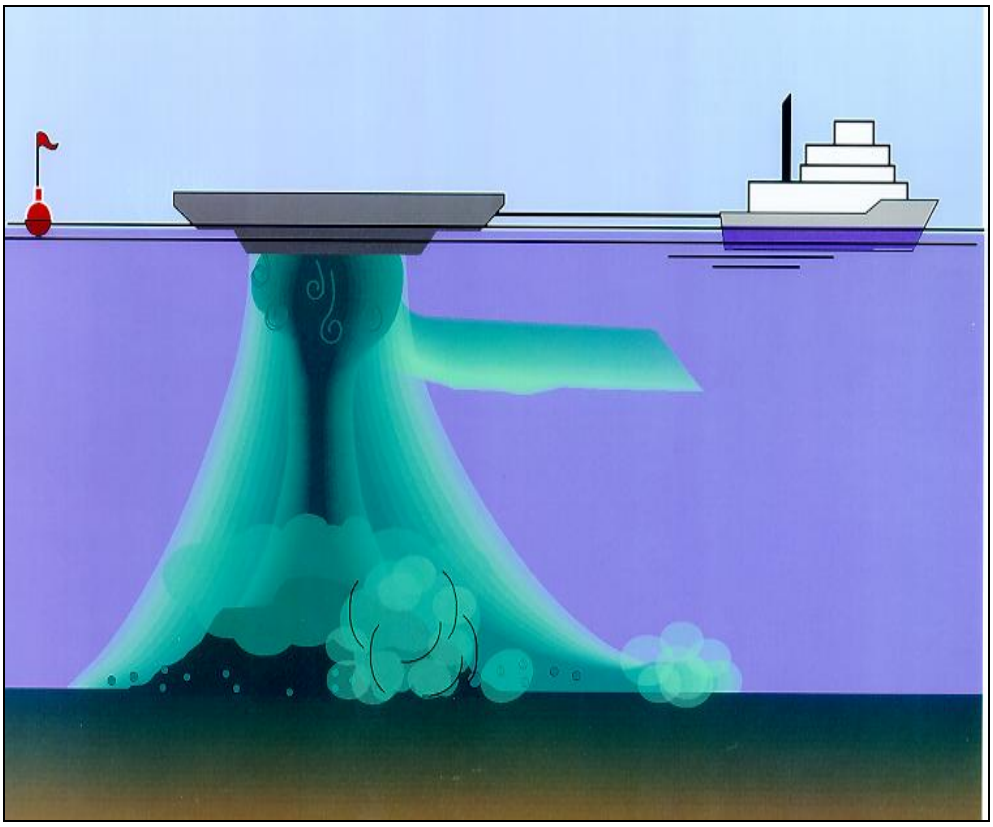

Figure 7: Conceptual diagram showing the general behaviour of sediments dumped from a hopper barge and the vertical distribution of material set up by entrainment and billowing (Source: ASA 2004)

Table 12: Initial vertical distribution of sediments in the water column set up by loss from the backhoe dredge.

Dumping	
Depth Above Seabed (m)	**% of Sediments**
12	2
9.6	2
7.2	2
4.8	2
2.4	92

8.6 Background TSS Concentration

Given that the model only reports the TSS concentrations from material generated by dredging operations, it was necessary to include the background concentrations to the model results to understand the collective effect.

Because the turbidity due to suspended solids within Port Curtis is highly variable, BMT-WBM selected to use satellite-derived data collected between February and April during the years 2007-2009 to determine the likely background concentrations. A number of quality control measures were employed during the analysis, including a comparison between recently composed satellite data (November 2009) with water samples measured by Vision Environment (VE) at the same time as the satellite passed over. Spatial estimates of average background TSS were subsequently provided to APASA for use in the data analysis as a 250 m by 250 m gridded dataset covering Port Curtis.

Because the satellite derived data proved to be highly variable, most likely due to interference with the sensors, APASA carried out some additional manipulation and smoothing:

a) Areas around the edges with values < 5 mg/L were removed as this was assumed to be affected by water level variation (hence a false signal over time);

b) Isolated spikes, which were above 60 mg/L (only 34 points out of 32,000) were removed and set to 60 mg/L on the basis that the estimates were likely to be erroneous;

c) Areas with no background data (mainly within the Narrows) were set to the average TSS value of the entire dataset (~ 20 mg/L);

d) The edited data was interpolated onto a grid the same size as the model results to allow direct addition of background and above background estimates on a common grid, which was set to 40 x 40 m; and

e) Finally, linear smoothing was conducted of the gridded background data to reduce noise in the data assumed to be due to erroneous measurements

Figure 8 shows the interpreted average background TSS concentrations used as part of the modelling assessment. Higher average turbidity levels (25 – 50 mg/L) were generally represented along the main channels.

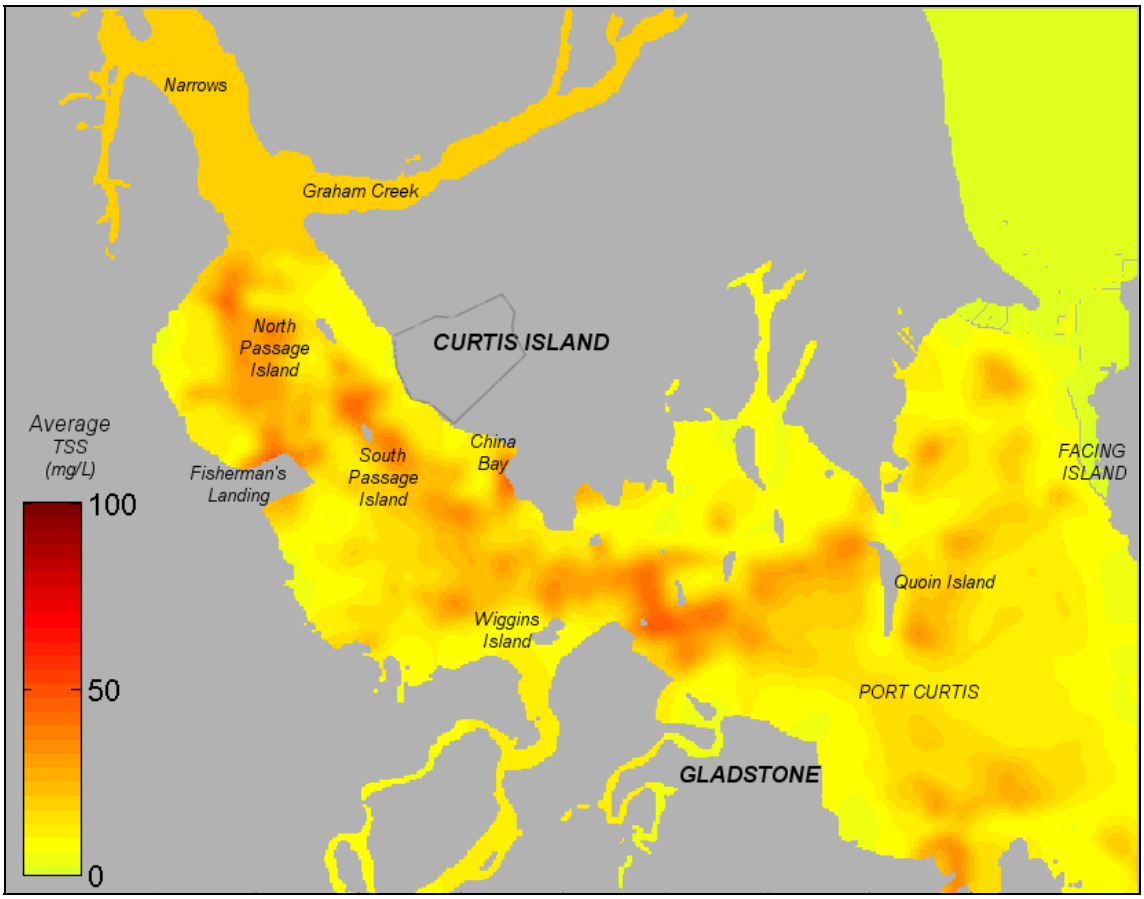

Figure 8: Map showing the average total suspended solids concentrations interpreted from satellite derived data from February to April 2007 – 2009.

8.7 Distribution of Seagrasses

Department of Primary Industries and Fisheries (DPI) is currently remapping the spatial distribution of seagrass meadows and species assemblages within Port Curtis. However, as this information was not available at the time of this study, the DPI survey from November 2002 was used as an indicator of seagrass meadow locations (see Figure 9).

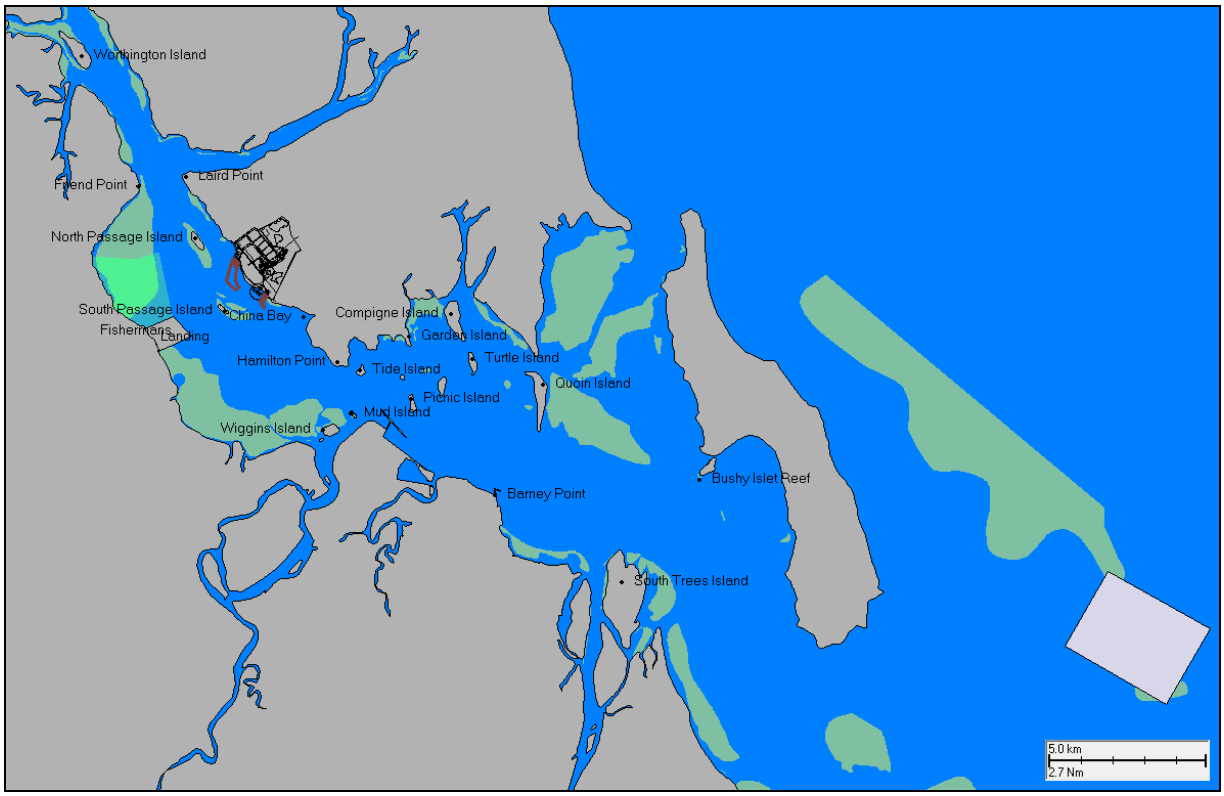

Figure 9: Location of seagrass meadows (pale green shading) within the port limits of Port Curtis, during November-December 2002 (source: DPI).

8.8 Analysis of Model Results for TSS and Sedimentation

Each of the three dredge scenarios were comprised of multiple independently modelled dredge operations. To gain an understanding of the overlapping sediment sources and in turn cumulative effects, the individual model outputs were amalgamated for each scenario.

The model results are presented in a number of forms to highlight the spatial and temporal patterns of effect that were predicted:

- Images of the model predicted TSS and sedimentation patterns due to the individual sediment sources;
- Time-series graphs of maximum predicted TSS concentrations as a function of time for known sensitive receptor habitats (Figure 10);
- Depth averaged median (i.e. the 50th percentile value), 80th and 95th percentile TSS contours calculated at hourly intervals for each depth layer and location (represented as 0.5 m depth layers within each 40 m x 40 m grid cell within the model domain). The median values indicate a more typical result, while the 80th and 95th percentiles reveal increasingly extreme upper values over time.

- Median and 95th percentile sedimentation rate contours were calculated from hourly predicted changes in sediment thickness at each location (represented by 40 m x 40 m grid cell within the model domain). These plots provide a summary for each location to identify locations that may be at higher risk from sedimentation.

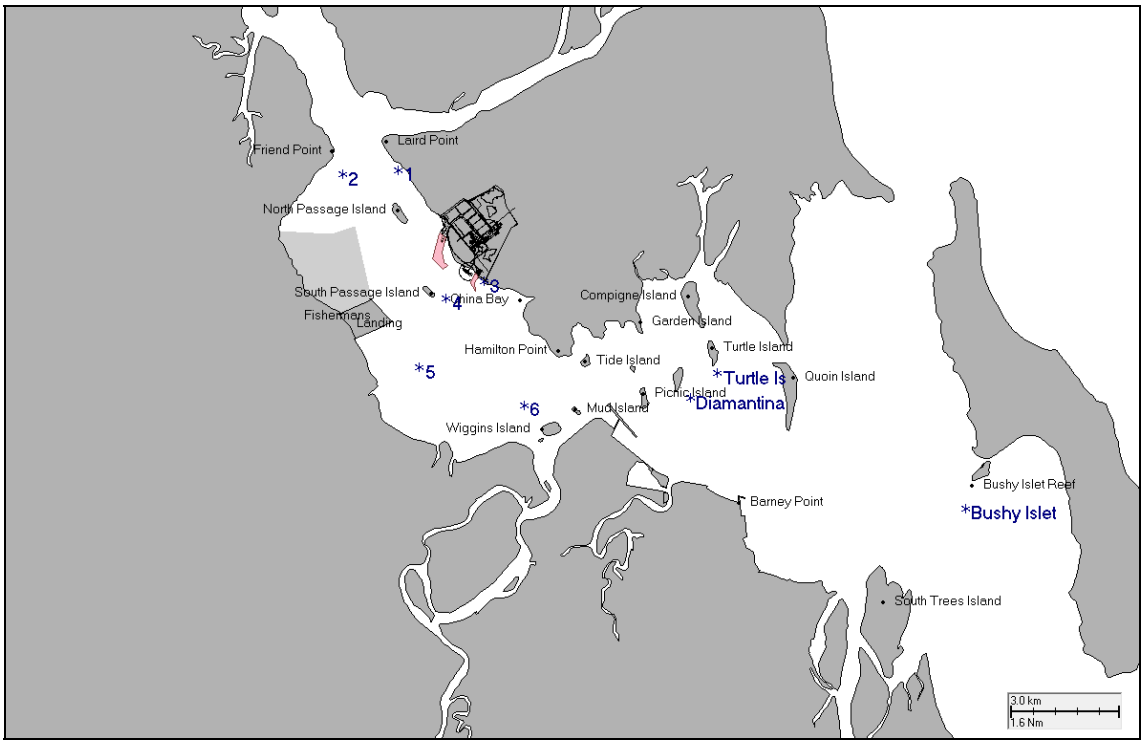

Figure 10: Location of time-series output sites.

8.9 Change in Available Light to Seagrasses

Because an increase in the levels of turbidity can reduce the availability of light and, in turn, the productivity of seagrasses, a key objective of this study was to relate the predicted TSS concentrations to the difference in the amount of light, pre and post-dredging for the three dredging scenarios.

This involved the following 10 step process:

Step 1) Add calculations for the average background TSS (Section 8.6) to modelled calculations of TSS due to dredging operations to derive spatial and temporal estimates of the combined TSS concentrations.

Step 2) Derive relationship of TSS to light attenuation coefficients (k_d), This relationship was estimated by BMT-WBM as a step-wise process:

a) Review Port Curtis field measurements provided by Vision Environment to derive the locally-specific relationship between turbidity and K_d;
b) Convert the local turbidity-k_d association to a local TSS concentration – K_d relationship;

Based on the above analysis, the recommended site specific relationships for deriving k_d from TSS concentrations are:

For TSS: 0 to 5 mg/L $K_d = 0.0774(TSS) + 0.5175$

For TSS: > 5 mg/L $K_d = 0.0395(TSS) + 0.7064$

Step 3) Determine the level of light at the water surface (I_o) using six-hourly solar radiation data for Gladstone, derived from a global atmospheric model.

Step 4) Calculate the amount of light reaching the seabed (I_z) over the model domain, using the following equation;

$$\frac{I_o}{I_z} = \exp^{-z.k_d}$$

where: I_o and I_z are the amounts of light at the surface and depth z, respectively and k_d is the light attenuation coefficient.

Step 5) Divide I_o by I_z to calculate the *fraction* of surface irradiance measured at depth *z*.
These calculations were adjusted to account for

a) Periods of exposure to day light hours only (by removing all time steps during hours of darkness)
b) Periods when a given section of seagrass bed was exposed above sea level (by removing all time steps for sections when the local water depth was reduced to 1m LAT)

Step 6) Calculate the 50th (or median), 80th and 95th percentile light levels received at the seabed separately for the background case and for the background plus dredging case.

Step 7) Compare the calculated time-series of I_z for each cell between the background case and the background plus dredging case, to determine the change in amount of light expected for each cell (40 m by 40 m).

Step 10) Generate 50th and 95th percentile plots of the difference in light (%) reaching the seabed, as a result of the dredging operation. Plots showed contours surrounding areas where the light levels would be reduced by 5, 10, 15, 30, 40 and 50%.

9 MODEL RESULTS

9.1 General Observations

9.1.1 Cutter Suction Dredging

Since the CSD cutter head will suspended material near the seabed, modelling predicted significantly higher suspended sediment concentrations at the bottom (~ 100 mg/L above ambient for Scenario 3) and reducing concentrations toward the water surface (~ 10 mg/L). Horizontally, the plumes were concentrated around the MOF and construction dock, with concentrations decreasing exponentially as a function of distance and current strength from these areas of operation. As an illustration of this outcome, Figure 11 is a snapshot showing predicted TSS concentrations generated by the cutter head while dredging within the MOF footprint (Stage 2), under a sample ebb and flood peak current. The plan view shows the highest concentration at any vertical level within each 40 m x 40 m cell. The cross-section shows the vertical distribution along the plume axis, as indicated by the dotted line. These results are shown as additions to the background TSS concentrations.

During the out-going tide the sediment plume is advected south-east from the dredge operation toward Tide Island (refer to Figure 12), which is approximately 5.5 km south-east from the MOF dredge footprint. At this stage the TSS concentrations are reduced to 15 – 30 mg/L above background. At the turn of the tide, the plume is pushed back up the main channel towards the mouth of Graham Creek and the Narrows (see Figure 13) at lower concentrations (~ 5 mg/L above ambient).

At times in the simulation, isolated patches of plumes reach concentrations expected to be visibly above background (5 mg/L). This results when sediment plumes collide with land masses (i.e. South Passage Island) and form break-away plumes, and/or sediment is resuspended. Resuspension of the fine (< 130 µm) dredged sediment was a common occurrence due to the strong currents (up to 2 m/s) scouring the seabed within the vicinity of the operational site.

The bottom thickness was predicted to increase over time adjacent to the cutter head, mainly due to the settlement of coarser sediment. In contrast, finer sediment is predicted to advect in the general direction of the prevailing currents when the tide is flowing. The duration of the slack tides was also indicated to be long enough for some of the finer sediments to momentarily settle, with a higher proportion settling during the slacks over the neap tides. As the current speeds increased, the finer sediments in the main channels were predicted to

resuspend. However, locations where current speeds were relatively low, resulted in a local build up of sediments.

With the on-going re-suspension of dredged sediments, the distribution of deposits was predicted to be ever-evolving and more wide-spread as the dredging operation continues. Figure 14 and Figure 15 highlight the change in the thickness and distribution of deposits as hourly time-series plots, during a sample flood and ebb tide.

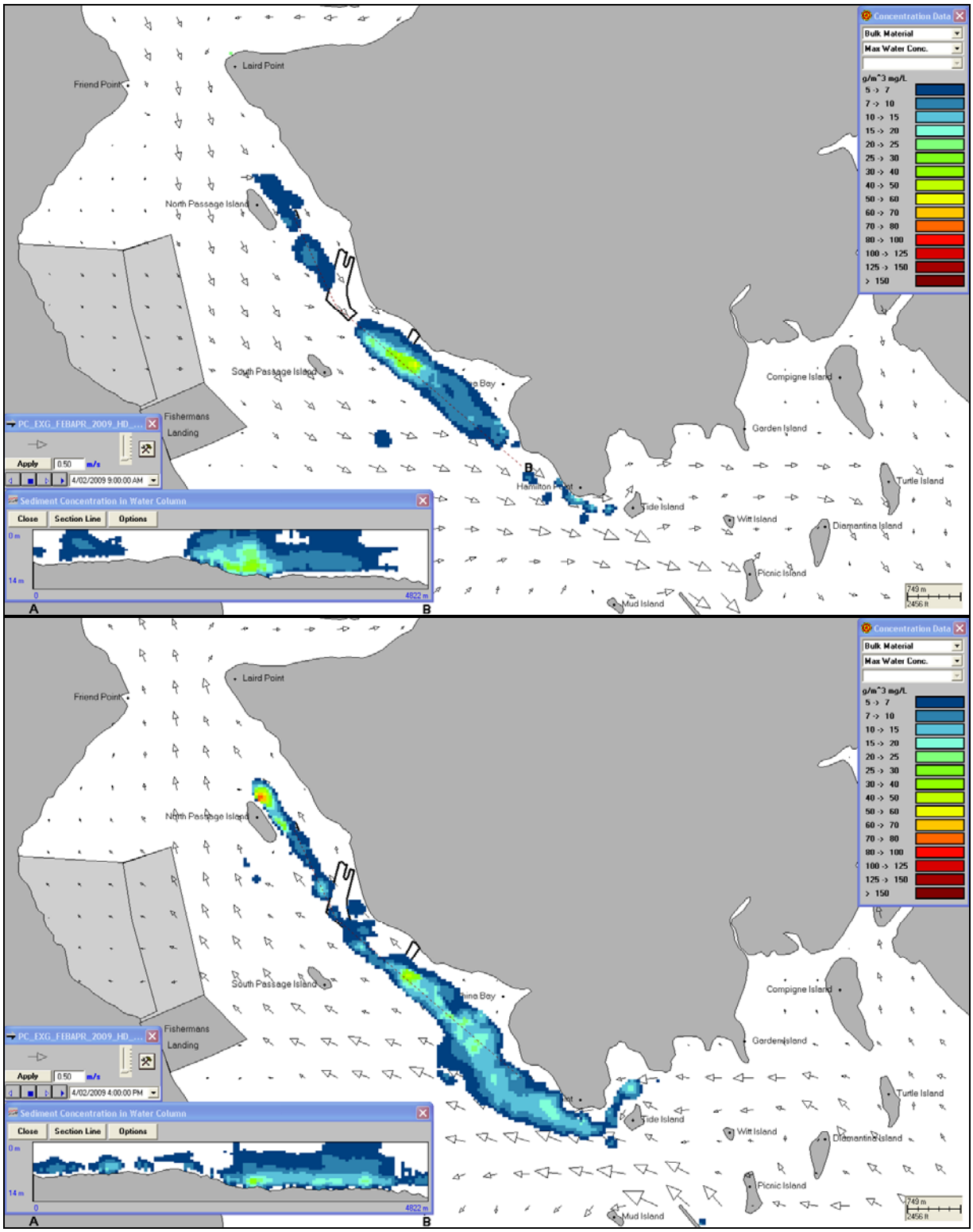

Figure 11: Snapshot of the maximum predicted suspended sediment concentration plume (above background) generated from loss at the cutter head while dredging within the MOF (stage 2) during a sample February 2009, ebb (top) and flood (bottom) peak current.

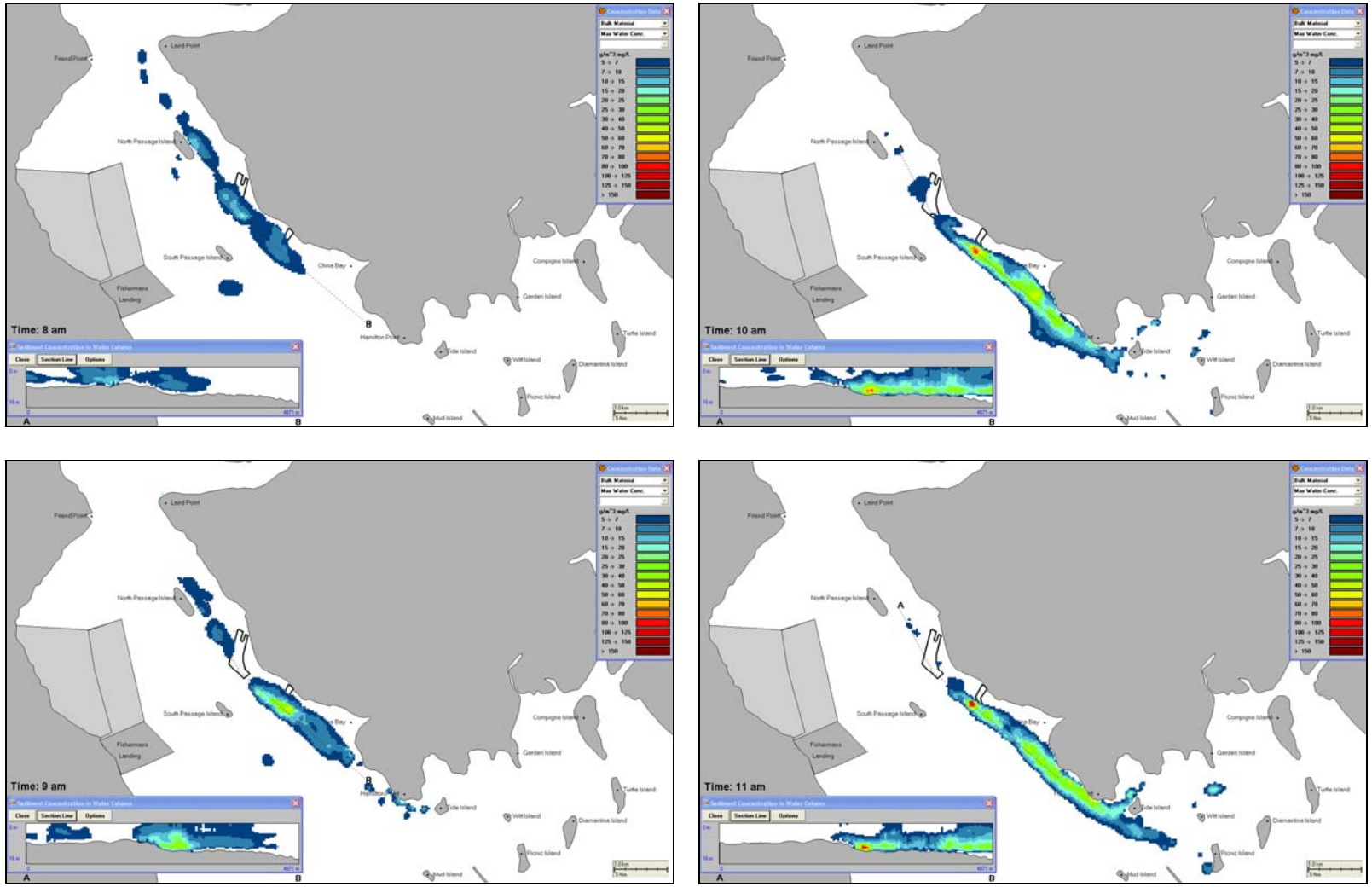

Figure 12: Hourly time-series plots (8 am, 9 am, 10 am and 11 am 4th February 2009) of maximum TSS plumes (mg/L) generated from loss at the cutter head while dredging within the MOF (stage 2).

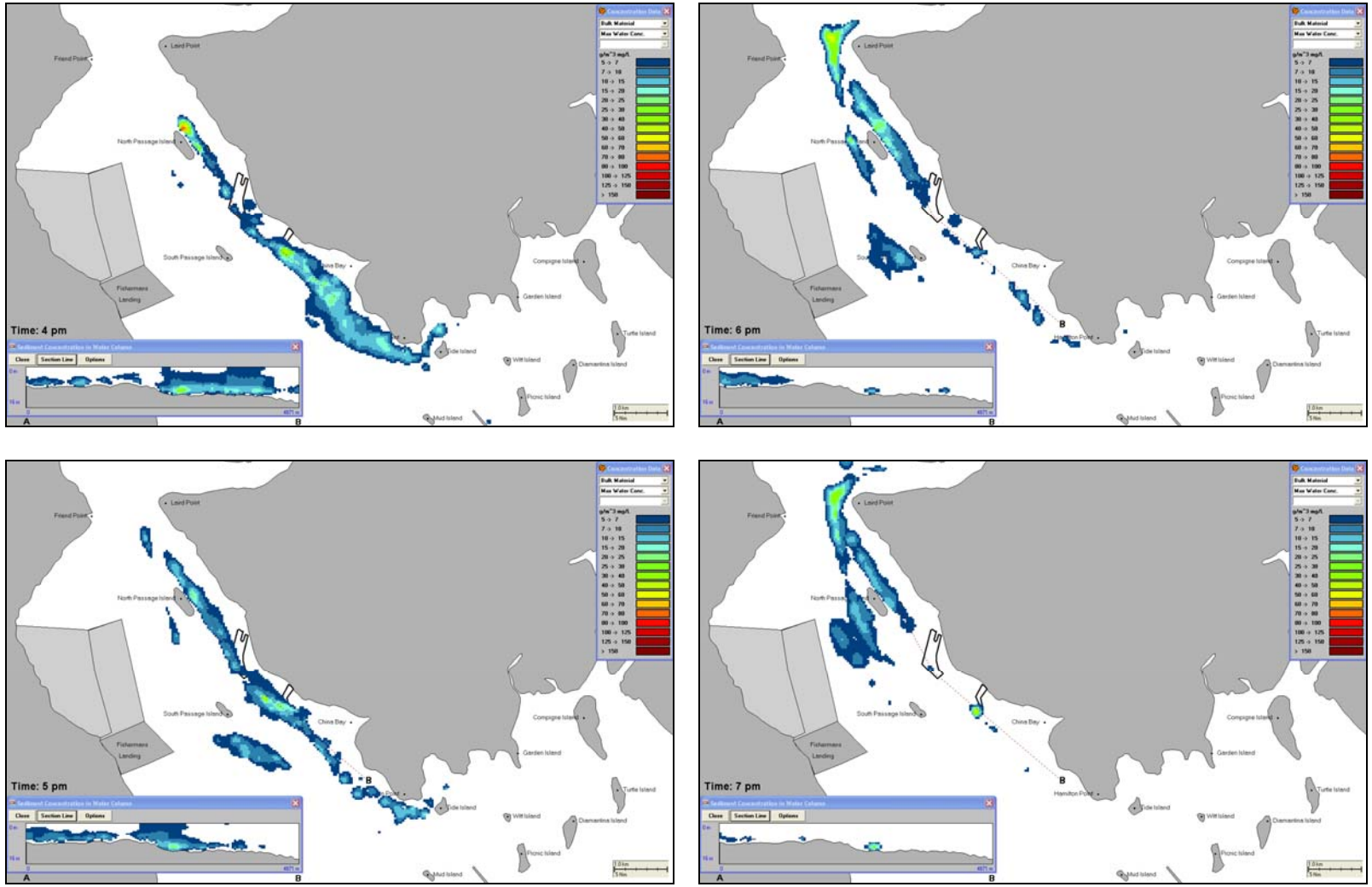

Figure 13: Hourly time-series plots (4 pm, 5 pm, 6 pm and 7 pm 4th February 2009) of maximum TSS plumes (mg/L) generated from loss at the cutter head while dredging within the MOF (stage 2).

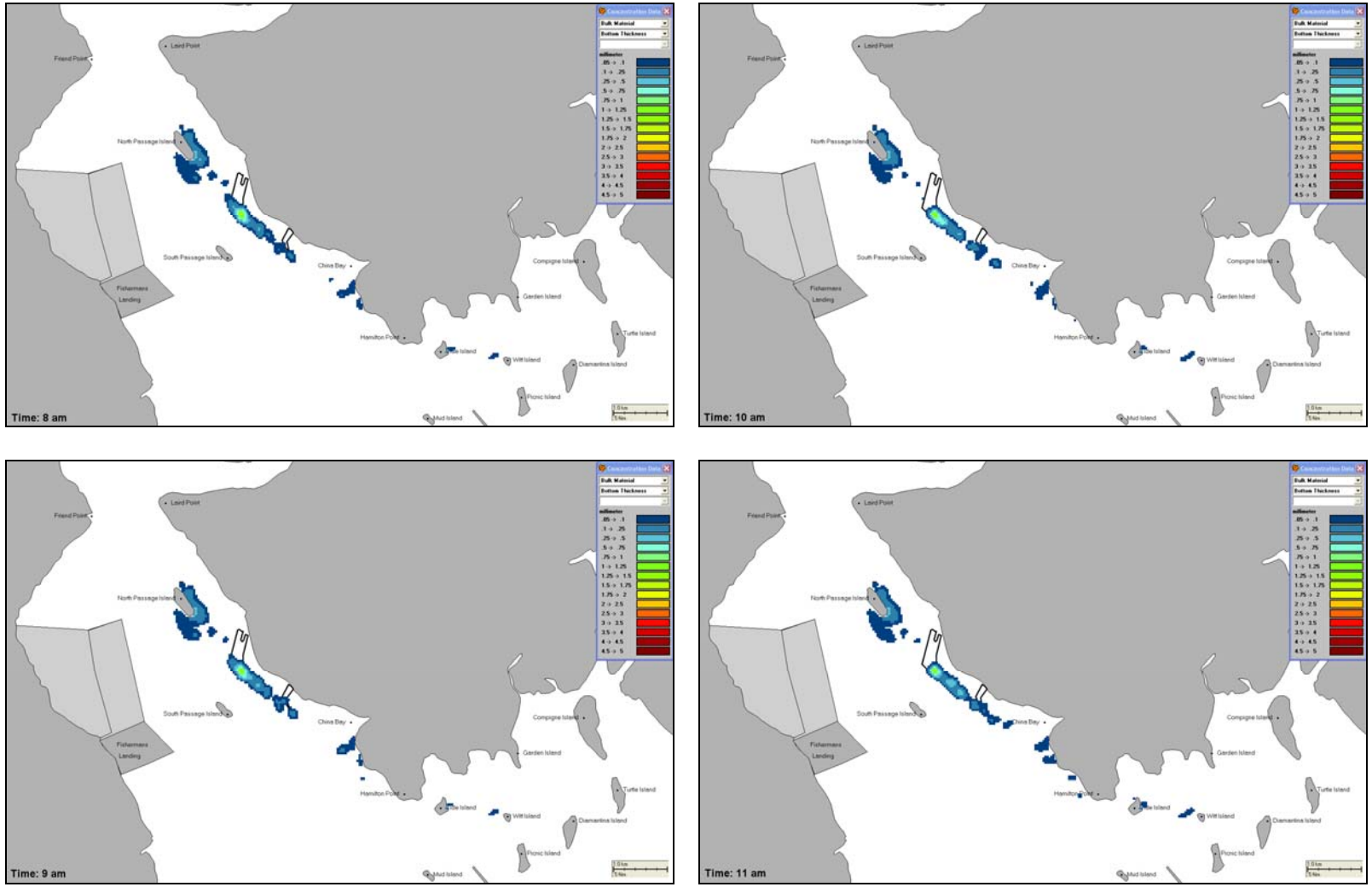

Figure 14: Hourly time-series plots (8 am, 9 am, 10 am and 11am 4th February 2009) of bottom thickness (millimetres) generated from loss at the cutter head while dredging within the MOF (stage 2).

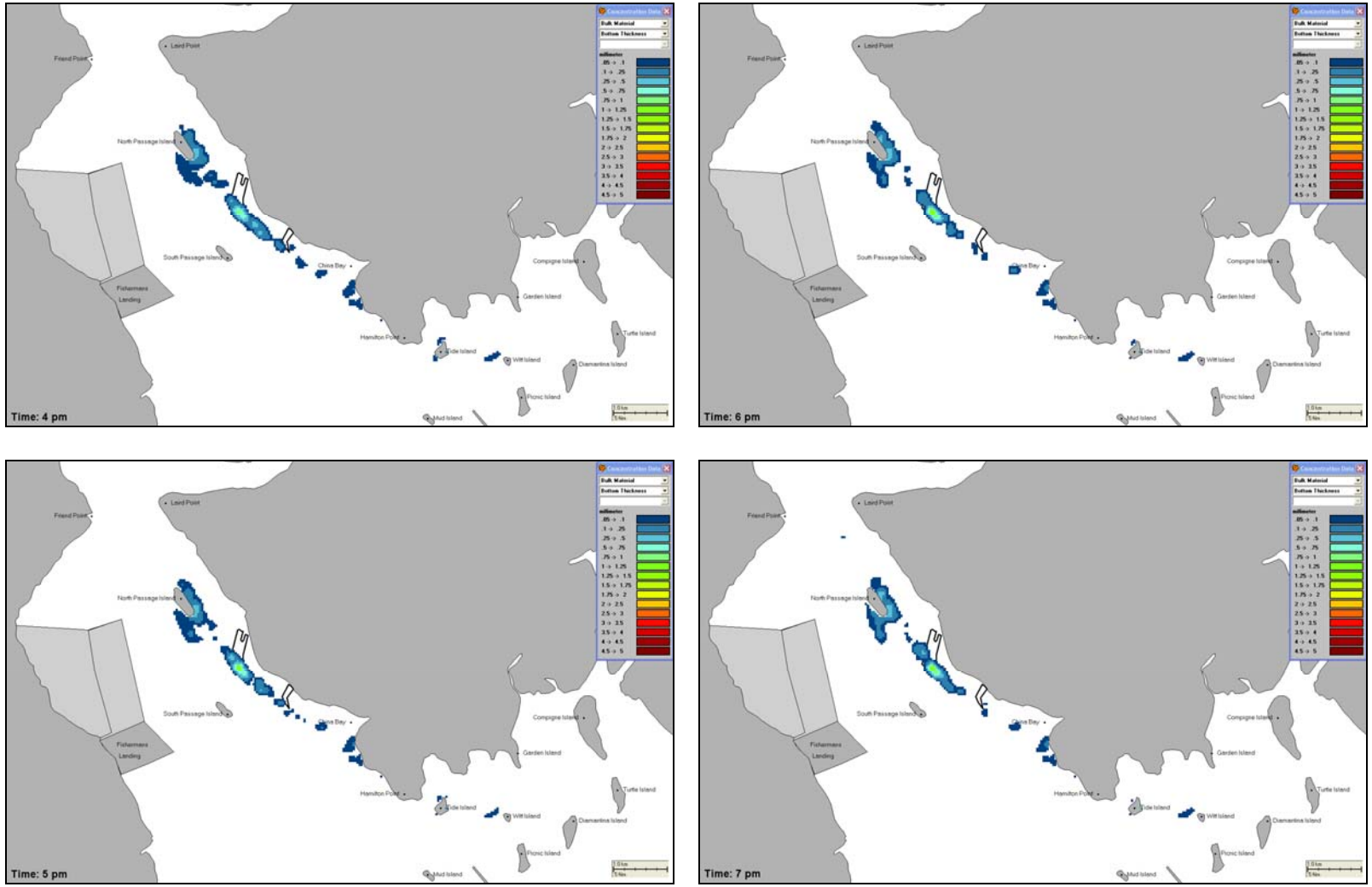

Figure 15: Hourly time-series plots (4 pm, 5 pm, 6 pm and 7 pm 4th February 2009) of bottom thickness (millimetres) generated from loss at the cutter head while dredging within the MOF (stage 2).

9.1.2 Tail-Water Discharge

The tail-water discharge produced limited plumes, with the highest TSS concentrations (< 50 mg/L above ambient) occurring immediately adjacent to the discharge cell (within 300 m) and dropping down to 5 mg/L (above ambient) at the north-east point of the reclamation site (~ 2.2 km). During the flood tides, the fine sediment (< 75 µm) is expected to migrate towards Friend Point, resulting in episodic spikes of low concentrations (5 mg/L above ambient). In the following ebb tide, the material is expected to re-disperse back toward the northern sector of the proposed reclamation site. Figure 16 demonstrates the movement of the tail-water plume as hourly plots, commencing at the start of an out-going tide.

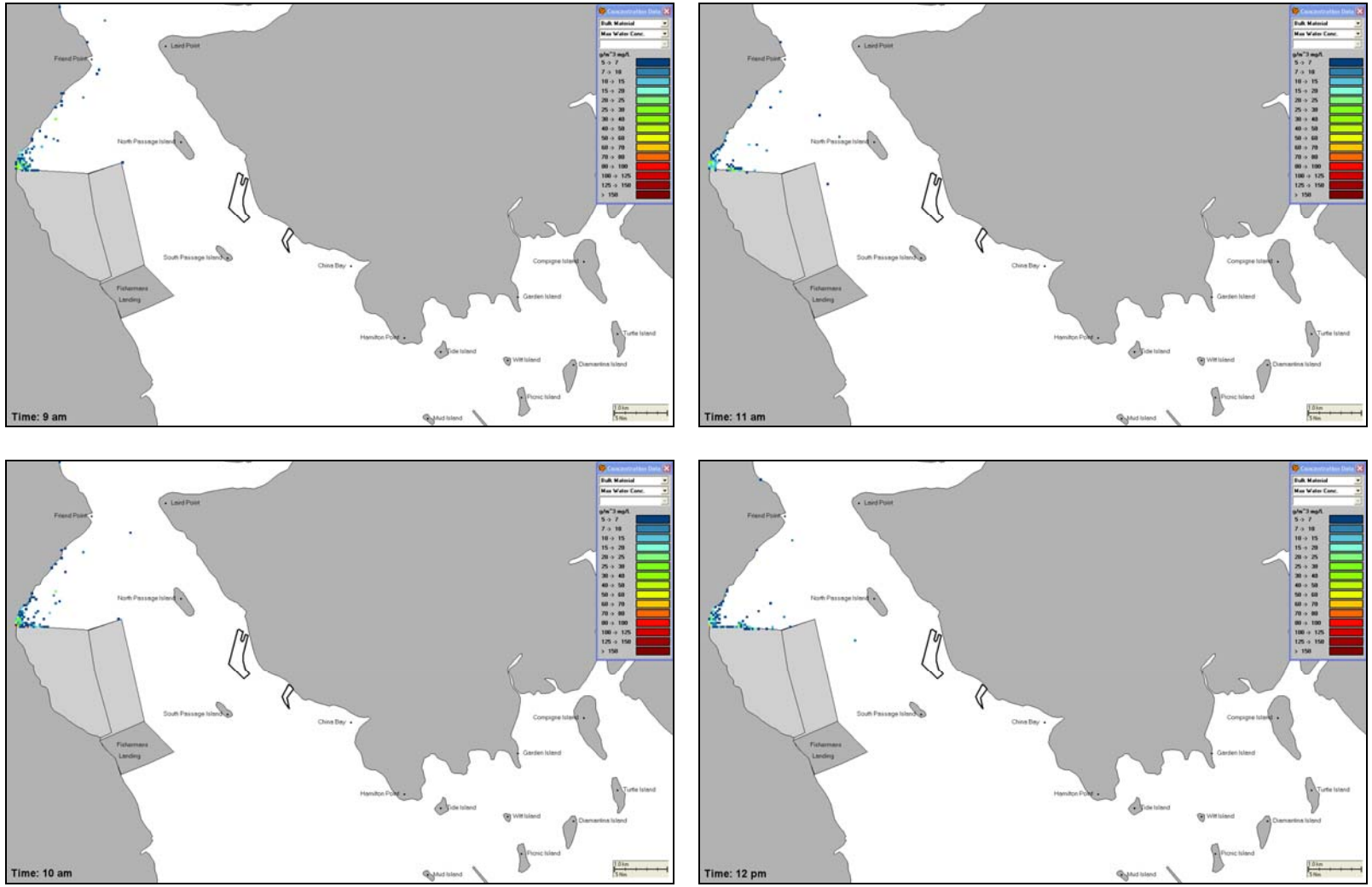

Figure 16: Hourly time-series plots (9 am, 10 am, 11 am and 12 pm 4th February 2009) of maximum TSS plumes (mg/L) generated by the tail-water discharge at the north-western sector of the reclamation site.

9.1.3 Backhoe Dredging

In contrast to the CSD simulations, work with a BHD was predicted to be more widespread throughout the water column but to still be more concentrated towards the seabed (Figure 17 and Figure 18). In this case, the sediments will initially be released throughout the water column and will have a low proportion of coarse particles. Hence entrainment will be reduced and the fine sediments will have a greater distance to sink to the bed, allowing for the material to be carried by the current and to build up over a sequence of tidal oscillations.

The plume was predicted to advect south-east beyond Tide Island during ebb tides and north-west to Laird Point during flood tides. Plume concentrations were predicted to vary over time due to the current magnitudes.

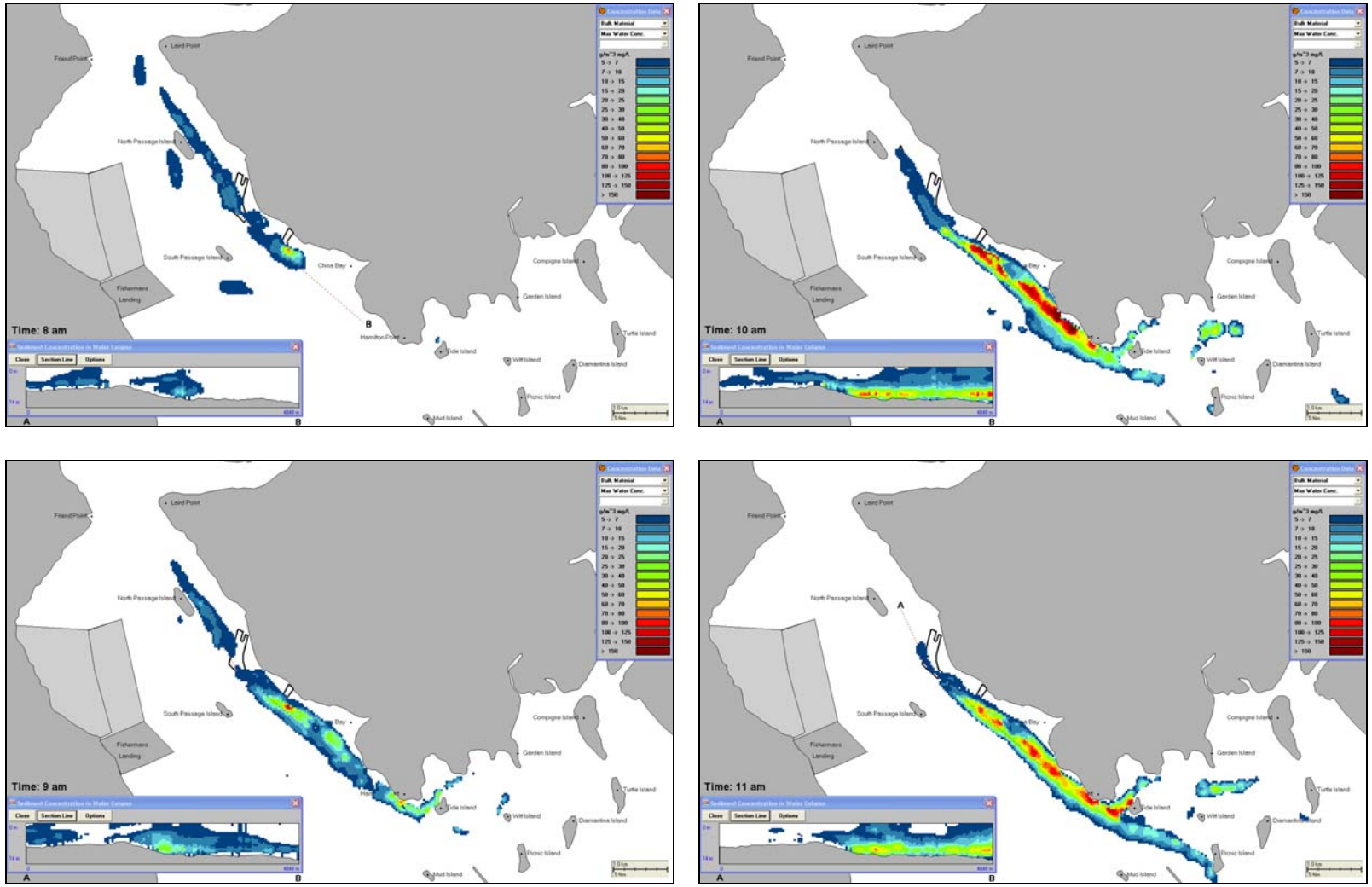

Figure 17: Hourly time-series plots (8 am, 9 am, 10 am and 11 am 4th February 2009) of maximum TSS plumes (mg/L) generated from loss at the BHD bucket while dredging within the MOF (stage 1).

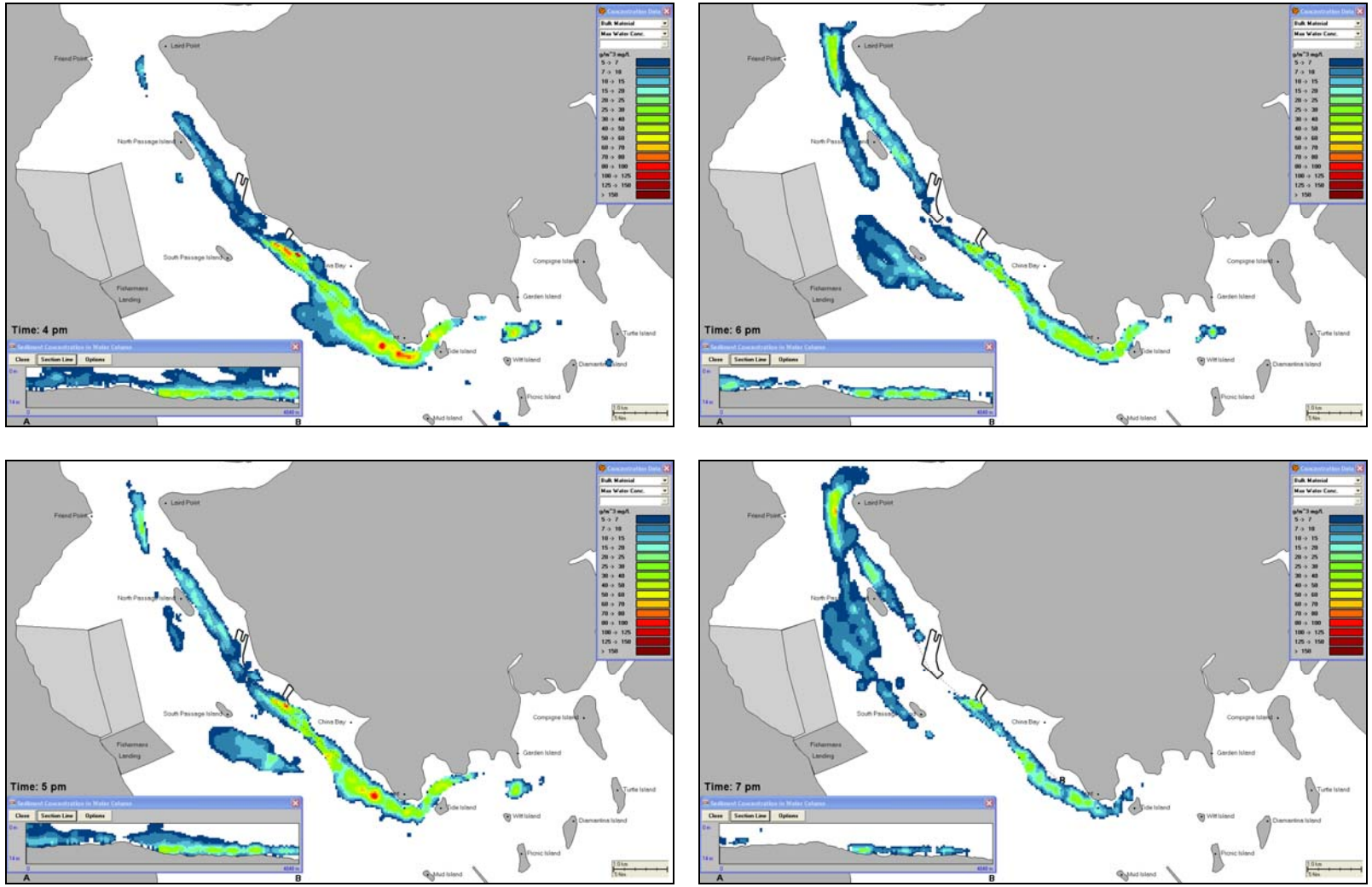

Figure 18: Hourly time-series plots (4 pm, 5 pm, 6 pm and 7 pm 4th February 2009) of maximum TSS plumes (mg/L) generated from loss at the BHD bucket while dredging within the MOF (stage 2).

9.1.4 Propeller Wash

Thrust from the SHB propellers in shallow waters is predicted to generate evolving suspended sediment plumes that would be detectable at the surface at concentrations of up to 50 to 80 mg/L (above ambient) immediately behind the vessel (Figure 22). Concentrations above 100 mg/L were predicted to develop in the water column after the vessel had passed. Coarser sediment was predicted to settle over a range of 10's of meters in a general north-west to south-east alignment with the tidal axis while plumes of finer particles were predicted to drift for 100's of meters and disperse with the tide.

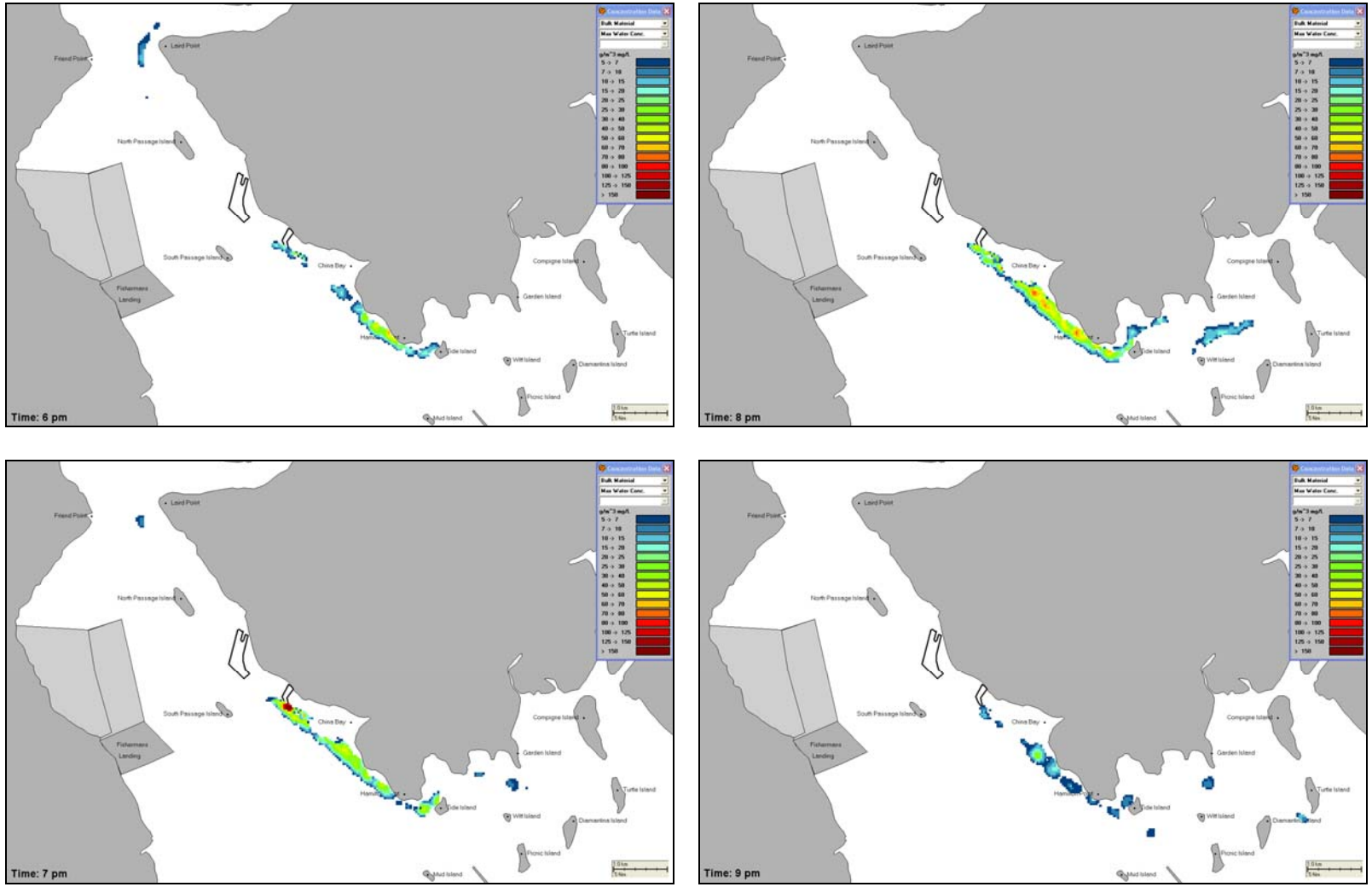

Figure 19: Hourly time-series plots (6 pm, 7 pm, 8 pm and 9 pm 1st February 2009) of maximum TSS plumes (mg/L) generated from the SHB propeller wash.

9.1.5 Disposal from Hopper Dumping

Disposal operations from SHBs were predicted to set up very high local TSS concentrations within the sinking plume, with the entrainment of coarser sediment expected to limit the suspension time for finer sediments. Given the strong currents which run east-west, simulations indicated that the major depositional axis would be along the east-west axis. The highest sedimentation rates occurred in the centre of the existing spoil ground and tapered off exponentially towards the edges. Figure 20 shows changes in the predicted bottom thickness (metres) within the GPC spoil ground at 2 day intervals at the beginning of the simulation (days 1, 3, 5 & 7). Figure 21 shows the predicted cumulative bottom thickness (meters) after 91-days of dredged sediment disposal within the GPC spoil ground. Note that while the thickest deposits (~ 0.5 m) are expected within the disposal area bounds, sediments are expected to settle beyond the bounds of the defined disposal area due to lateral displacement of the sinking sediments by the prevailing currents.

Table 13 presents the corresponding area of coverage as a function of thickness (in metres). The predicted maximum area of exposure was 41 km^2 above 0.001 m (or 1 mm). Seventy-nine percent of the area (or 32.2 km^2) had a thickness less than 0.01 m. Therefore, 8.88 km^2 would be covered by a mound higher than 0.01 m.

Table 13: Predicted area of coverage as a function of thickness, calculated from the 91-day disposal operation.

Bottom Thickness (metres)	***Area of coverage (km^2)***	***Percentage of cumulative area covered (%)***
Above 0.001	32.190	100.000
Above 0.010	3.712	21.622
Above 0.015	3.225	12.584
Above 0.030	0.523	4.732
Above 0.040	0.324	3.459
Above 0.050	0.463	2.672
Above 0.075	0.222	1.545
Above 0.100	0.289	1.006
Above 0.200	0.060	0.303
Above 0.3 -> 0.4	0.055	0.158
Above 0.400	0.010	0.024

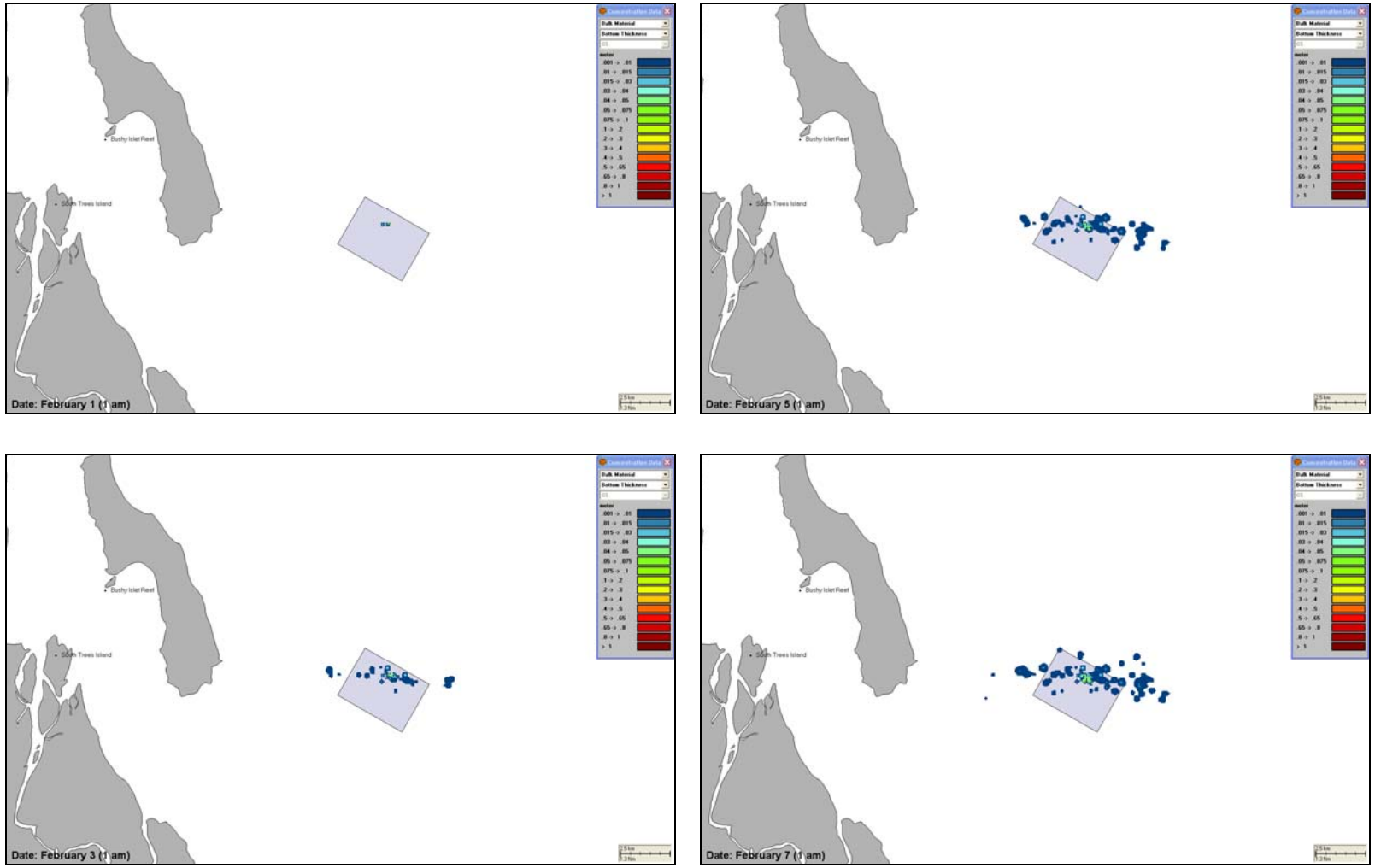

Figure 20: Predictions for the change in bed height (m) above background due to 1 week of disposal of dredged sediment within the Gladstone Port Corporation existing spoil ground. Note that some settlement is predicted to fall beyond the disposal area.

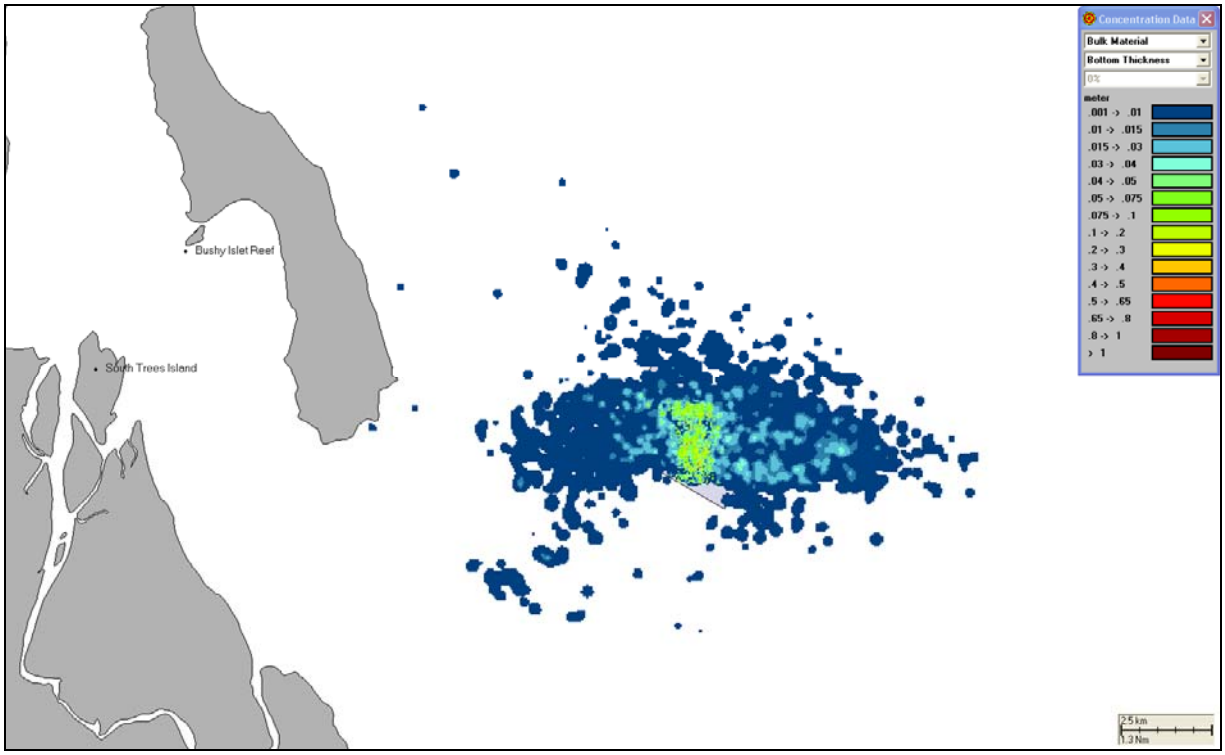

Figure 21: Cumulative bottom thickness (metres) from 91-days of discharge at a rate of 6 discharges per day into the centre of the Gladstone Port Corporation existing spoil ground.

9.2 Scenario 1 Cumulative Results

9.2.1 Time-Series Graphs of Maximum TSS Concentrations

Figure 22 to Figure 24 compare the maximum TSS concentrations predicted over time at 9 defined locations (see Figure 10) as a result of CSD dredging at MOF stage 1 and the construction dock, combined with the tail-water discharge. Each graph depicts the highest concentration at any depth within the water column, with average background TSS estimates included.

Site 1 is predicted to reach a peak concentration of 20 mg/L (8 mg/L above ambient) 8 days into the dredge operation, with a second spike of ~22 mg/L, 13 days later. Predicted concentrations at site 1 were then largely reduced to background for the remainder of the time-series. Site 3 is predicted to receive periods of extended and more varied increases in TSS concentrations in comparison to site 1. Numerous events with concentrations > 18 mg/L (8 mg/L above ambient) are predicted with a maximum > 26 mg/L (16 mg/L above ambient).

Sites 4 and 5 are characterised by more intermittent pulses of increased concentrations with clusters of events occurring either side of the 26/02/2009. Concentration increases are predicted to be the same at the two locations (~ 4 mg/L). No increases of background TSS concentrations are predicted for site 6 (Figure 23).

Figure 24 shows 2 clusters of concentration increases occurring during two periods of ~10 days at Turtle Island. A maximum concentration of 25 mg/L (5 mg/L above background) was predicted for Diamantina. No increase in TSS concentrations is predicted for Bushy Islet.

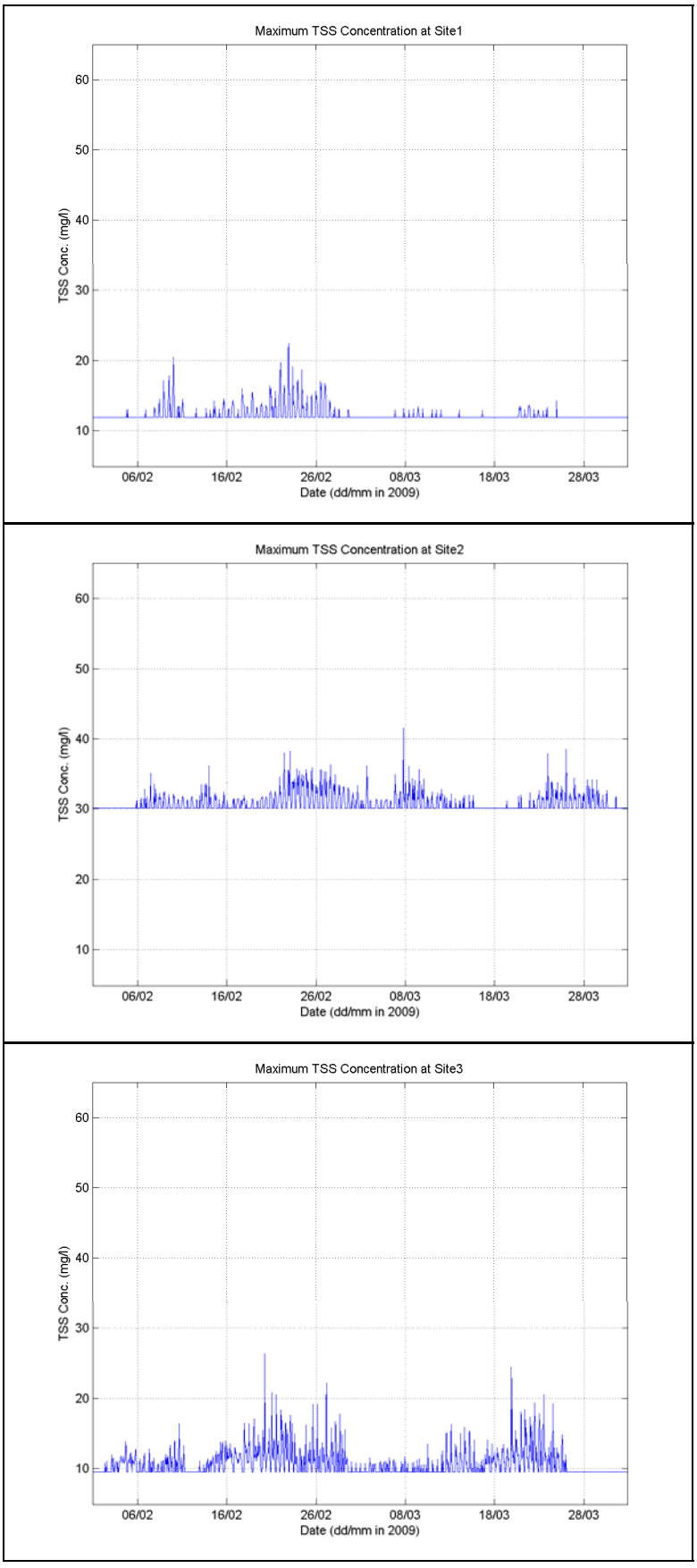

Figure 22: Time-series graphs of maximum predicted TSS concentration (above background) at sites 1, 2 and 3. Results are based on sediment sources identified in Scenario 1.

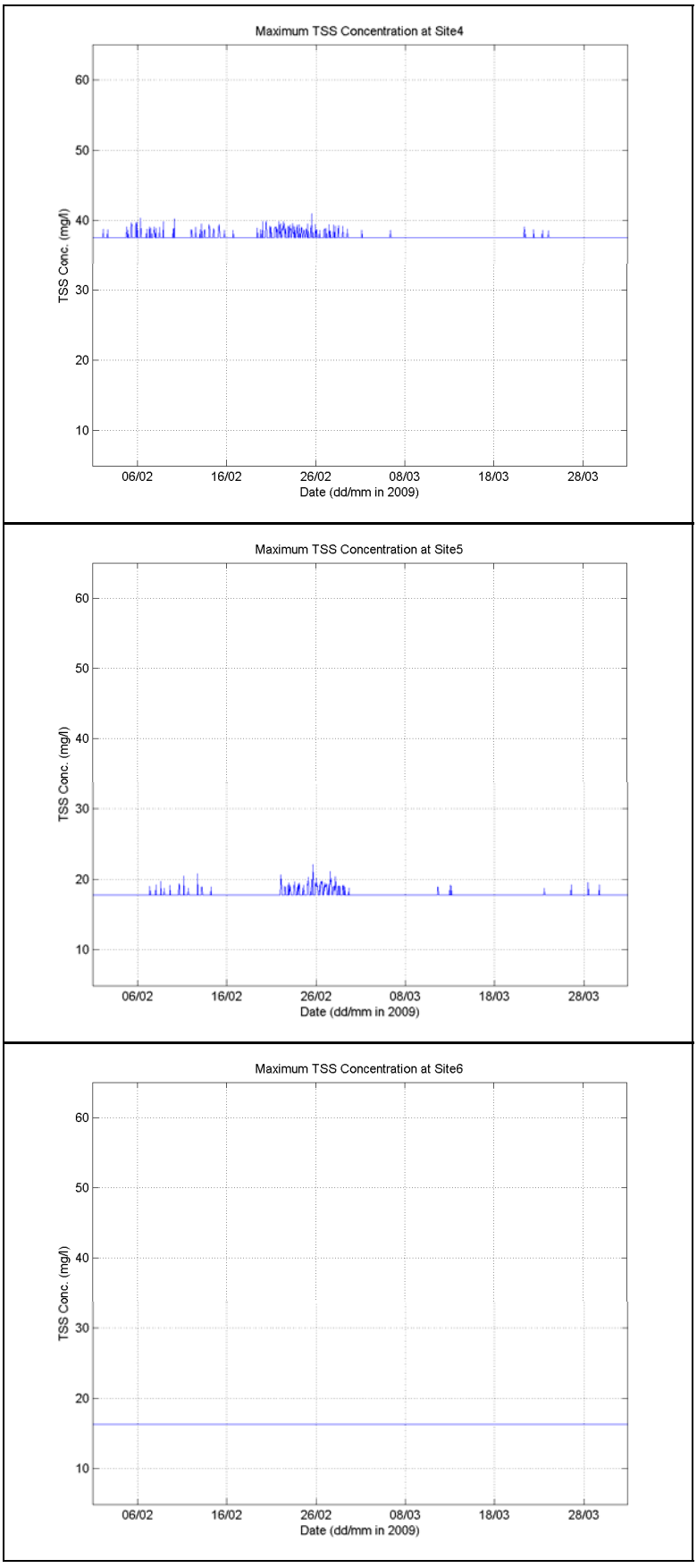

Figure 23: Time-series graphs of maximum predicted TSS concentration (above background) at sites 4, 5 and 6. Results are based on sediment sources identified in Scenario 1.

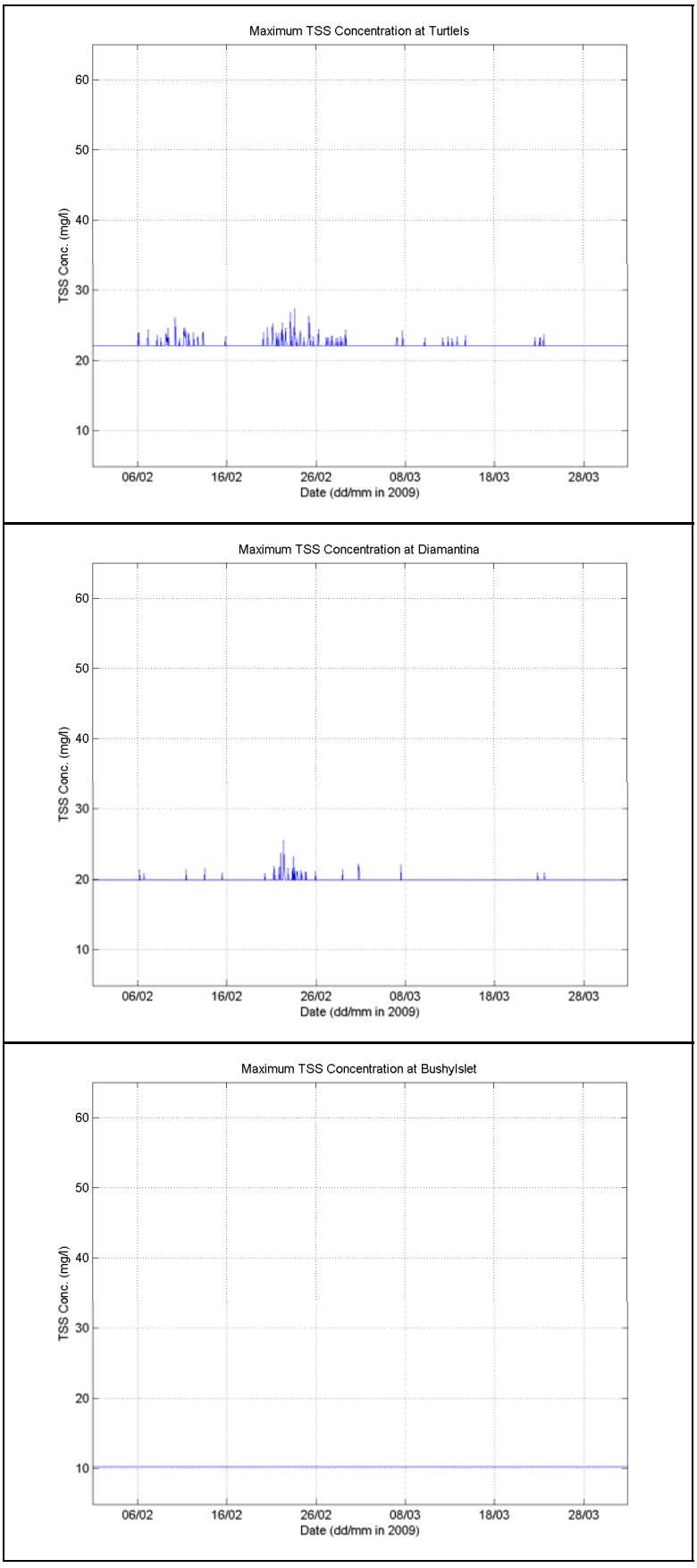

Figure 24: Time-series graphs of maximum predicted TSS concentration (above background) at Turtle Island, Diamantina and Bushy Islet. Results are based on sediment sources identified in Scenario 1.

9.2.2 Percentile Analysis of depth averaged TSS concentrations

Figure 25 to Figure 27 present depth averaged TSS percentile plots, with and without average background estimates added. Discussion of the contour maps will focus on the direct effect of the dredge operations, i.e. percentile values calculated without the background TSS concentrations added because they show the magnitude of dredging effects. A comparison of the plots with and without background TSS highlights locations where exceedances of given light reduction thresholds are expected, irrespective of dredging inputs, due to the ambient turbidity of the waterway. The 50^{th}, 80^{th} and 95^{th} percentiles should be interpreted as 50%, 80% or 95% of the time, respectively.

The 50^{th} percentile estimates of the depth averaged TSS concentration shown in Figure 25 (top) indicate an increase of 5 mg/L (above ambient) for waters directly adjacent to the MOF and construction dock, and a 25 to 50 mg/L increase immediately adjacent to the tail-water discharge location. Dredging discharges are not expected to add to the median levels of the ambient concentrations beyond these locations.

The 95^{th} percentile estimates (see Figure 27 top) indicate a predicted concentration contour of 5 mg/L stretching from Graham Creek in the north, along the western shoreline of Curtis Island, North and South Passage Islands. Occurrences of 10 mg/L concentrations (above background) were predicted next to the MOF and Friend Point. While 25 mg/L concentrations were indicated within 300 m from the tail-water outfall, along the shorelines of the construction dock, North passage and Tide Island. Pockets of 25 mg/L were predicted along the shorelines of the construction dock, North passage and Tide Island.

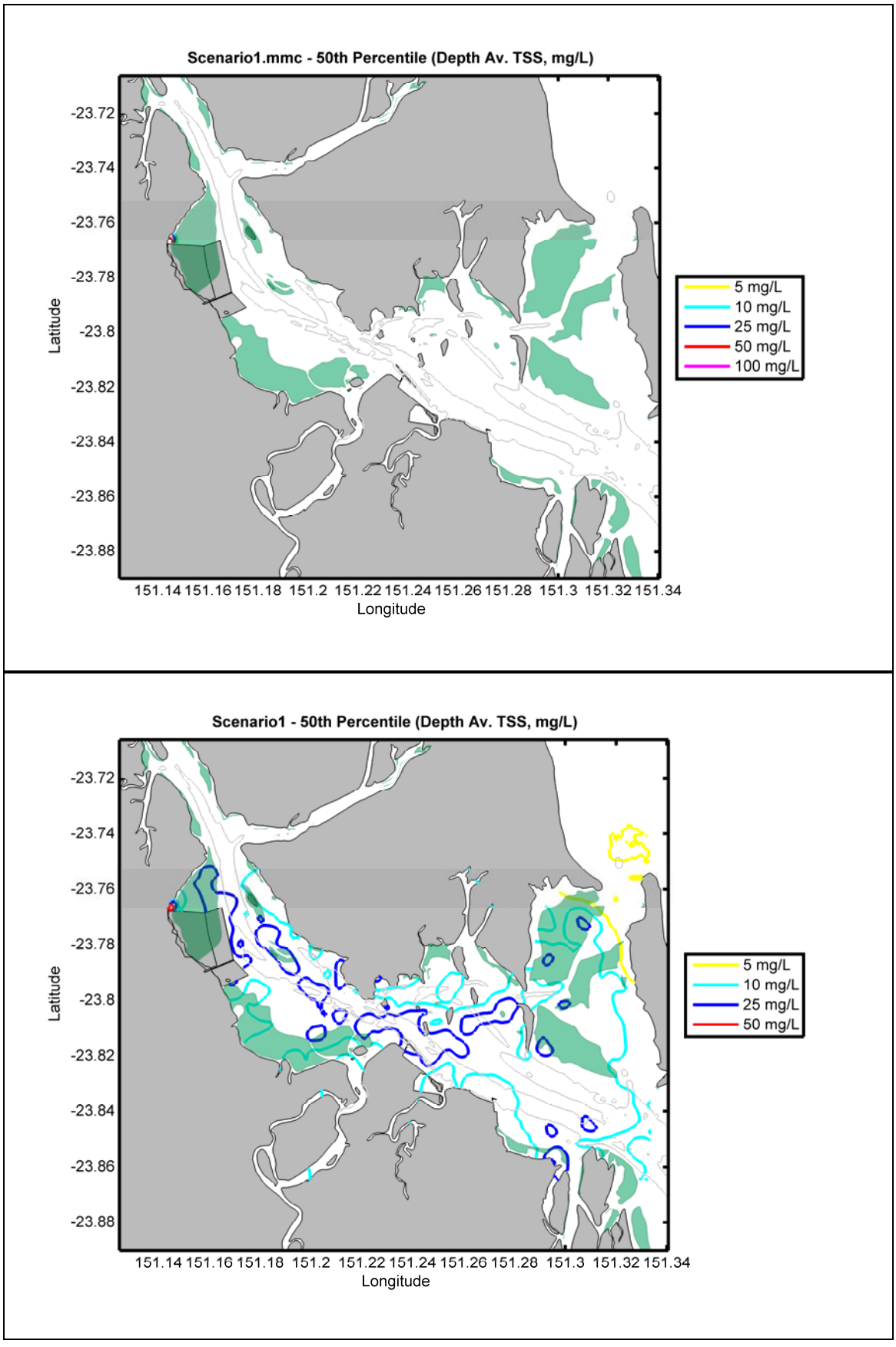

Figure 25: Scenario 1 TSS depth-averaged 50th percentile concentration contour plots without (top) and with background levels included (bottom).

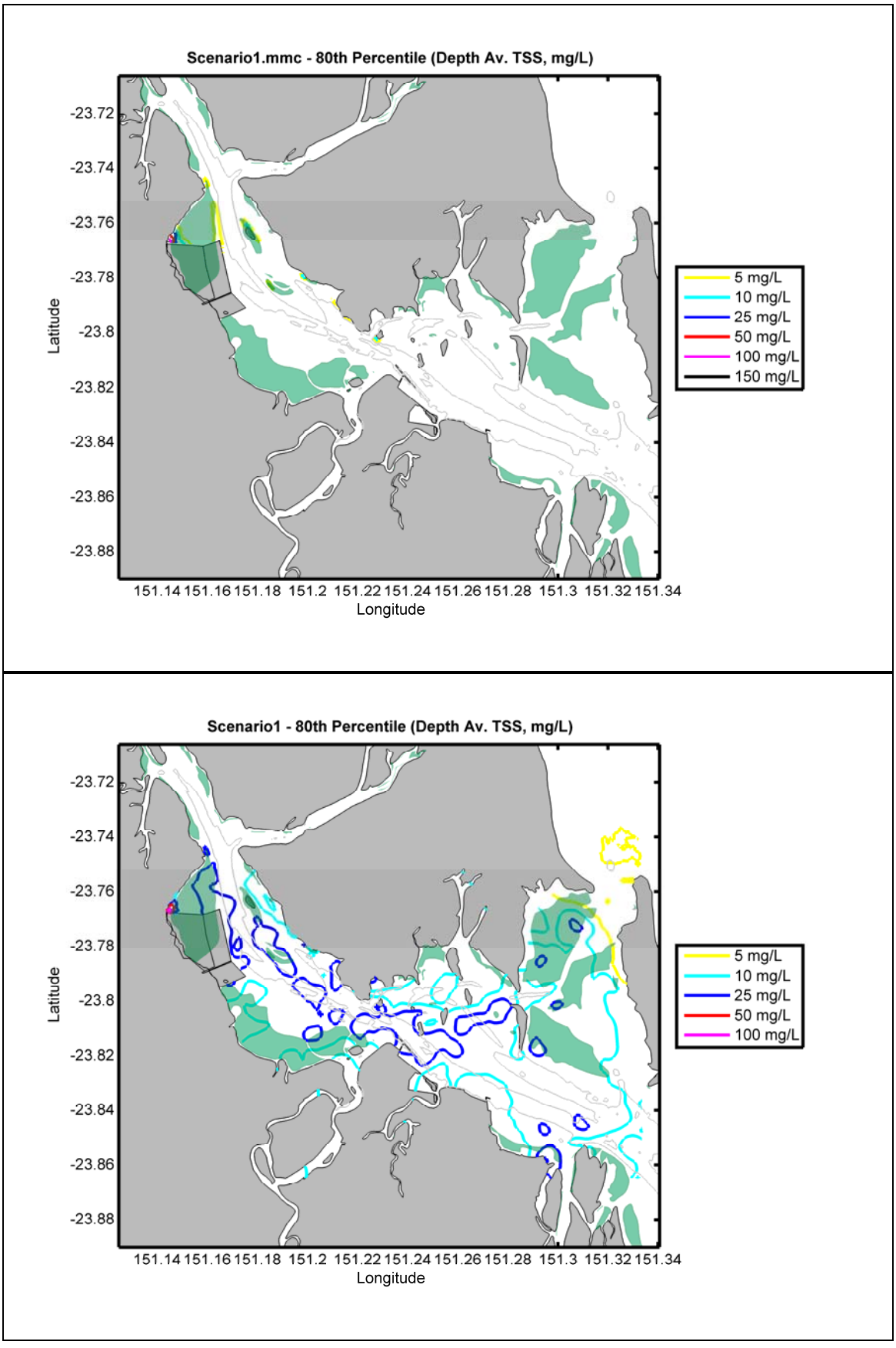

Figure 26: Scenario 1 TSS depth-averaged 80th percentile concentration contour plots without (top) and with background levels included (bottom).

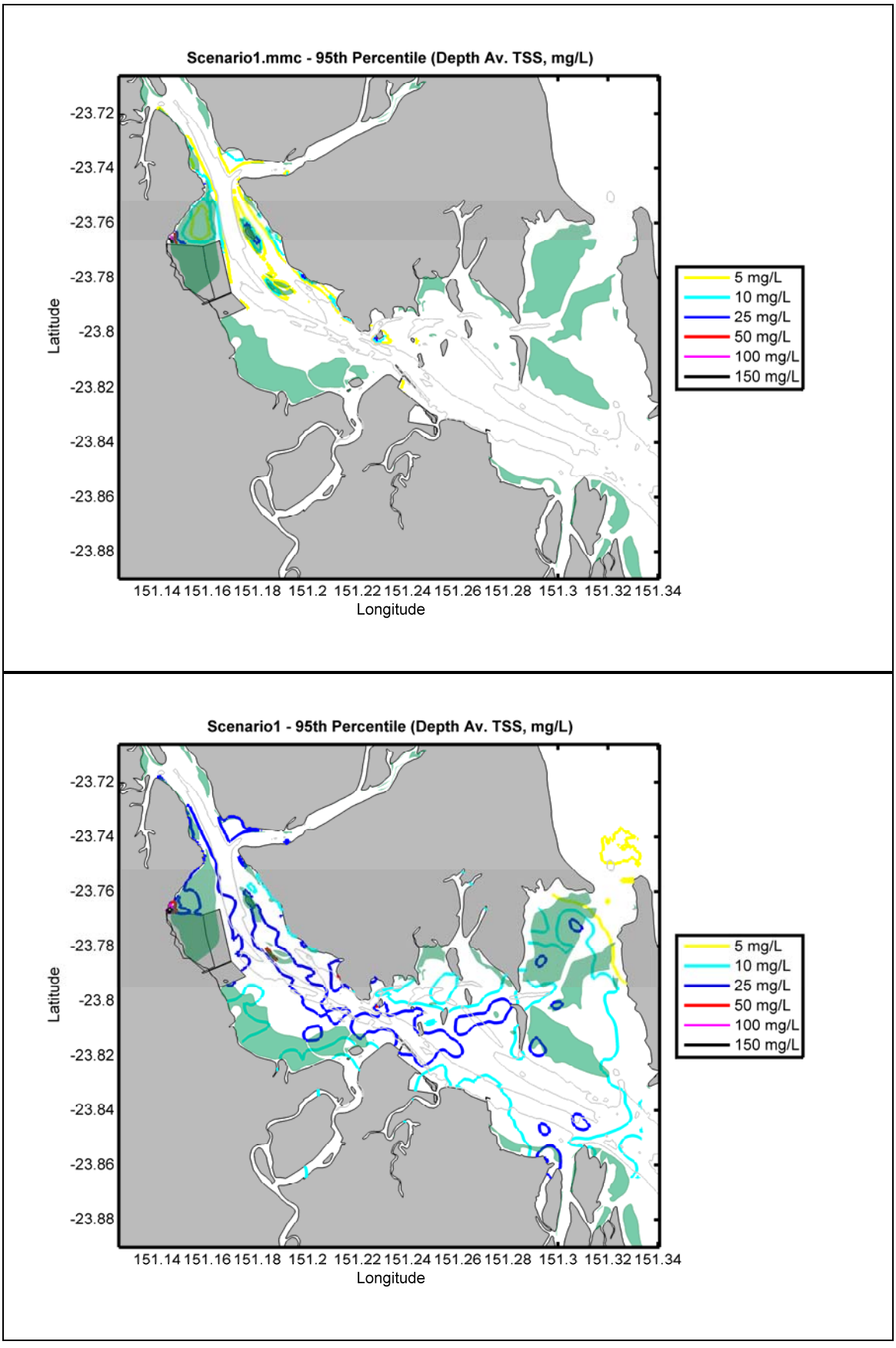

Figure 27: Scenario 1 TSS depth-averaged 95th percentile concentration contour plots without (top) and with background levels included (bottom).

9.2.3 Sedimentation Plots

The 50th and 95th percentile of the predicted sedimentation rate, as a result of the dredge operations of Scenario 1, are presented in Figure 28 and Figure 29.

The 50th percentile estimates indicate a small area adjacent to the tail-water discharge site characterised by a sedimentation rate >2 g/m^2/day but < 5 mg/L. The 95th percentile estimate indicates two distinct areas would be influenced by sedimentation rates up to 5 g/m^2/day, respectively. These areas occur along the western shoreline of Curtis Island from the MOF site to areas surrounding Hamilton Point and adjacent the tail-water discharge site along the northern bounds of the proposed reclamation site north of Fisherman's Landing. Additional areas characterised by sedimentation rates of 2 g/m^2/day include a small area adjacent the shoreline north-east of Barney Point and areas surrounding and to the north of Picnic Island. Increased sedimentation rates of 10 g/m^2/day are predicted to occur at the immediate vicinity of the MOF dredge location and immediately adjacent the tail-water discharge site. Predicted rates of 25 g/m^2/day can be observed at the north-eastern tip of Tide Island, suggesting this location would be a site where sediments accumulate.

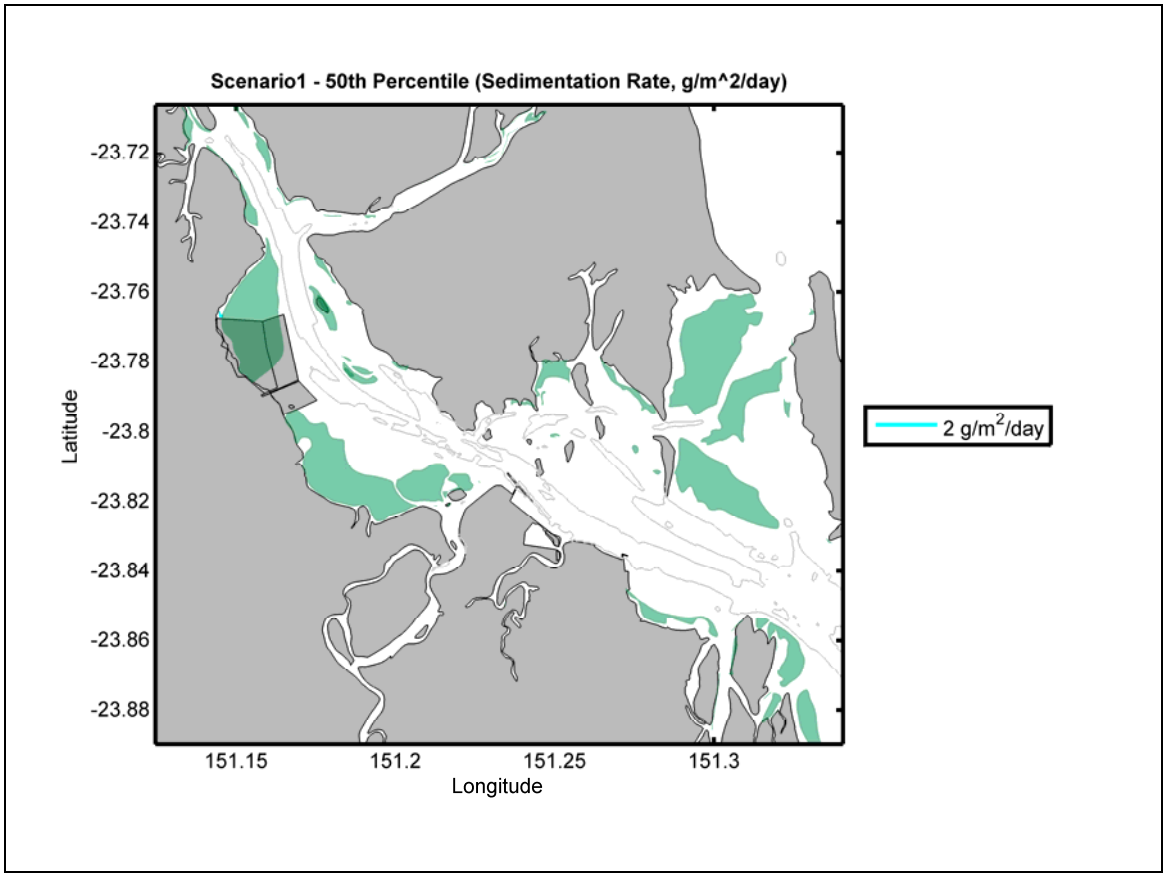

Figure 28: Predicted 50th percentile sedimentation rate (g/m^2/day) from dredging operations in Scenario 1.

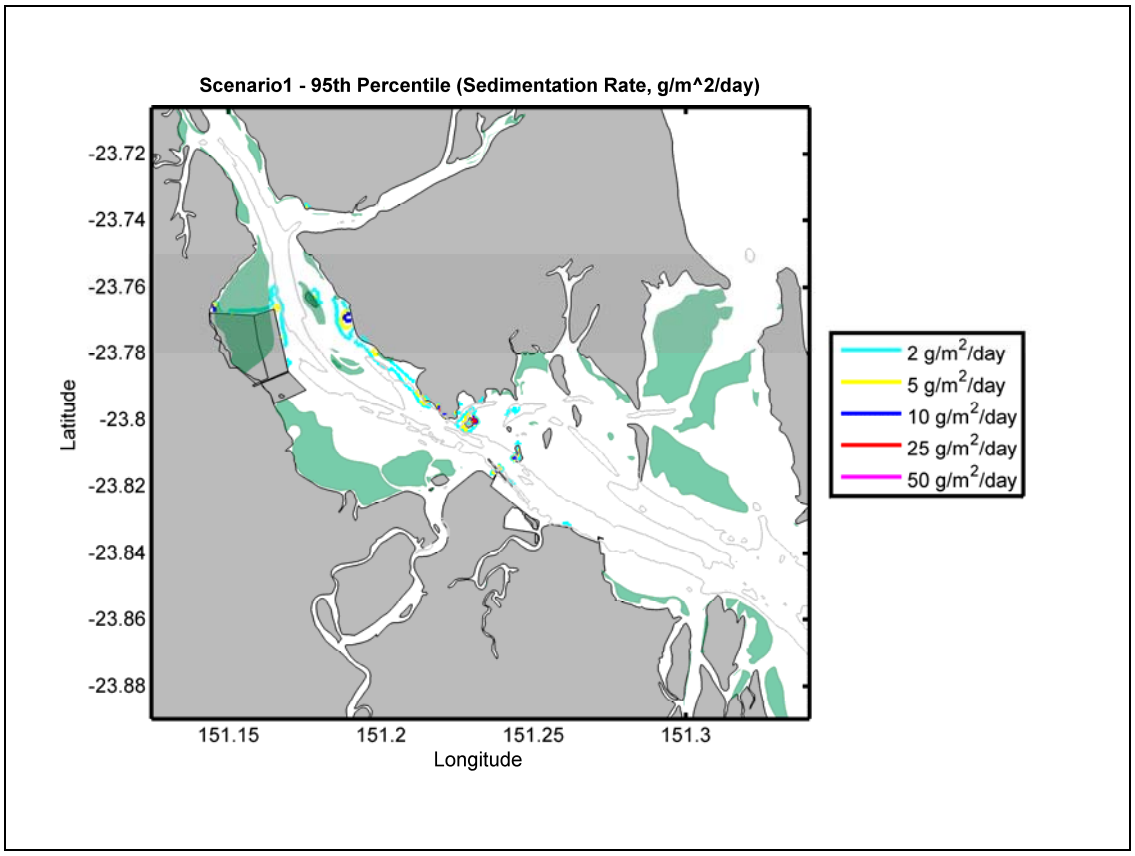

Figure 29: Predicted 95th percentile sedimentation rate (g/m^2/day) from dredging operations in Scenario 1.

9.2.4 Difference in the Proportion of Light Reaching the Seabed

Median (i.e. 50th percentile) and 95th percentile maps have been generated of the amount (%) of light reaching the seabed under ambient conditions (i.e. pre-dredging). Each map is defined by six contours enclosing areas where the light reaching the seabed would be reduced by 5, 10, 15, 30, 40 and 50% of incident light. Plots are also shown of the median and 95th percentile of the difference in the available light reaching the seabed that is expected with the addition of dredging plumes.

In general, the estimates for background alone indicate that there will be 50% reduction of light over a large part of the waterway due to the ambient turbidity. The 50th percentile map (Figure 32) indicates a further reduction of 1% in available light at the fringe of the seagrass meadow north of Fisherman's Landing proposed reclamation site with the addition of dredging plumes. Up to 25% reduction in the available light is indicated immediately around the proposed tail-water outfall. The percentage difference drops down to a 2% reduction within 300 m.

The 95th percentile map (Figure 33) shows a 2% reduction in light for seagrass meadows south of Fisherman's Landing and a 15% reduction in available light for seagrass meadows at

North and South Passage Islands. The seagrasses adjacent to Laird Point are likely to experience 10% less light, whereas meadows north of the Fisherman's Landing reclamation site are expected to experience reductions ranging between 5 and 25%, depending on proximity to the tail-water outfall.

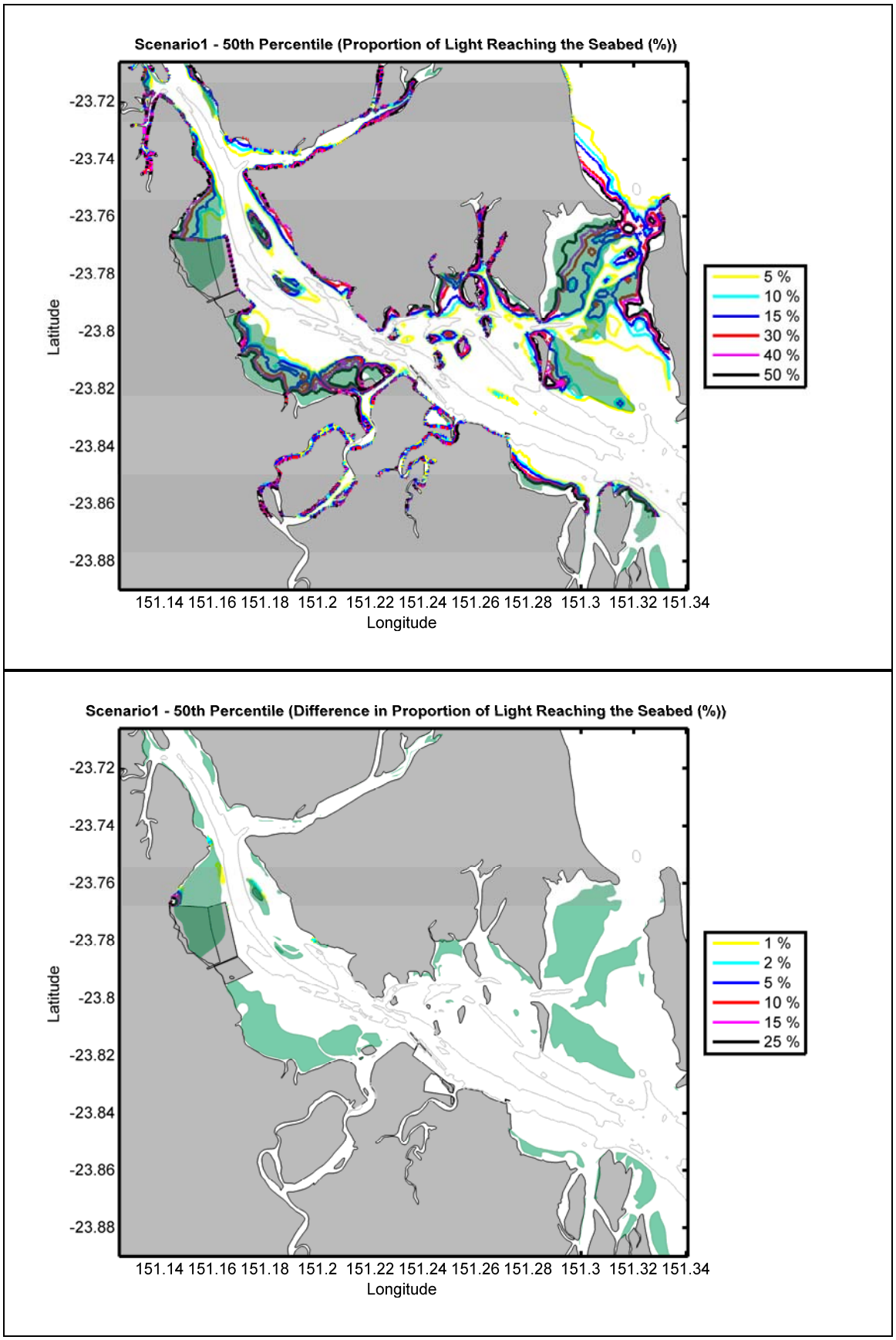

Figure 30: Scenario 1 - Fiftieth percentile plots of the (top) proportion of light (%) reaching the seabed pre-dredging; and (bottom) difference in light (%) reaching the seabed as a result of the dredging operation.

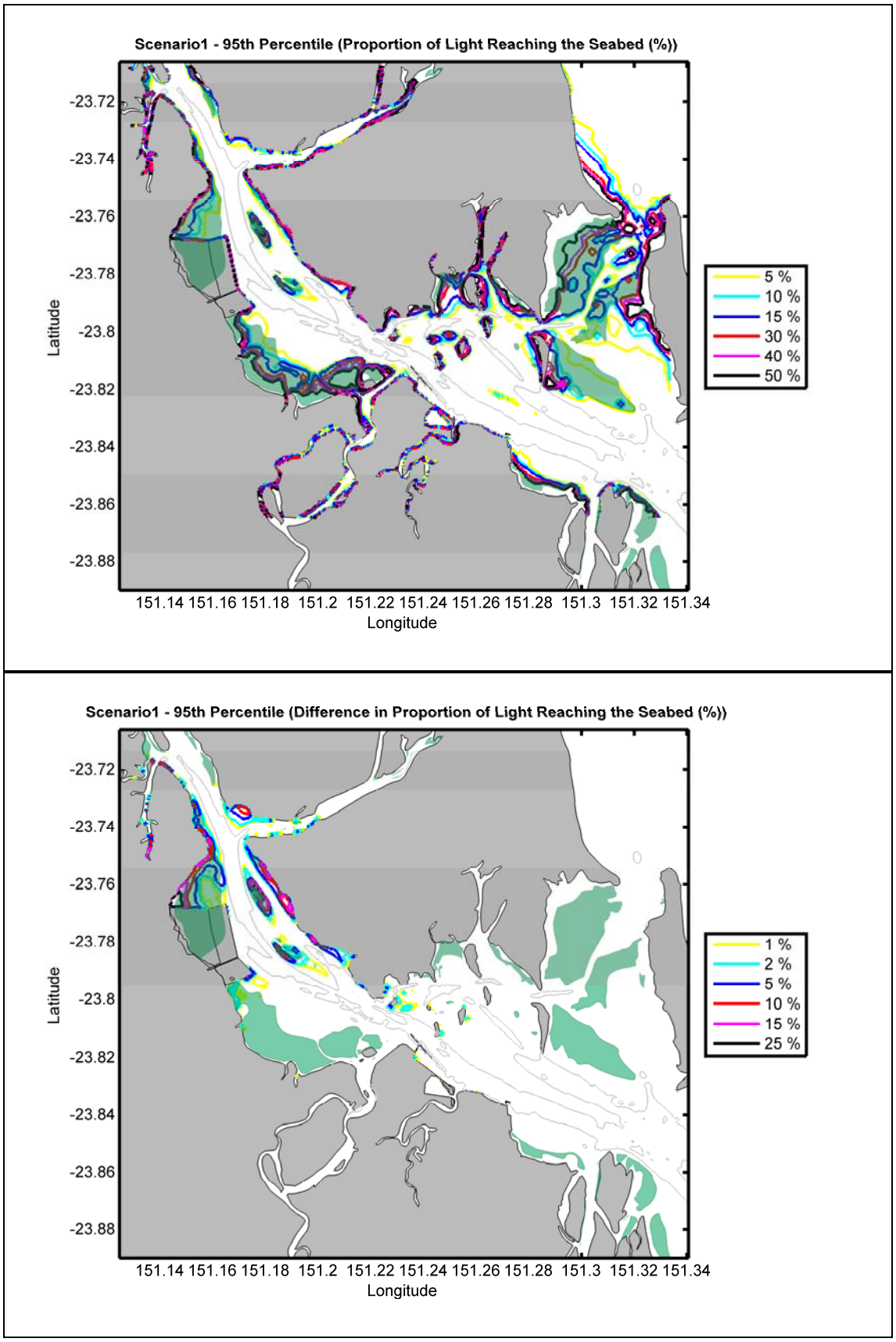

Figure 31: Scenario1 - Ninety-fifth percentile plots of the (top) proportion of light (%) reaching the seabed pre-dredging; and (bottom) difference in light (%) reaching the seabed as a result of the dredging operation.

9.3 Scenario 2 Cumulative Results

9.3.1 Time-Series Graphs of Maximum TSS Concentrations

Figure 32 to Figure 34 compare the maximum TSS concentrations predicted over time at the 9 defined locations (Figure 10) due to the plumes generated by BHD dredging at MOF stage 1 and the construction dock, and propeller wash generated by the SHB vessels. Each graph depicts the highest concentration at any depth within the water column, with background TSS included.

Due to the nature of the plumes generated by the BHD operations and propeller wash, Sites 1 to 3 are characterised by highly elevated concentrations on a near-daily basis. Elevated concentration peaks show a cyclic pattern indicating the influence of the spring/neap tidal regime on the TSS concentrations within the Port environment. A spike of 62 mg/L (50 mg/L above background) was predicted for site 1. A single TSS event of 130 mg/L over the 91 day operation was predicted at site 3.

Figure 33 shows a similar time-series trend for sites 4 and 5 with near-daily increases of background TSS concentrations. Maximum concentrations also follow cyclic patterns presumably as a result of the tidal regime of the Port. Peaks at site 4 typically exceed 42 mg/L (background was 37 mg/L), while at site 5 TSS was above 26 mg/L (background level 17 mg/) on numerous occasions.

As observed at sites 1 to 5, Turtle Island and Diamantina are also predicted to be characterised by near-daily increases in background TSS concentrations over a cyclic pattern (Figure 34). Increases in TSS concentrations are predicted to be greater in waters surrounding Turtle Island in comparison to Diamantina with a larger number of events > 40 mg/L (background level 19 mg/L) and a number of peaks occurring > 60 mg/L. A single spike of 140 mg/L occurred at Turtle island (120 mg/L above background). No increases in TSS concentrations are predicted for Bushy Islet.

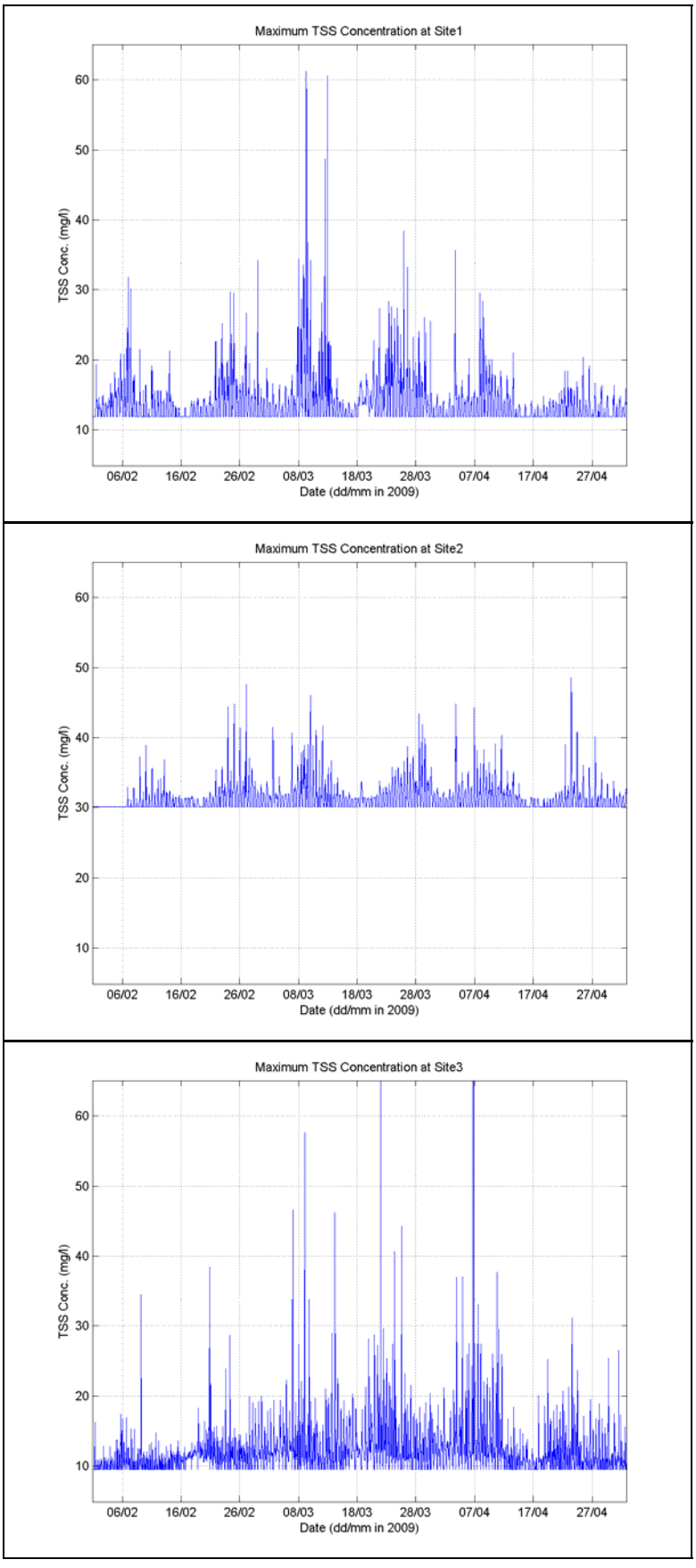

Figure 32: Time-series graphs of maximum predicted TSS concentration (above background) at sites 1, 2 and 3. Results are based on sediment sources identified in Scenario 2.

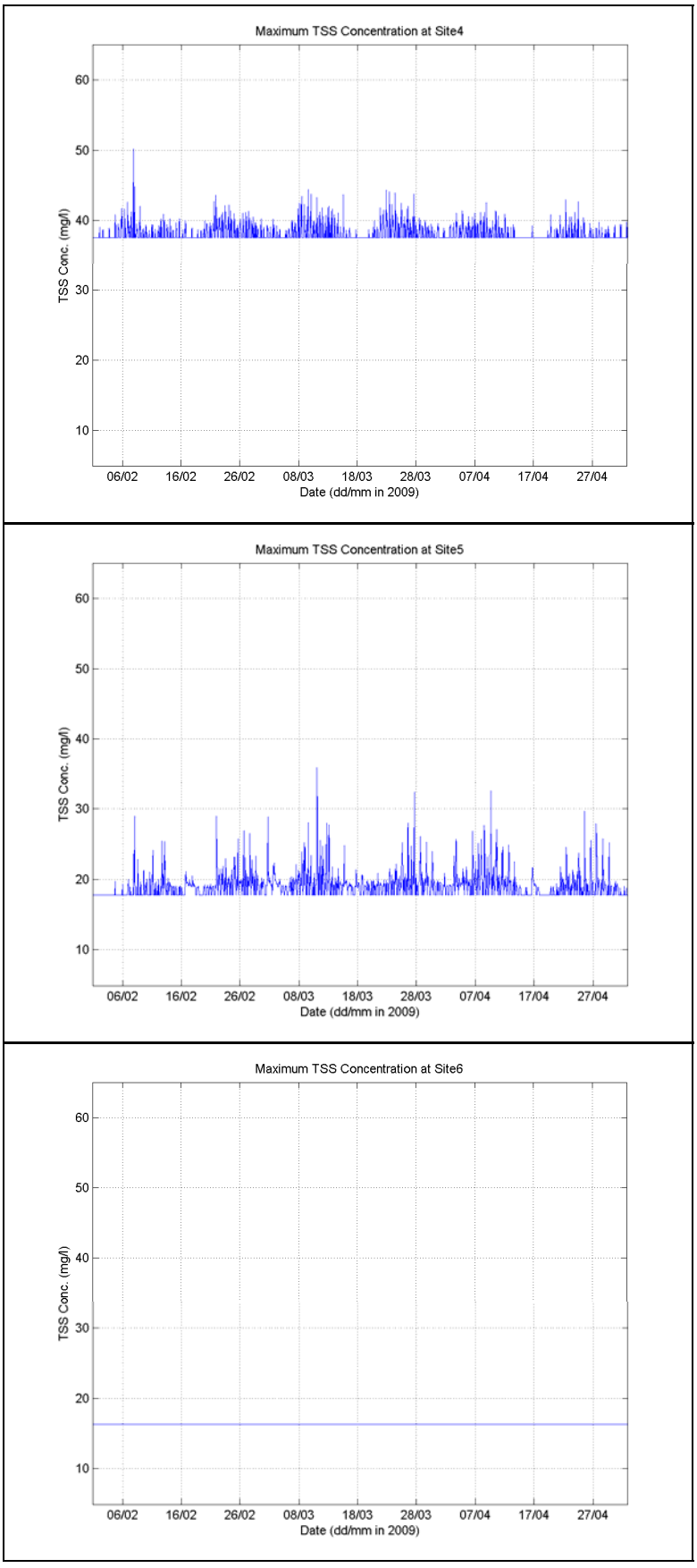

Figure 33: Time-series graphs of maximum predicted TSS concentration (above background) at sites 4, 5 and 6. Results are based on sediment sources identified in Scenario 2.

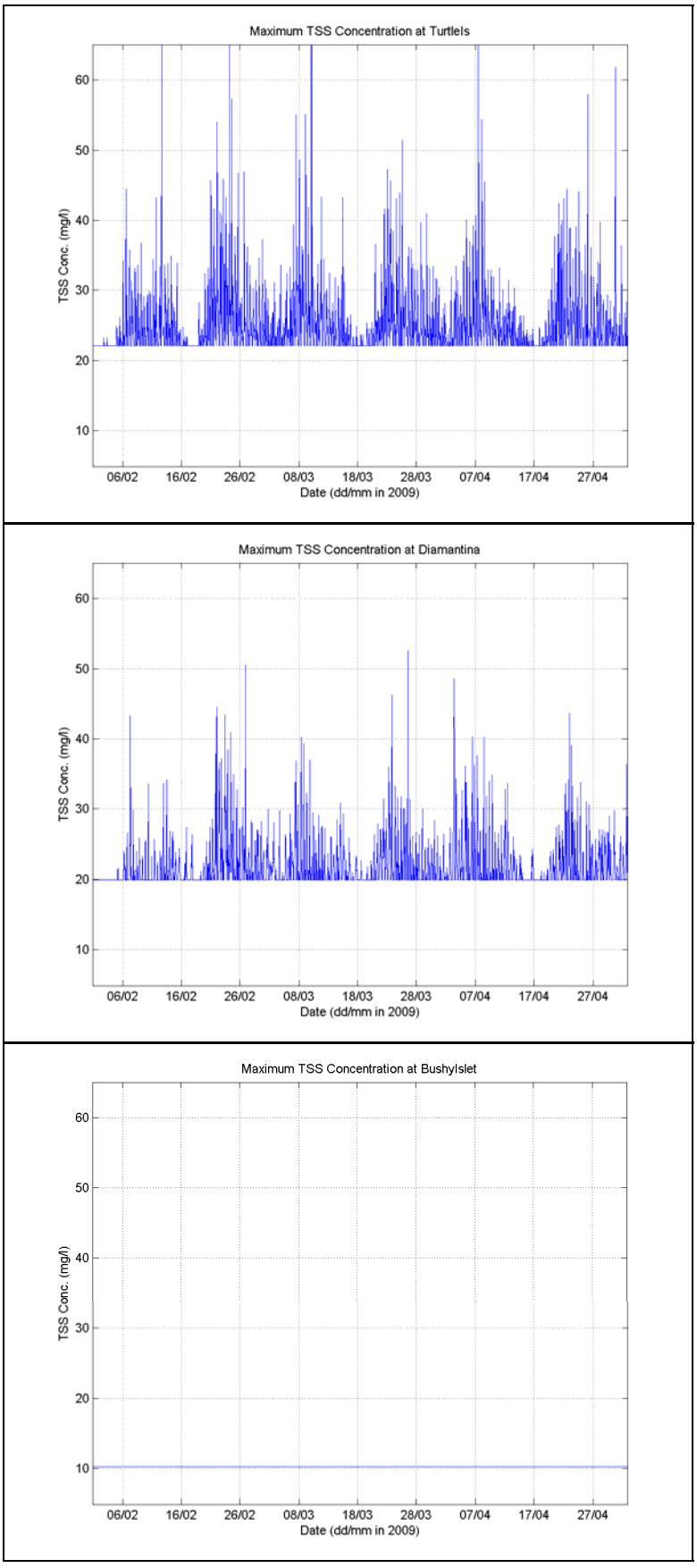

Figure 34: Time-series graphs of maximum predicted TSS concentration (above background) at Turtle Island, Diamantina and Bushy Islet. Results are based on sediment sources identified in Scenario 2.

9.3.2 Percentile Analysis of Depth Averaged TSS concentrations

The depth averaged TSS median percentile plot shown in Figure 35 (top) indicates waters adjacent to the construction dock and Tide Island, reaching 5 mg/L (above ambient).

The 80th percentile map suggests an increase of 5 mg/L at the entrance of Graham Creek, North Passage Island and waters nearby the MOF and construction dock sites. An increase of 5 mg/L concentration was also predicted for Tide Island ~ 5 km from the MOF. Concentrations of 10 mg/L extended over the south-west corner of Tide Island, shallow waters on the western side of Curtis Island and at the north and south areas of North Passage Island.

Based on the 95th percentile statistics (Figure 37 top), predicted concentrations of 5 mg/L would stretch over 16 km from waters south of Turtle Island to the north of Graham Creek. A concentration increase of 10 mg/L was predicted to occur along the fringes of the seagrass meadows, 3.5 km north of Fisherman's Landing. Regular peaks of 25 mg/L are predicted within waters surrounding the MOF and construction dock dredge areas.

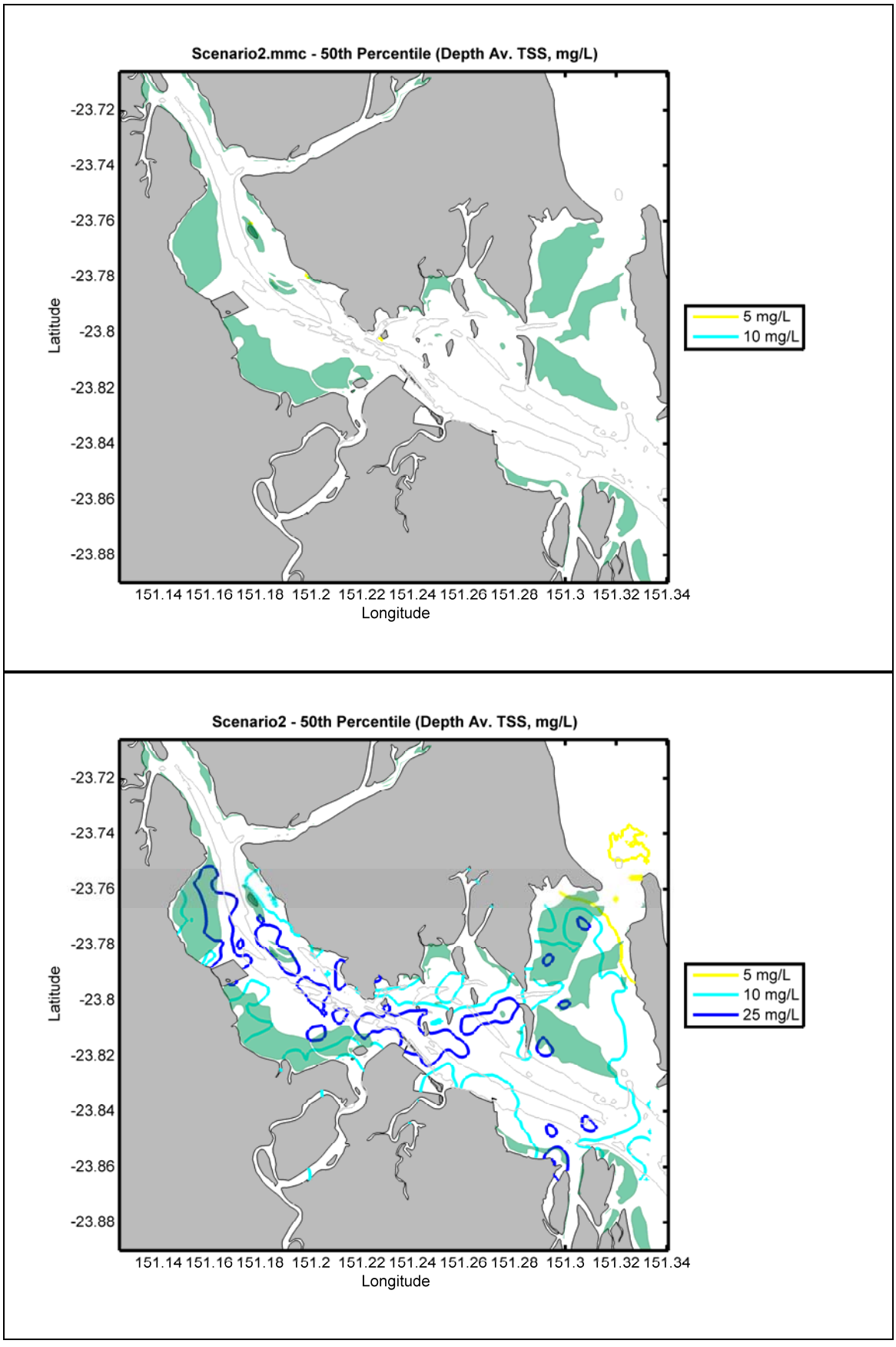

Figure 35: Scenario 2 TSS depth-averaged 50th percentile concentration contour plots without (top) and with background levels included (bottom).

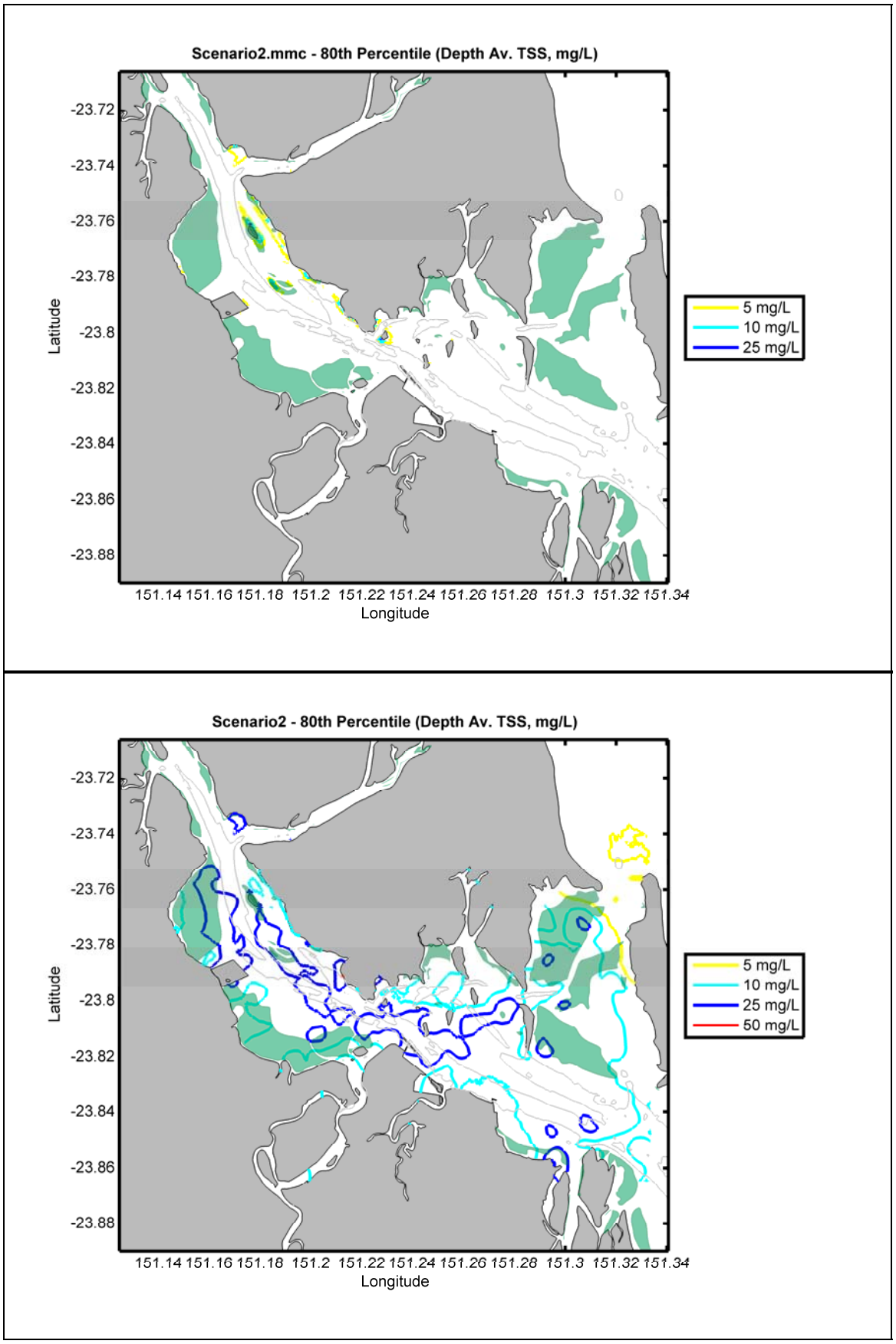

Figure 36: Scenario 2 TSS depth-averaged 80th percentile concentration contour plots without (top) and with background levels included (bottom).

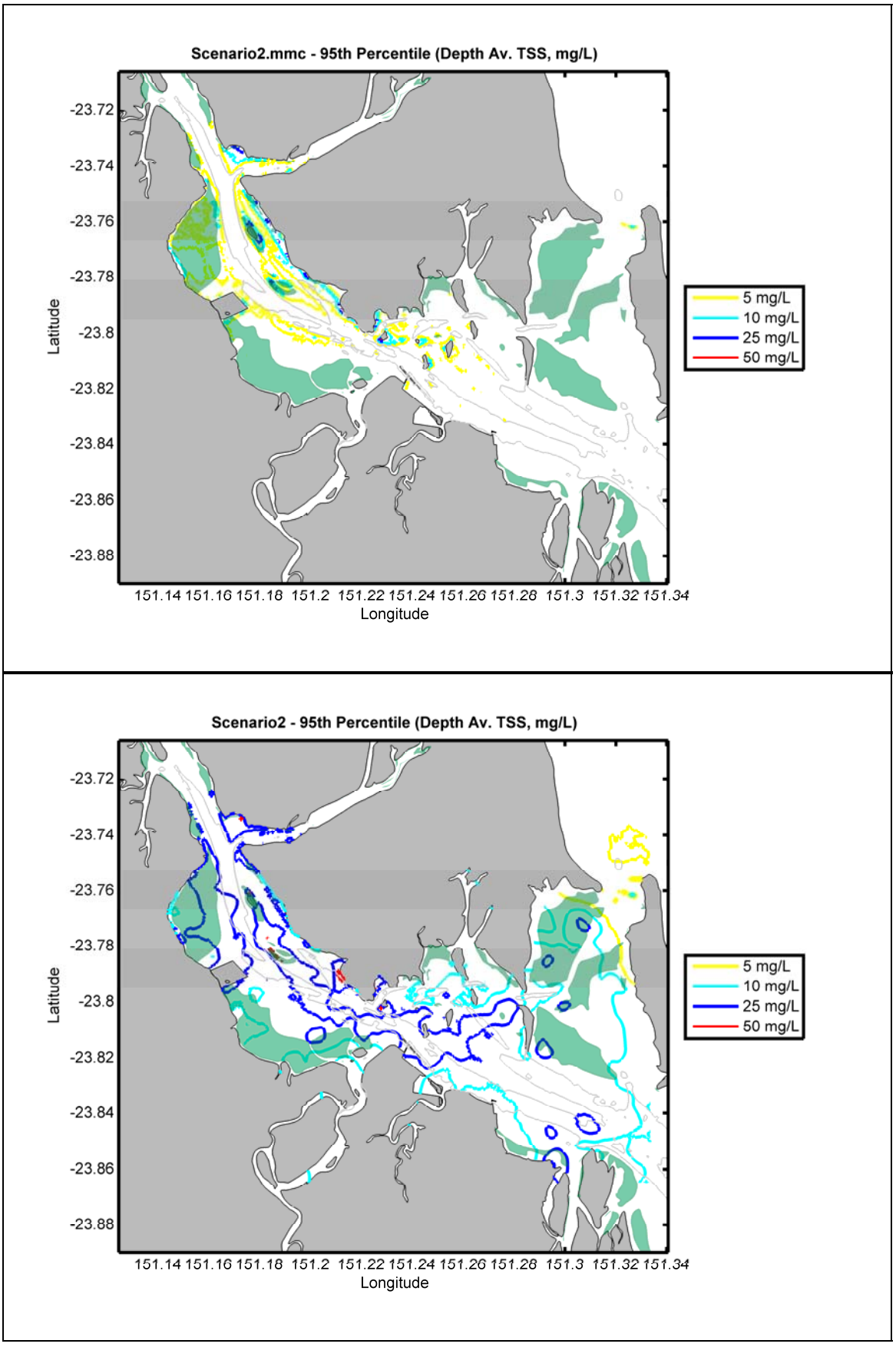

Figure 37: Scenario 2 TSS depth-averaged 95th percentile concentration contour plots without (top) and with background levels included (bottom).

9.3.3 Sedimentation Plots

Figure 38 and Figure 39 are the 50th and 95th percentile sedimentation rate maps, respectively, as a result of the Scenario 2 dredge operations.

The median percentile plot (Figure 38) indicates a 2 g/m^2/day sedimentation rate surrounding the MOF and construction dock regions, and south at Hamilton Point. A sedimentation rate of 5 g/m^2/day is predicted within the immediate vicinity of the MOF dredge area.

The 95th percentile map (Figure 39) shows extended areas of increased sedimentation rates resulting from the BHD operations, ranging between 2 and 100 g/m^2/day. Predicted areas characterised by rates of 2 g/m^2/day occur along the length of the estuary from the Narrows and Graham Creek in the north to the deep channel waters at the entrance of the Port. Closely banded with these areas are zones predicted to incur rates of 5 g/m^2/day. Sedimentation rates surrounding Hamilton Point and the small group of adjacent islands are predicted to be > 5 g/m^2/day with rates as high as 100 5 g/m^2/day. Elevated sedimentation rates > 25 g/m^2/day are also predicted for a small region to the east of Fisherman's Landing, along the western side of Curtis Island within the direct vicinity of the MOF and construction dock sites and the entrance of Graham Creek.

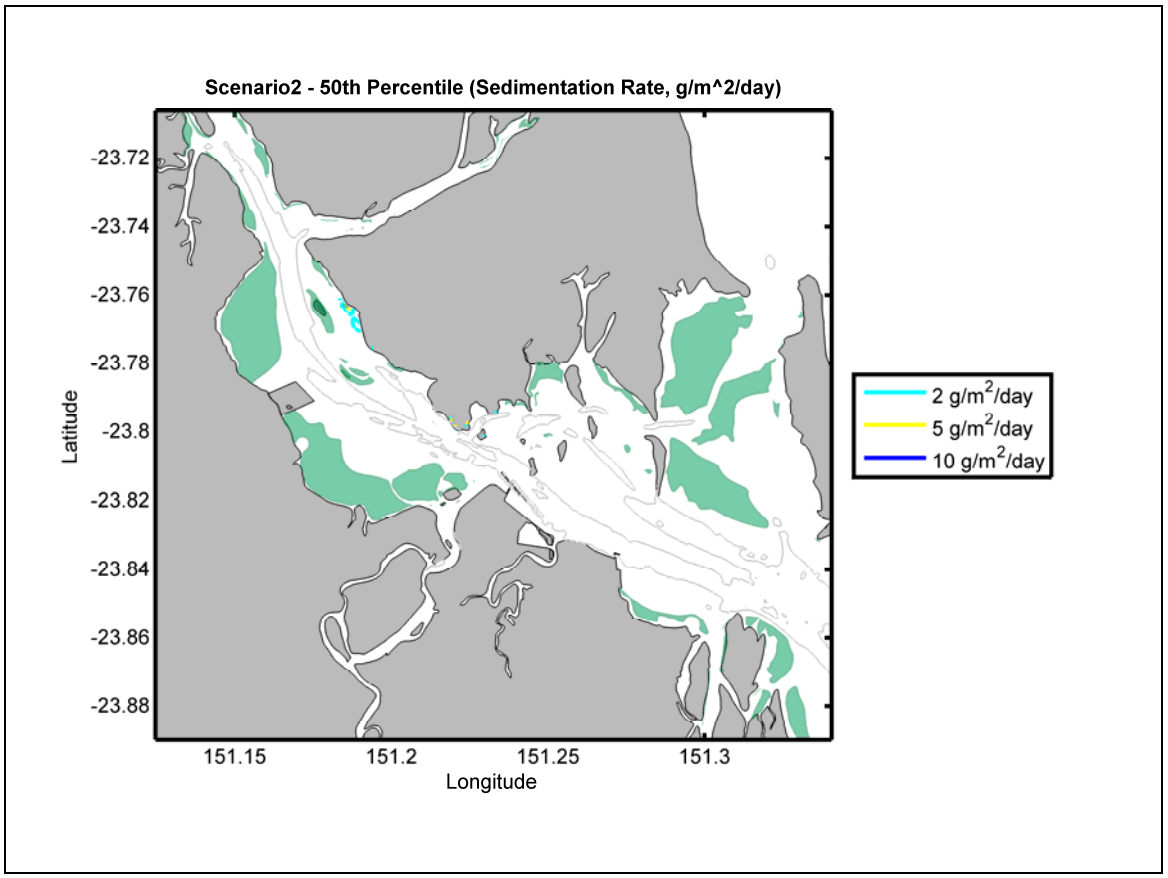

Figure 38: Predicted 50th percentile sedimentation rate (g/m^2/day) from dredging operations in Scenario 2.

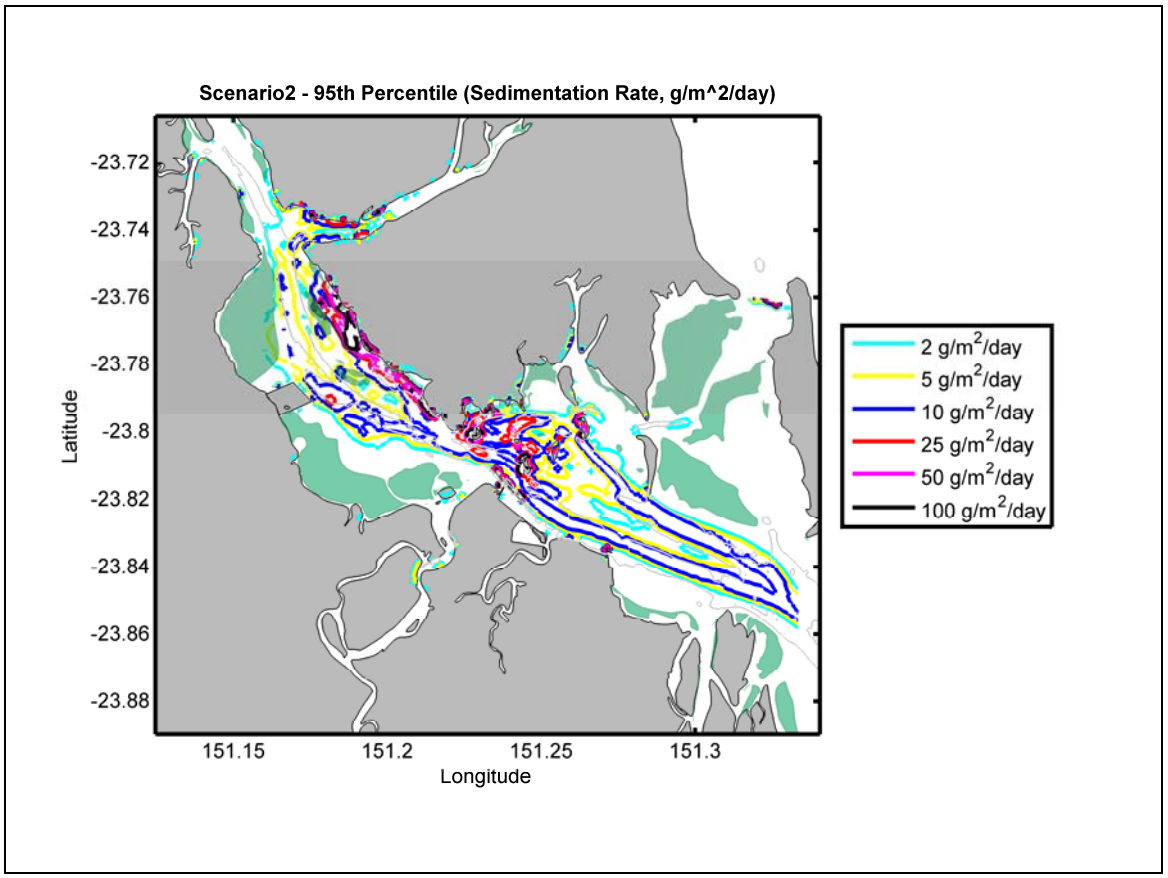

Figure 39: Predicted 95th percentile sedimentation rate (g/m^2/day) from dredging operations in Scenario 2.

9.3.4 Difference in the Proportion of Light Reaching the Seabed

Median and 95th percentile maps of the available light reaching the seabed pre and post dredging and are presented in Figure 40 and Figure 41.

The 50th percentile map shows a 2 to 5% reduction in available light for seagrass meadows north and south of Fisherman's Landing, compared to the ambient estimate. Up to 10% reduction in available light is indicated at the tip of North Passage Island. Seagrass meadows adjacent to Laird Point and South Passage Island could potentially receive 5% less light.

The 95th percentile map shows 10% less available light west of Compigne Island and 5% less light near Garden Island. The seagrass meadows along the coastline south of Fisherman's Landing could have 5 to 10% less available light. For seagrasses adjacent to Laird Point, North and South Passage Island's the indicated difference in available light was 15%. Finally, the change in available light was indicated to be highest (~ 15%) for the seagrass located along the coast, north of Fisherman's Landing.

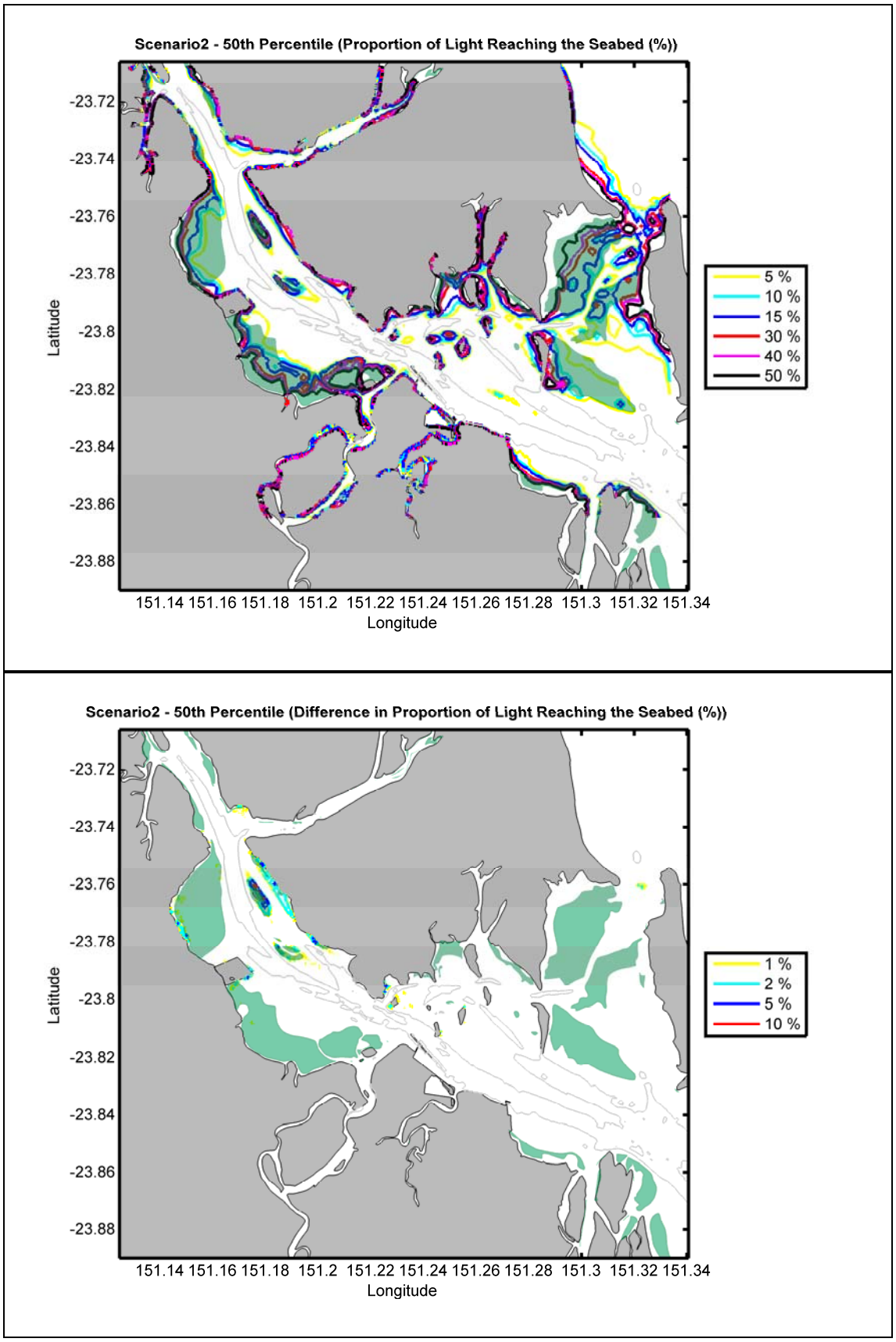

Figure 40: Scenario 2 - Fiftieth percentile plots of the (top) proportion of light (%) reaching the seabed pre-dredging; and (bottom) difference in light (%) reaching the seabed as a result of the dredging operation.

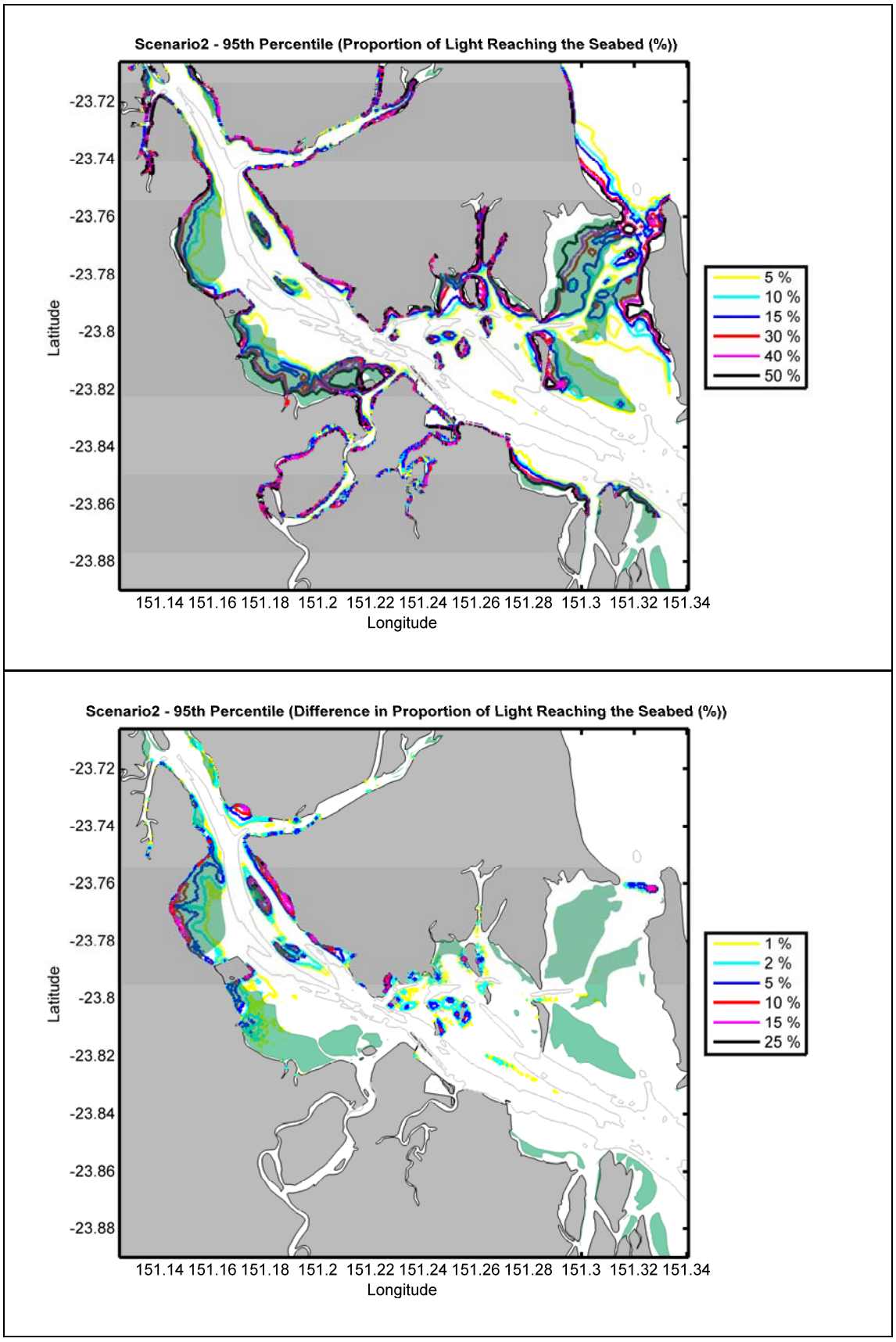

Figure 41: Scenario 2 - Ninety-fifth percentile plots of the (top) proportion of light (%) reaching the seabed pre-dredging; and (bottom) difference in light (%) reaching the seabed as a result of the dredging operation.

9.4 Scenario 3 Cumulative Results

9.4.1 Time-Series Graphs of Maximum TSS Concentrations

Figure 42 to Figure 44 compare the maximum predicted TSS concentrations over time at the same 9 locations (see Figure 10) due to the plumes generated by the larger CSD dredging at MOF stage 2 and tail-water discharges. Each graph depicts the highest concentration at any depth within the water column, with background TSS included.

Figure 42 indicates that the increase in background concentrations at Site 1 typically occurred within the second half of the dredge operations. Within this time 2 peak periods are identified where levels exceeded 18 mg/L (6 mg/L above ambient). In comparison, much larger concentrations are predicted for site 2. The influence of the tidal regime is again evident with cyclic patterns of minimum and maximum concentrations occurring during the modelled period. Concentrations of 70 mg/L or greater are predicted to occur at least 5 times. Site 3 also shows a near daily occurrence of elevated TSS concentrations with a maximum concentration of 80 mg/L (70 mg/L above ambient). Similar to site 1, peak concentrations are predicted to occur in the latter half of the modelled period.

Site 4 is characterised by intermittent peaks > 42 mg/L (5 mg/L above background). Concentrations at site 5 show cyclic pulses above the background and TSS levels typically exceeded 20 mg/L with maximum concentration nearing 28 mg/L (10 mg/L above ambient). No increase in TSS concentrations is predicted for site 6.

Figure 44 shows pulses of increased concentrations at Turtle Island and Diamantina over the model duration. Typically, sustained periods of increased concentrations are more frequent at Turtle Island with concentrations predicted to be 6 mg/L above ambient (22 mg/L). Maximum concentrations at Turtle Island and Diamantina are predicted to be ~ 38 and 32 mg/L, respectively. No increases in TSS concentrations are predicted for Bushy Islet.

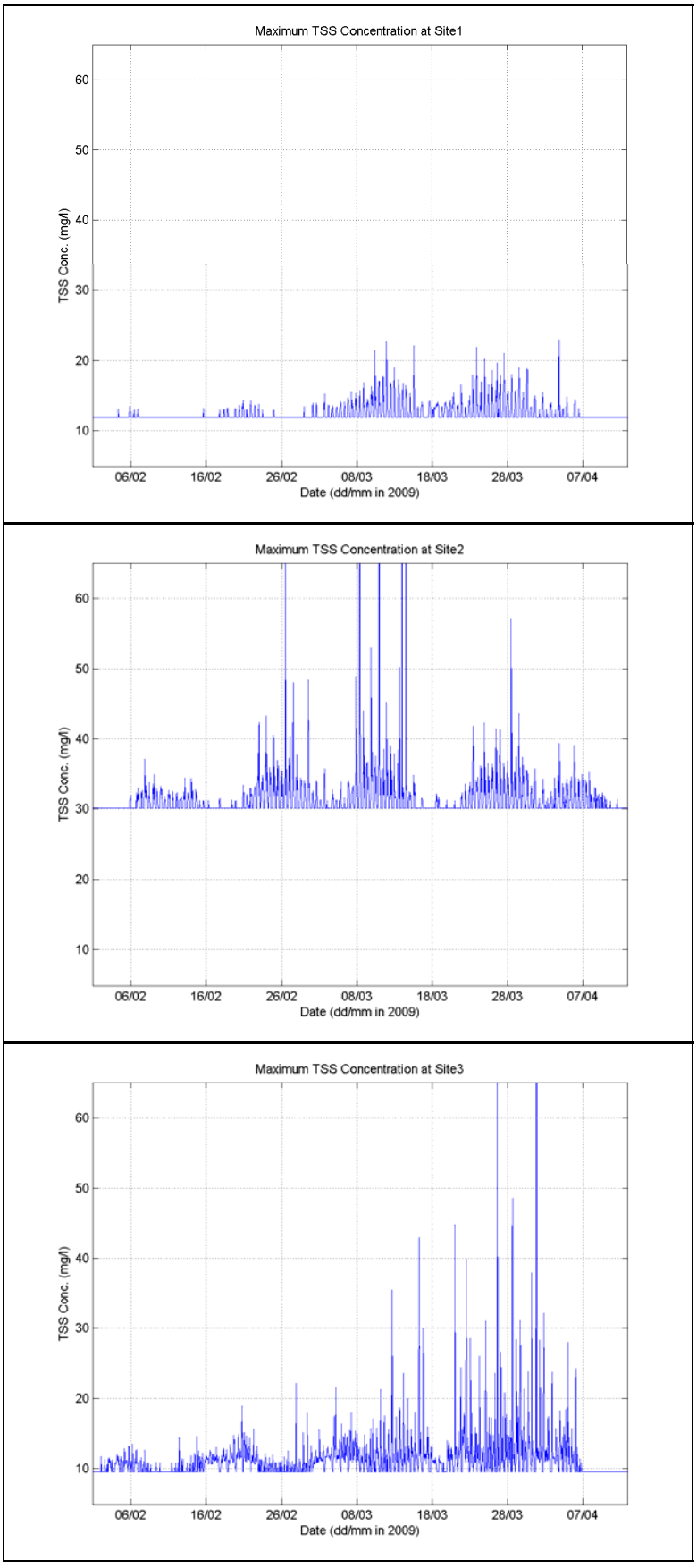

Figure 42: Time-series graphs of maximum predicted TSS concentration (above background) at sites 1, 2 and 3. Results are based on sediment sources identified in Scenario 3.

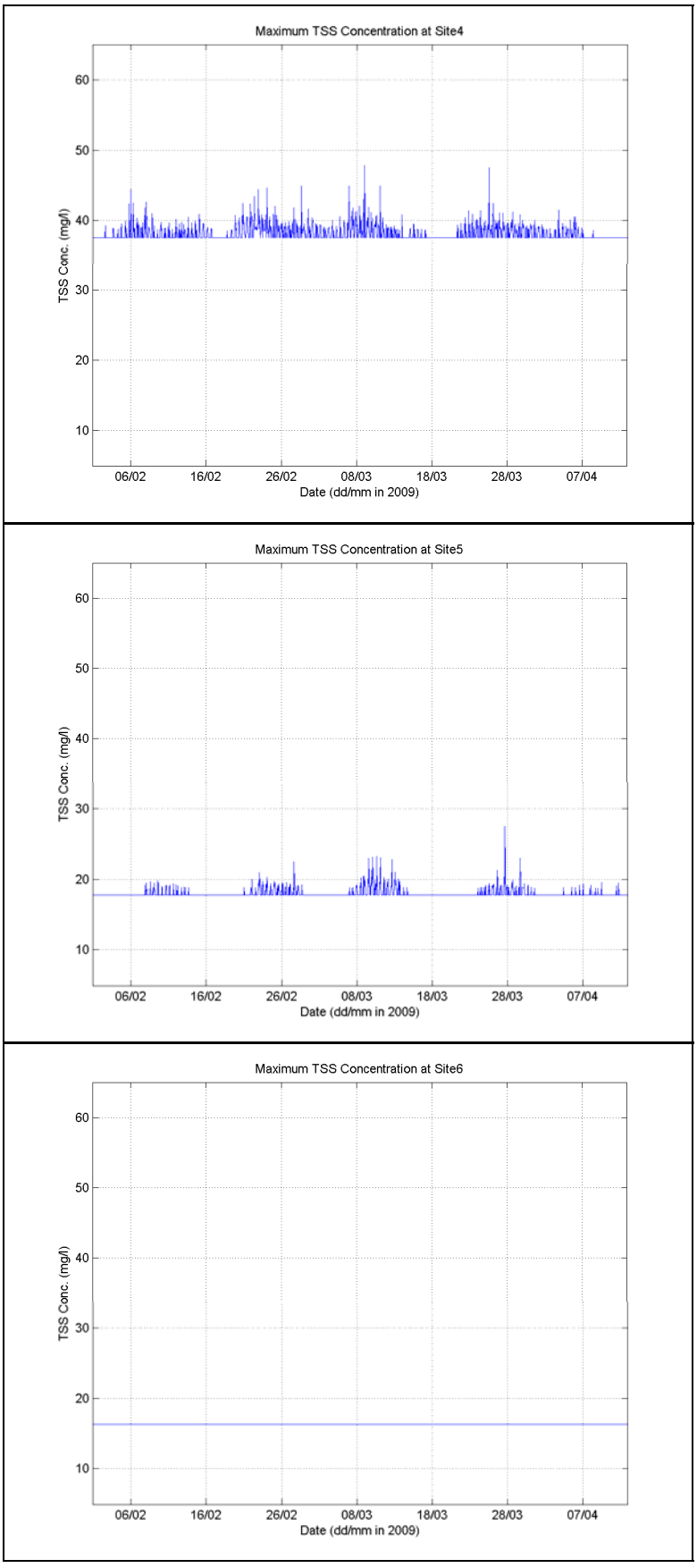

Figure 43: Time-series graphs of maximum predicted TSS concentration (above background) at sites 4, 5 and 6. Results are based on sediment sources identified in Scenario 3.

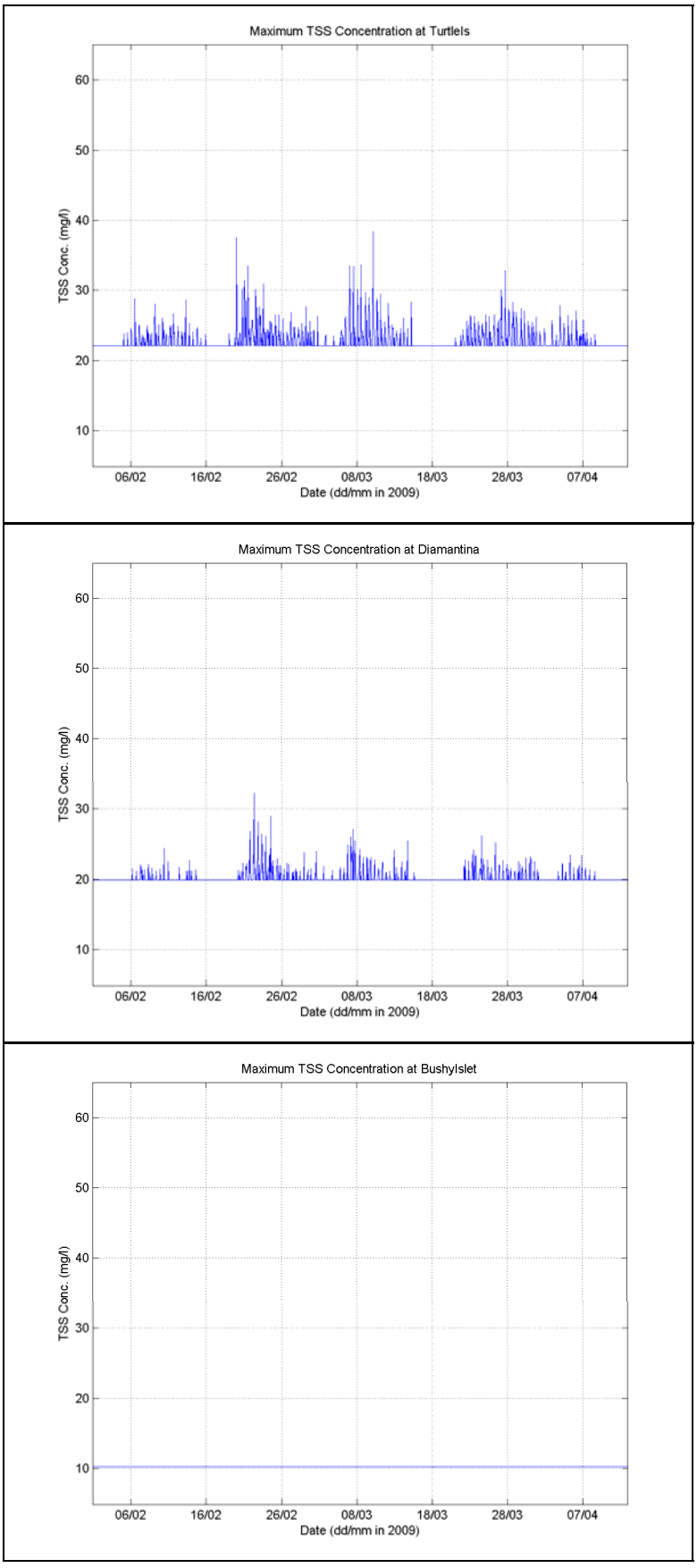

Figure 44: Time-series graphs of maximum predicted TSS concentration (above background) at Turtle Island, Diamantina and Bushy Islet. Results are based on sediment sources identified in Scenario 3.

9.4.2 Percentile Analysis of Depth Averaged TSS Concentrations

Figure 45 to Figure 47 show the 50th, 80th and 95th depth-averaged TSS percentile values, as a result of the dredge operations of scenario 3, with and without addition of background. As previously noted, background turbidity results in exceedance of the defined thresholds and discussion of the contour maps will focus on the additional effect of the dredge operations, i.e. percentile plots without the background TSS concentrations added.

The 50th percentile map shown in Figure 45 (top) suggests that additional concentrations of 5 mg/L will occur in waters adjacent to North Passage Island, Tide Island and the north-east point of the reclamation site. Additional concentrations ranging from 25 to 50 mg/L were estimated for waters immediately adjacent to the tail-water discharge location.

The 95th percentile assessment indicated that increased concentrations of 5 mg/L would extend ~ 16.5 km from Graham Creek in the north to waters surrounding Picnic Island (see Figure 47 top). Concentrations of 10 mg/L were predicted for waters surrounding both North and South Passage Islands, Tide Island, and also nearby the tail-water discharge site. Additional concentrations up to 50 mg/L are predicted for waters in the south-west corner of Tide Island, North Passage Island and in the immediate vicinity of the tail-water discharge site. A maximum additional concentration of 100 mg/L was predicted to occur at the tail-water discharge site.

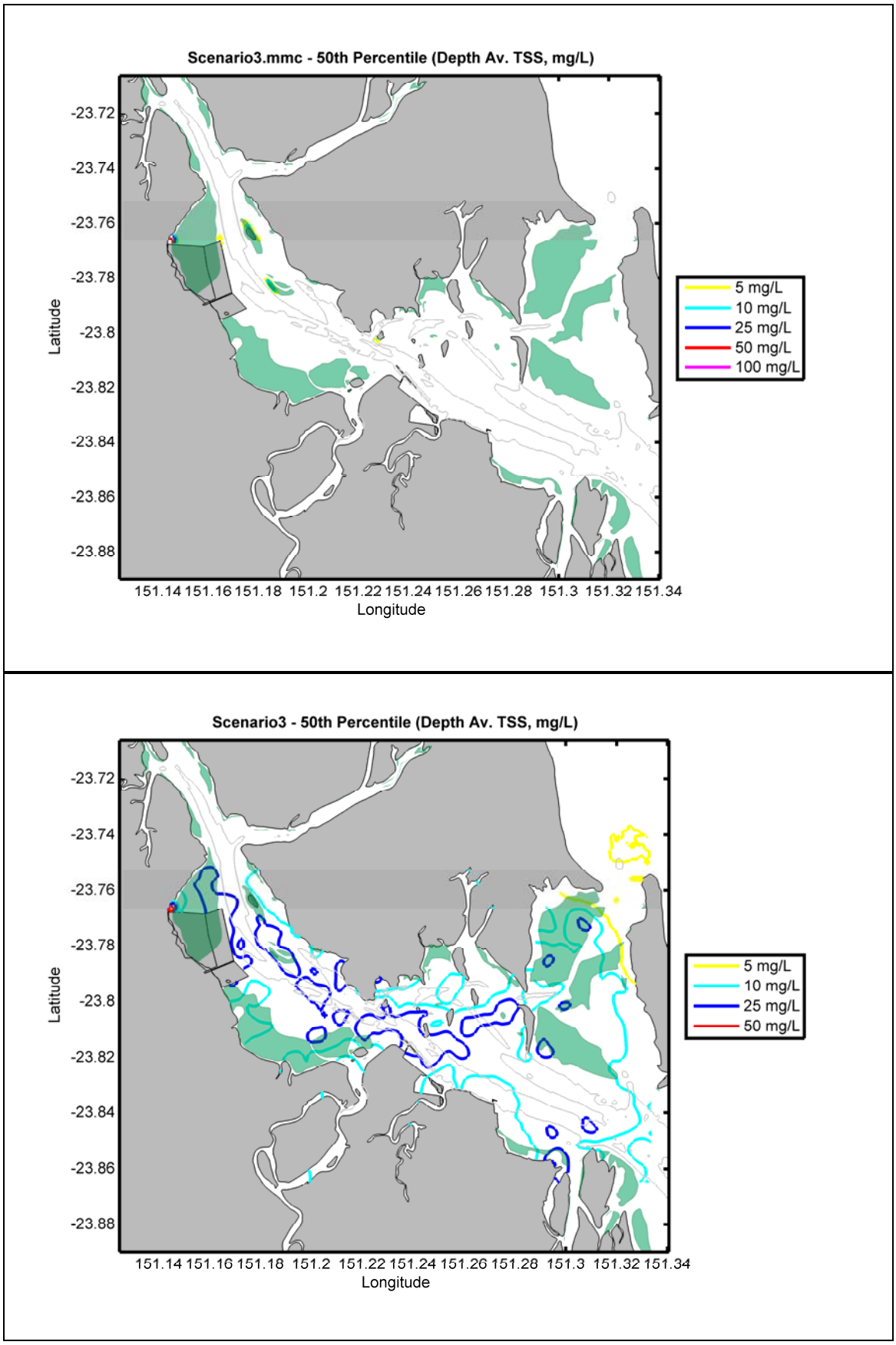

Figure 45: Scenario 3 TSS depth-averaged 50th percentile concentration contour plots without (top) and with background levels included (bottom).

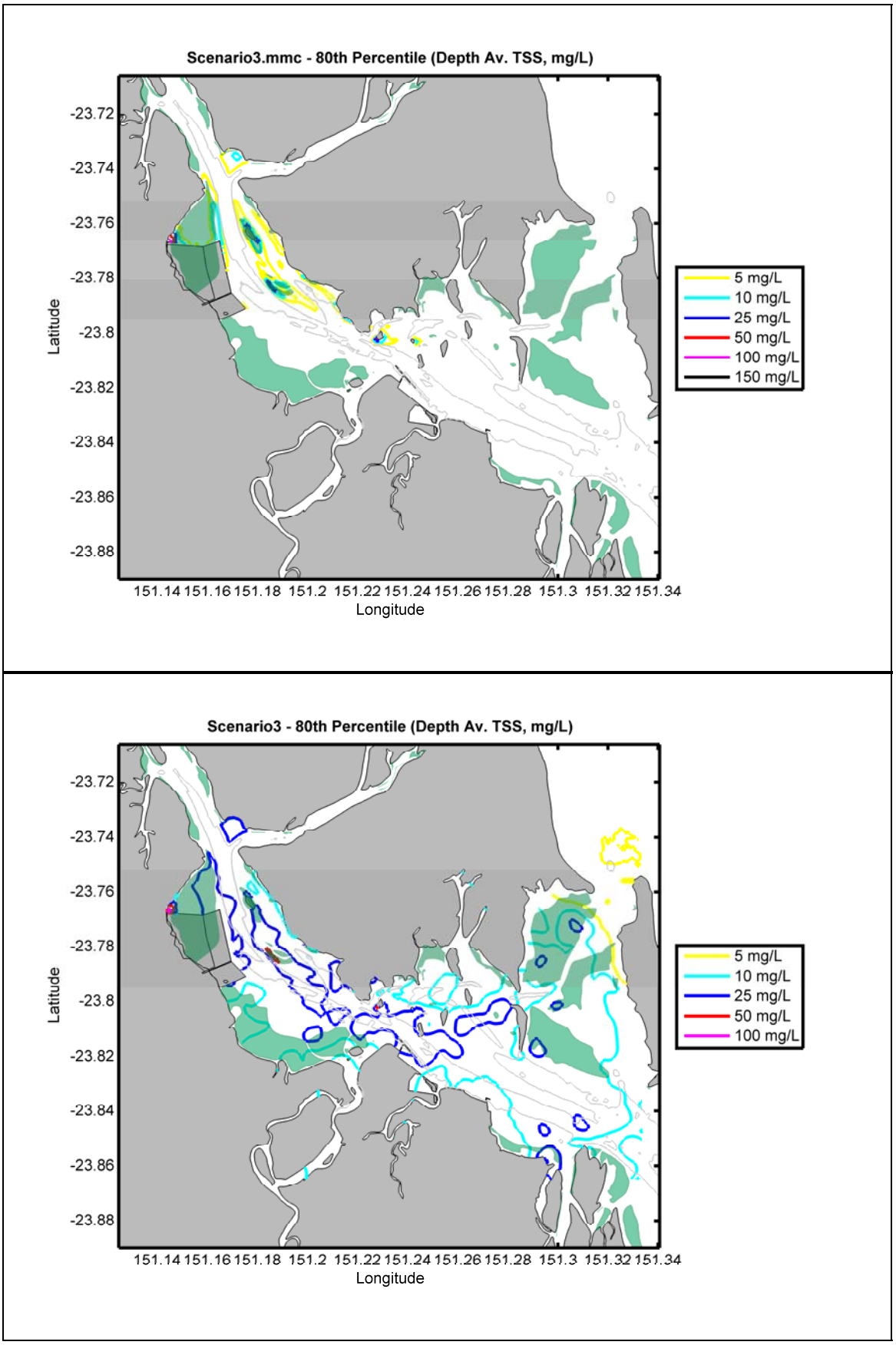

Figure 46: Scenario 3 TSS depth-averaged 80th percentile concentration contour plots without (top) and with background levels included (bottom).

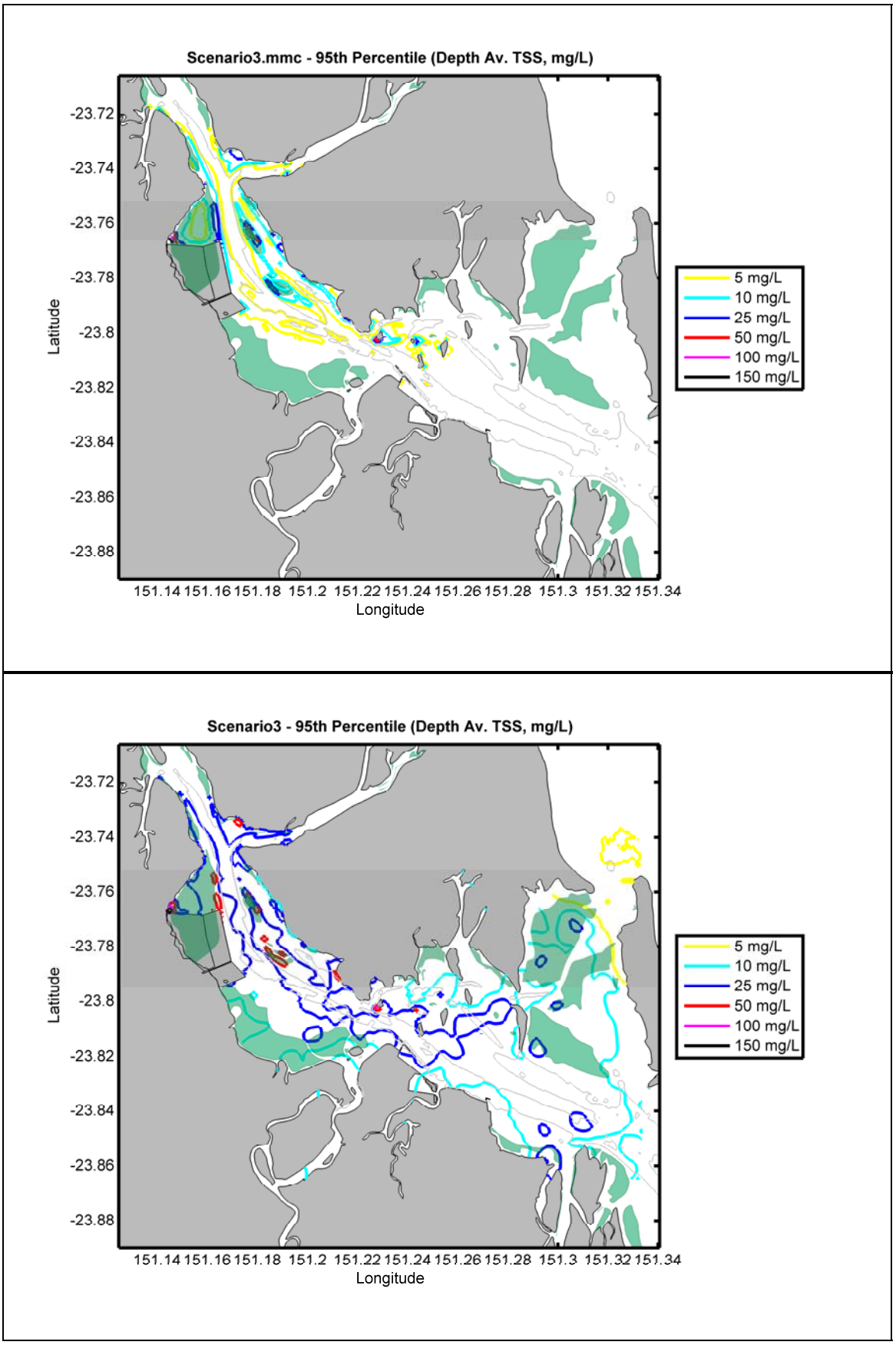

Figure 47: Scenario 3 TSS depth-averaged 95th percentile concentration contour plots without (top) and with background levels included (bottom).

9.4.3 Sedimentation Plots

Analysis of the 50th and 95th percentile sedimentation rates, are presented in Figure 48 and Figure 49.

The median percentile map (Figure 48) indicates a localized sedimentation rate of 2 g/m^2/day directly adjacent to the tail-water discharge site.

The 95th percentile map (see Figure 49) shows sedimentation rates ranging between 2 and 100 g/m^2/day. Predicted sedimentation rates of 2 g/m^2/day are indicated over a predominantly continuous contour from waters between Barney Point and South Trees Island, to Friend Point and Laird Point in the north of the estuary. Predicted sedimentation rates of 5 g/m^2/day or greater were scattered amongst Laird Point. Waters near the tail-water discharge site on the western side of Port Curtis and regions between the MOF and Picnic Island on the eastern side of the Port were characterised by typically more continuous areas. zones where predicted sedimentation rates reached 25 g/m^2/day or greater were concentrated at entrance of Graham Creek, North Passage Island and immediately adjacent the proposed land reclamation site in the northern region of the Port and surrounding Hamilton Point and Picnic Island with the central Port region.

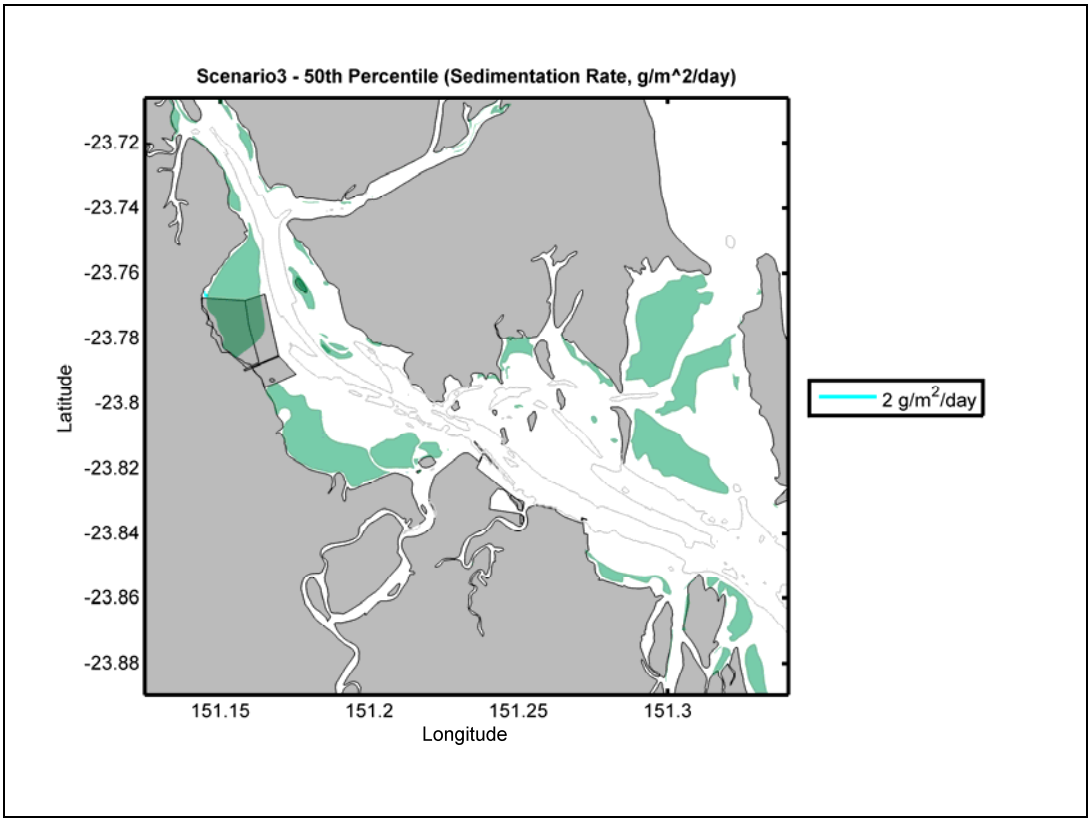

Figure 48: Predicted 50th percentile sedimentation rate (g/m^2/day) from dredging operations in Scenario 3.

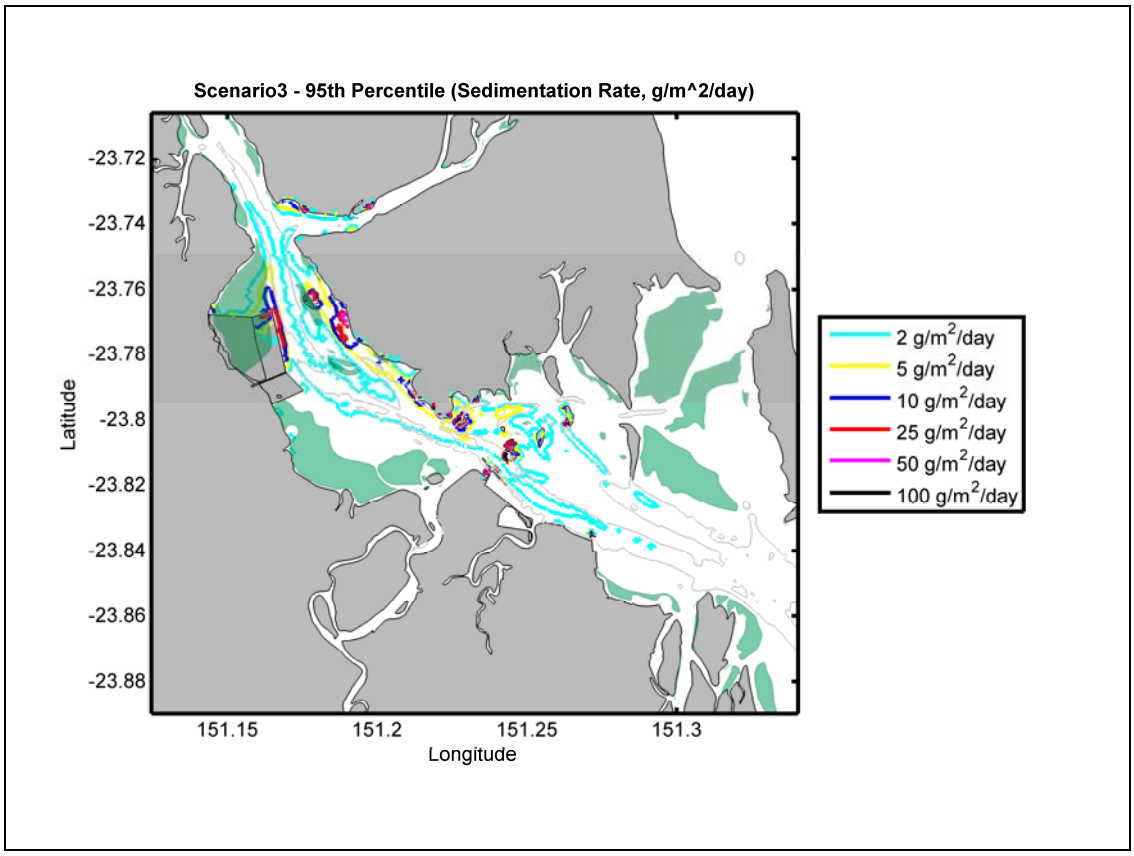

Figure 49: Predicted 95th percentile sedimentation rate (g/m²/day) from dredging operations in Scenario 3.

9.4.4 Difference in the Proportion of Light Reaching the Seabed

The top figures of Figure 50 and Figure 51 show the median and 95th percentile maps for the amount of light (%) reaching the seabed under ambient conditions (i.e. pre-dredging). The bottom figures represent the difference in the available light reaching the seabed with the addition of dredging effects.

The 50th percentile estimates indicate a 5% reduction in available light for seagrasses at South Passage Island and 10% at North Passage Island. Two-percent less light is indicated for meadows adjacent to the proposed construction dock. The seagrass meadows north of the proposed reclamation site are expected to experience 2% less light along the fringes and 25% less at the south-western corner adjacent to the proposed tail-water outfall.

Finally, the 95th percentile estimates indicate a 15% change in available light for meadows adjacent to Hamilton Point and along the western coastline of Curtis Island. Seagrasses located at North and South Passage Islands could receive 10% less light. There was a potential difference of 1 to 2% for meadows south of Fisherman's Landing and 2 to 25% change for seagrasses north of Fisherman's Landing.

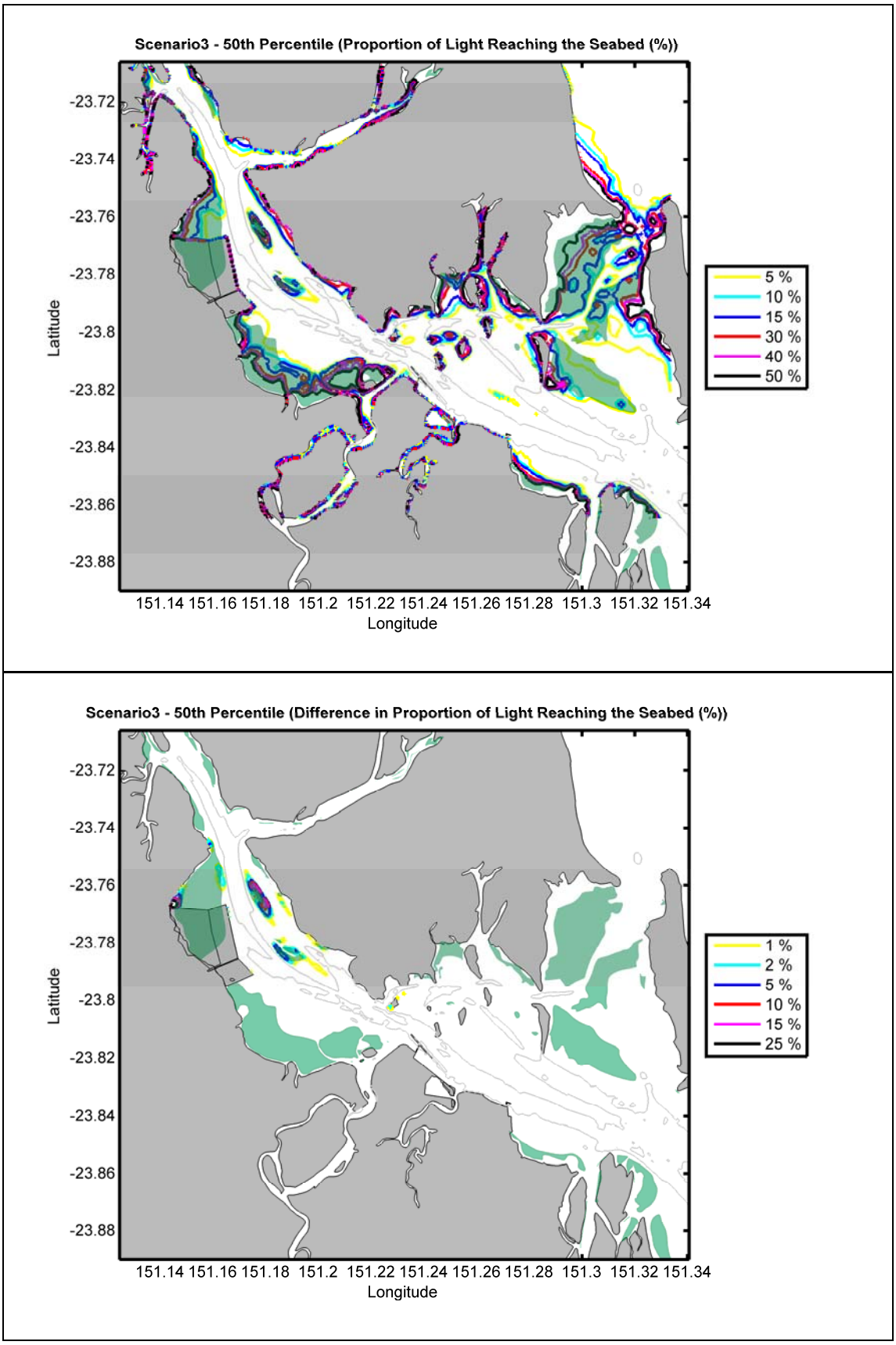

Figure 50: Scenario 2 - Fiftieth percentile plots of the (top) proportion of light (%) reaching the seabed pre-dredging; and (bottom) difference in light (%) reaching the seabed as a result of the dredging operation.

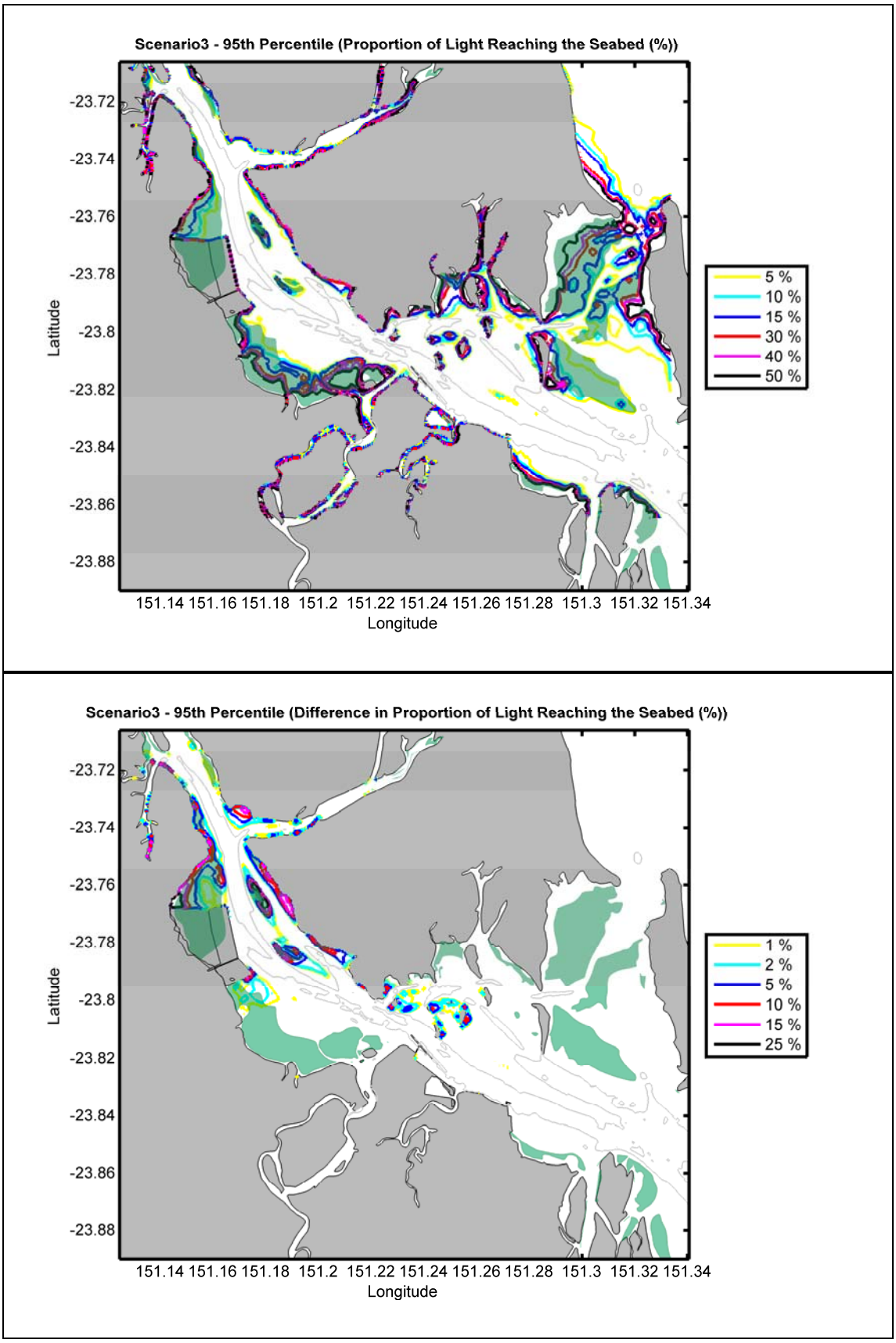

Figure 51: Scenario 2 - Ninety-fifth percentile plots of the (top) proportion of light (%) reaching the seabed pre-dredging; and (bottom) difference in light (%) reaching the seabed as a result of the dredging operation.

10 REFERENCES

Anchor Environmental (2003). Literature Review of effects of resuspended sediments due to dredging operations. Prepared for Los Angeles Contaminated Sediments Task Force. Los Angeles California, June 2003.

ASA, 2004. *SSFATE user manual*. Asia-Pacific Applied Science Associates.

Blaauw, H.G. and van de Kaa, E.J., 1978. *Erosion of bottom and sloping banks caused by the screw race of manoeuvring ships*. Publication 202. Waterloopkundig Laboratorium Delft Hydraukic Laboratory. The Netherlands. pp. 12.

BMT-WBM, 2009. *Water and Environment*, viewed 7 December 2009, < http://www.wbmpl.com.au/Services%20&%20Capabilities/?/273/Water%20and%20Environment>.

GHD Pty. Ltd. 2009. *Marine Water and Sediment, Chapter 8*. Fisherman's Landing Northern Expansion. Environmental Impact Statement. Prepared Gladstone Ports Corporation, Gladstone, Australia. 55p.

Hayes, D. & Wu, PY (2001) Simple approach to TSS source strength estimates. Proc. Of Western Dredging Association, WEDA XXI. Houston, TX. 25-27 June 2001.

Lin, J., Wang, H.V. ,Oh, J.-H., Park, K., Kim, S.-C., Shen, J., Kuo, A.Y., 2003. A new approach to model sediment resuspension in tidal estuaries. *Journal of Coastal Research* 19, 76-88.

Swanson, J., Isaji, T., Clarke, D., Dickerson, C. 2004 *Simulations of dredging and dredged material disposal operations in Chesapeake Bay, Maryland and Saint Andrew Bay, Florida*. Proceedings of the 36th TAMU Dredging Seminar, WEDA XXIV, 6-9 July 2004, Orlando Fl.

Swanson J.C., Isaji T., Galagan C., 2007, *Modeling the Ultimate Transport and Fate of Dredge-Induced Suspended Sediment Transport and Deposition*. Proceedings of Wodcon 2007, Lake Buena Vista, Florida.

Teeter, A.M. 1998 *Cohesive sediment modelling using multiple grain classes, Part 1: settling and deposition.* Proceedings of INTERCOH 98 – Coastal and Estuaries Fine sediment Transport: Processes and Applications, South Korea.

US Army Corps of Engineers, 2008. *Dredging Operations and Environmental Research Program - The Four Rs of Environmental Dredging: Resuspension, Release, Residual, and Risk.* Washington, DC

Van Rijn L.C., 1989, *Sediment Transport by Currents and Waves,* Rep. H461, Delft Hydraul. Lab., Delft, Netherlands